Experimental and Numerical Investigation of the Bone-Screw in Axial Pull-Out Test

DIPLOMARBEIT

zur Erlangung des akademischen Grades

Diplom-Ingenieur

im Rahmen des Studiums

Biomedical Engineering

ausgeführt am

Institut für Analysis und Scientific Computing

Univ.-Klinik für Orthopädie und Traumatologie der Medizinischen Universität Innsbruck

Institut für Werkstoffe und Produktion der Universität Aalborg

unter der Anleitung von

Ao.Univ.Prof. Dipl.-Ing.Dr.sc.med.Dr.techn.Dr.rer.nat. Frank Rattay

Univ. Prof. Dipl.-Ing.(FH) Dr. Werner Schmölz

Dr. Matin Afshar

Eingereicht von

Saman Khodabakhshi

Matrikelnummer 1425238

Abstract

Pedicle screw fixation is a widely used technique for spinal stabilization, especially in patients with osteoporosis or other conditions that affect bone quality. The mechanical stability of pedicle screws is influenced by bone density and structural properties, which can be evaluated using both experimental and numerical methods. The purpose of this study was to evaluate the pull-out strength of pedicle screws in vertebral trabecular bone using both experimental testing and finite element analysis (FEA).

In the experimental phase, pull-out tests were performed on normal, osteopenic, and osteoporotic vertebral specimens, followed by micro-CT imaging to assess bone microarchitecture, including bone volume fraction (BV/TV) and trabecular thickness. Since direct integration of micro-CT data into FEA was not feasible, BV/TV values were used to estimate apparent bone density and assign material properties in the FE model. Finite element simulations were then performed using a homogeneous material approach for comparison with experimental pull-out forces (PPF). The results showed a strong correlation between FE and experimental pull-out forces, with an average discrepancy of approximately 10%. However, variations between FE and experimental PPF were observed in different bone quality groups, especially in osteoporotic bone. In addition, a mesh sensitivity analysis was performed to determine the optimal mesh size for accurately capturing screw-bone interactions.

Despite certain limitations, including material homogeneity assumptions and segmentation challenges in micro-CT data, this study demonstrates the feasibility of using FEA to predict pedicle screw pull-out strength. The results improve computational modeling techniques for spinal fixation and highlight the importance of bone quality in surgical outcomes. Future studies should focus on refining FE modeling approaches, incorporating patient-specific bone structures, and integrating advanced material models to improve prediction accuracy.

Zusammenfassung

Die Fixation mit Pedikelschrauben ist eine weit verbreitete Technik zur Stabilisierung der Wirbelsäule, insbesondere bei Patienten mit Osteoporose oder anderen Erkrankungen, die die Knochenqualität beeinträchtigen. Die mechanische Stabilität von Pedikelschrauben wird durch die Knochendichte und strukturelle Eigenschaften beeinflusst, die sowohl experimentell als auch numerisch bestimmt werden können. Ziel dieser Studie war es, die Ausreißfestigkeit von Pedikelschrauben im trabekulären Wirbelknochen sowohl experimentell als auch mittels Finite-Elemente-Analyse (FEA) zu untersuchen. In der experimentellen Phase wurden Auszugsversuche an normalen, osteopenischen und osteoporotischen Wirbelkörperproben durchgeführt, gefolgt von Mikro-CT-Aufnahmen zur Bewertung der Mikroarchitektur des Knochens, einschließlich des Knochenvolumenanteils (BV/TV) und der Trabekeldicke. Da eine direkte Integration der Mikro-CT-Daten in die FEA nicht möglich war, wurden die BV/TV-Werte zur Abschätzung der scheinbaren Knochendichte und zur Zuweisung von Materialeigenschaften im FE-Modell verwendet. Anschließend wurden Finite-Elemente-Simulationen mit einem homogenen Materialansatz durchgeführt, um sie mit den experimentellen Auszugskräften (PPF) zu vergleichen. Die Ergebnisse zeigten eine starke Korrelation zwischen den FE- und den experimentellen Auszugskräften mit einer durchschnittlichen Abweichung von etwa 10 %. Es wurden jedoch Unterschiede zwischen FE- und experimentellen PPF in verschiedenen Knochenqualitätsgruppen beobachtet, insbesondere bei osteoporotischem Knochen. Zusätzlich wurde eine Netzempfindlichkeitsanalyse durchgeführt, um die optimale Netzgröße für eine genaue Erfassung der Schrauben-Knochen-Interaktionen zu bestimmen.

Trotz einiger Einschränkungen, einschließlich Annahmen zur Materialhomogenität und Segmentierungsproblemen bei Mikro-CT-Daten, zeigt diese Studie die Durchführbarkeit der Verwendung der FEA zur Vorhersage der Ausreißfestigkeit von Pedikelschrauben. Die Ergebnisse tragen zur Verbesserung der computergestützten Modellierungstechniken für die Wirbelsäulenfixation bei und unterstreichen die Bedeutung der Knochenqualität für das chirurgische Ergebnis. Zukünftige Studien sollten sich auf die Verfeinerung von FE-Modellierungsansätzen, die Integration patientenspezifischer Knochenstrukturen und die Einbeziehung fortgeschrittener Materialmodelle konzentrieren, um die Vorhersagegenauigkeit zu verbessern.

Table of Contents

List of Abbreviations and Symbols

AD	Apparent Density (g/cm^3)
BMD	Bone Mineral Density (mg/cm^3)
BV	Bone volume (cm^3)
BV/TV	Bone volume fraction
CFR	Carbon Fiber-Reinforced
CT	Computed Tomography
CTC	Computed Tomography colonography
d^i	Inner hollow diameter (mm)
d_{peak}	Peak pull-out displacement (mm)
d^{thr}	Average thread diameter (mm)
$d^{thr,i}$	Inner thread diameter (mm)
$d^{thr,o}$	Outer thread diameter (mm)
DXA	Dual-energy X-ray Absorptiometry
E	Elastic Modulus (MPa)
FEA	Finite Element Analysis
F_{peak}	Peak pull-out force (N)
HU	Haunsfield Unit
ISCD	International society forclinical densitometry
ISM	Inner Solid Medium
µCT	Micro Computed Tomography
MRI	Magnetic Resonance Imaging
OSM	Outer Solid Medium
PEEK	Polyaryl-Ether-Ether-Ketone
POO	Pull-Out Object
PPD	Peak pull-out displacement (mm)
PPF	Peak pull-out force (N)
qCT	Quantitative Computed Tomography
S_{slope}	Pull-out stiffness (N/mm)
σ_u	Ultimate stress (MPa)
σ_y	Yield stress (MPa)
TV	Total volume (cm^3)
Tb.Sp	trabecular separation (mm)
Tb.Th	trabecular thickness (mm)
VSP	Variable Screw Placement
WHO	World Health Organization

1. Introduction

1.1 Research Objective (Motivation)

Bone fractures are a common occurrence and can result from road traffic accidents, falls, sports injuries, and other causes. Statistically, a common site for femur fracture in trauma patients is the femoral diaphysis [1][2]. An epidemiological study has shown that approximately 9.9 fractures of the femoral shaft occur per 100,000 adults per year, with a higher incidence in older women and young men [3]. In 2002, the American National Osteoporosis Foundation reported that more than 500,000 vertebral compression fractures occur each year and that more than a quarter of American women over the age of 65 suffer from vertebral compression fractures [4][5]. Taiwan's Ministry of Health reported that 12.5% of elderly men and 20% of elderly women suffer from vertebral compression fractures due to osteoporosis [6]. Vertebral fracture is considered one of the classic hallmarks of osteoporosis and is increasingly recognized as a significant public health problem due to its association with back pain and disability [7][8]. In many cases, bone drilling is required to perform a surgical procedure in which screws, wires and fixation plates are inserted to immobilize and align the bone and help it to heal properly. The success rate of these procedures depends on the patient's recovery time and the biomechanical extraction strength of the inserted screws [9]. The pedicle screw as a spinal implant was first described by Boucher et al [10]. in the 1950s and was reintroduced by Roy-Camille et al [11]. Multiple test methods, including insertion torque, pull-out, push-in, and bending tests [12], can be employed to estimate bone screw fixation. Researchers have carried out numerous studies to investigate pull-out strength and the factors that can influence it [13][14][15][16][17][18]. The pedicle is the strongest part of the vertebra. It is a cylinder of cortical bone surrounding a small amount of cancellous bone. The study of the horizontal and vertical diameters of the pedicle confirms that there is no problem in fixing a screw, and sometimes two [19]. Pedicle screw fixation is a standard technique in spinal stabilization, providing rigid bony fixation points for the attachment of internal fixation devices. The mechanical performance of pedicle screws depends on the biomechanical properties of the bone-screw interface, which in turn are influenced by the physical properties of the screw, such as length, pitch, outer and inner diameter, thread, and shaft design (cylindrical or cortical). It has also been found that low bone density in patients with osteoporotic bone can hurt the mechanical strength of the bone-screw interface. Axial pull-out tests have been extensively used to evaluate the fixation stability of pedicle screws in cadavers and animal bone, as well as in artificial materials with bone-like properties[20]. Micro-computed tomography (micro-CT)

is a non-destructive X-ray-based imaging technique that allows rapid digitization of specimens in three dimensions and can visualize the internal and external properties of a specimen. Micro-CT images contain information about the material and structure of the sample being examined, which can be used in combination with other examination techniques, such as mechanical testing or finite element modeling, to investigate the behavior of the sample under load concerning its composition and structure [21]. The pull-out test is a biomechanical experiment designed to evaluate the strength of the interface between a material (such as bone) and another material (such as an implant or screw) that is inserted into it. In addition to experimental testing, finite element analysis (FEA) is an effective method for evaluating pedicle screw fixation under different bone conditions. In this study, FE models based on micro-CT-derived bone properties were developed to simulate pedicle screw pull-out tests and to compare the numerical results with experimental measurements. Due to computational constraints, the micro-CT images were not used directly in the FE modeling. Instead, BV/TV (bone volume fraction) values of the bone-screw interface were extracted from the micro-CT scans and used to estimate apparent bone density, which was then used to assign material properties in the FE model.

The primary objective of this study was to compare FEA-derived pull-out forces with experimental results to evaluate the accuracy and predictive ability of FE models in assessing screw fixation strength in normal, osteopenic, and osteoporotic bone. The results of this research will help improve computational modeling techniques for bone-screw interaction and contribute to more reliable patient-specific surgical planning in the future.

1.2 Clinical context

1.2.1 Anatomy of the spine

The spine is a set of bones (vertebrae), intervertebral discs, and ligaments. The human spine contains 32 to 34 vertebrae: seven cervical (C1 to C7), twelve thoracic (T1 to T12), five lumbar (L1 to L5), five forming the sacrum, and three to five in the coccyx (Figure 1.1). Each vertebra is separated by flexible intervertebral discs, made up mainly of water and collagen, which allow the entire spine to move.

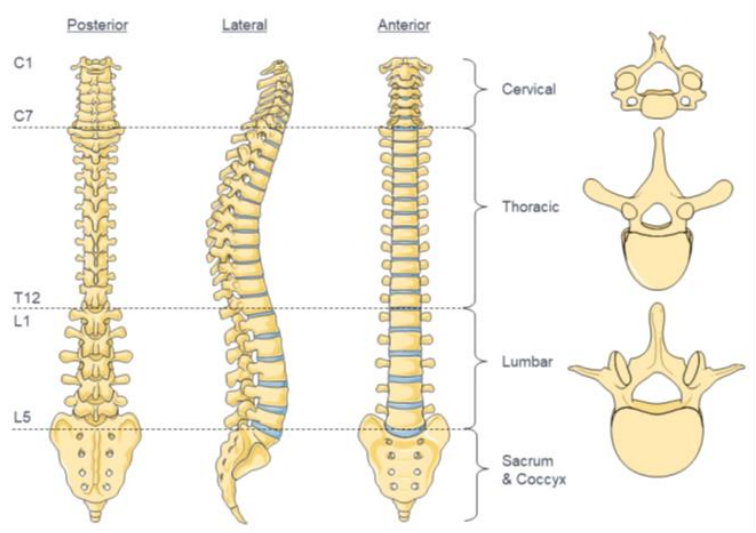

Figure 1.1. Anatomy of the spine. Vertebrae in yellow, disks in blue [22]

The anatomy of the vertebrae varies in shape and size depending on the level (cervical, thoracic, or lumbar). However, they all have the same basic components: a vertebral body, two transverse processes, a spinous process separated by laminae, and two pedicles (Figure 1.2). Together they form the spinal canal, which protects the spinal cord as it runs from the head to the sacrum.

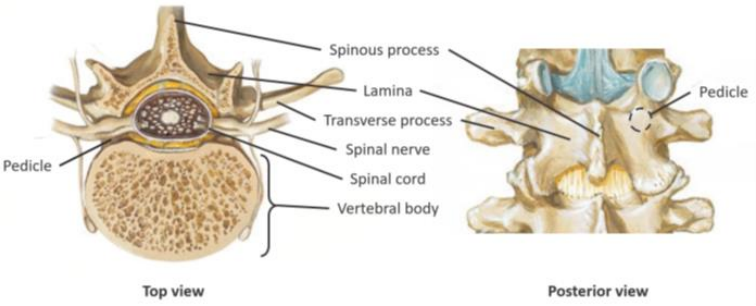

Figure 1.2. Anatomy of a lumbar vertebra [22]

The bone structure itself is also variable within a vertebra and evolves. The surface of the bone called the cortical bone, is much denser and stronger than the spongy (or cancellous) bone. Figure 1.3 shows the difference between these two layers of bone in a lumbar vertebra.

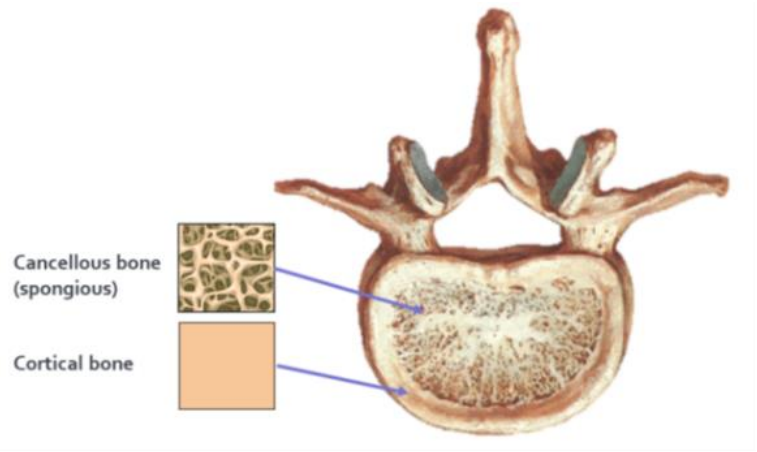

Figure 1.3. Cortical and spongious bone in a lumbar vertebra [22]

1.2.2 Anatomy of the human pedicle

The pedicle is a cylinder of bone located between the lamina and the vertebral body (Figure 1.2) and appears to play an important role in stabilising the screw [17]. Weinstein et al [23] summarised that approximately 60% of the tensile strength and load-to-failure of the thoracic and lumbar pedicles is in the pedicle itself, and the cancellous bone in the vertebral body adds another 15-20% of strength, while purchase in the anterior cortex provides a further 20-25% increase.

1.2.3 Osteopenia & Osteoporosis

Bones in the human body are constantly undergoing a process called remodeling, in which bone is resorbed by cells called osteoclasts, while new bone is created by cells called osteoblasts. This process is essential to maintain an adequate calcium balance in the body. However, an imbalance occurs naturally with aging, where osteoblastic activity begins to occur at a slower rate than that of osteoclasts. As this happens, bone density decreases. The maximum bone density a person will have occurs in the late teens to mid-twenties. After that, bone mass is lost at a rate of about 0.3% to 0.5% per year. However, this rate can be exacerbated by other conditions. For example, women can lose bone mass at a rate of 5% to 6% per year during the first five years after menopause. In addition, prolonged use of certain medications, such as corticosteroids, can further induce osteoporosis [24]. The clinical term "osteopenia" refers to a lower-than-normal bone mineral density (BMD) compared to others of the same age. Bone density measures the mass and strength of bone. Osteopenia weakens the bone compared to normal levels, but not enough to easily break or fracture vertebrae. Osteopenia itself does not cause any symptoms, but as the condition worsens over time, the risk of other harmful bone conditions, such as osteoporosis, increases dramatically [25].

The World Health Organization has suggested general descriptive categories for men and women based on DXA measurements. Osteoporosis occurs when the BMD value is 2.5 SD or more below the mean value for young female adults [26] [27]. It can be classified as either primary or secondary. Primary osteoporosis happens because of common physiological processes occurring within the body [26] [28]. This is further classified into two types: Postmenopausal osteoporosis is known as Type I and senile osteoporosis is Type II. Secondary osteoporosis occurs pathologically, possibly because of other diseases in the body, lifestyle choices, or as a side effect of certain medications [29].

1.2.4 Spine Disorder

The spine is made up of 26 bones called vertebrae that protect and support the spinal cord and nerves. Several conditions and injuries can affect the spine, which can damage the vertebrae, cause pain, and limit mobility. Numerous conditions can affect the spine from the neck to the lower back. Degenerative spine and disc disease: Arthritis, degenerative disc disease, herniated disc, spinal stenosis, spondylosis. Other Spine Conditions and Disorders: Scoliosis, Kyphosis, Spinal Fracture, Spinal Cord Injury, Neck Pain, Osteoporosis Vertebral Fractures, and... [28].

1.2.4.1 Causes of Spine Disorders

Spinal disorders have a variety of causes, depending on the condition. For some conditions, the causes are unknown. Common causes include Accidents or falls, Congenital disorders (present at birth), Inflammation, Infection, Hereditary disorders, Injuries ranging from minor to traumatic, Degenerative wear and tear associated with aging [28].

1.2.4.2 Treatment for Spine Disorders

Depending on the specific condition or injury, treatments may include

Surgery to replace discs, fuse (join) vertebrae, open the spinal canal, or repair nerves; Rehabilitation with physical therapy to strengthen and stretch the back and abdominal muscles [28].

1.2.4.3 Spinal Fusion

Spinal fusion is a procedure in which multiple levels of the vertebral body are immobilized and placed in a position that allows bone to form between them, creating a single spinal unit [30]. Adapted from arthrodesis, where joints are fused together to relieve pain, the primary goal of spinal fusion is to treat spinal instability [30] [31]. Various techniques are used to perform this procedure, including the placement of cages between the endplates of adjacent vertebrae, the use of bone grafts, bone morphogenetic proteins, and pedicle screws [30].

1.2.4.4 Pedicle Screws

Pedicle screws have been widely used in the treatment of spinal instability by spinal fusion for over half a century. The techniques probably originated with King et al [32] in the mid-1940s when he attempted to stabilize a lumbar spine by placing screws through the facets. In the late 1950s, Boucher et al [10] advanced King's idea by placing long screws through the pedicle, which led to the addition of a rod a few decades later to fuse multiple levels simultaneously [33]. Since then, pedicle screws have been considered the "gold standard" in spinal fusion technology.

It has been reported that over 50% of all money spent by hospitals on spinal implants in 2004 was spent on pedicle screws and their ancillary products such as rods, heads, and set screws [36]. Standard pedicle screws are manufactured in a variety of lengths and diameters depending on the size of the pedicle and vertebral body in which they are to be inserted. In 2004, most of these screws (75%) were placed in the lumbar levels. As a result, the most used diameter during this period was 6.5 mm (33%), and the two most common lengths were 40 mm (29%) and 45 mm (26%). However, screws as small as 3.5 mm in diameter and/or 14 mm in length were used, most likely for instrumentation in the smaller pedicles of the cervical spine [36]. The shaft of the screw typically consists of a single lead thread with a pitch more similar to wood screws to match the mechanical properties of the surrounding bone. The head of the screw often resembles a cup with a U-shaped cut-out to accommodate the rod used to connect pedicle screws at adjacent levels. The head may be either fixed to the screw or allowed to rotate freely, such as the polyaxial cannulated fenestrated pedicle screws used in this study. Pedicle screws are made of biocompatible materials such as stainless steel or titanium [36]. Similar to the anatomical directions used in the human body, the term distal was used to describe a location closer to the screw's head (Figure 1.4) [34][35][36][37][38].

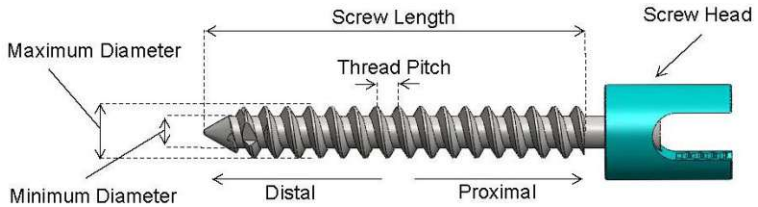

Figure 1.4. Standard pedicle screw

1.2.5 Pedicle screw placement

Several spinal procedures, such as scoliosis correction, require the insertion of screws into the vertebrae to fix two or more vertebrae together with metal rods. The pedicles are the strongest

accessible parts of the vertebral arch through a posterior (back) approach. These narrow spaces are used to insert pedicle screws, as shown in Figure 1.5, with appropriate stability.

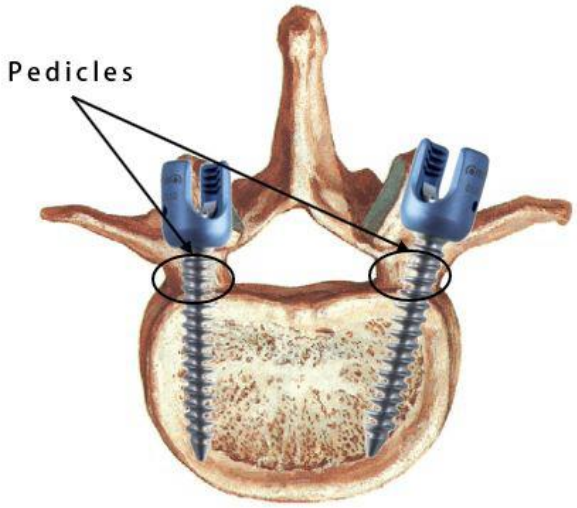

Figure 1.5. Top view of a lumbar vertebra with two pedicle screws inserted

Depending on the patient's anatomy, the pedicle width varies from up to 18 mm to 3.5 mm for thoracic and lumbar vertebrae [39]. The diameter of the screws used can be selected based on the estimated pedicle width from preoperative imaging. Surgeons tend to select the largest screw possible so that its threads can be fixed in the cortical layers of the pedicle. However, if selected too large, they may damage the vertebra. The optimal diameter is approximately 80% of the available width according to [40]. The screw length can also be adjusted to maximize the screw purchase to optimize fixation [41].

1.2.6 CFR Poly(aryl-ether-ether-ketone) Pedicle Screw

Metal-induced artifacts significantly hinder postoperative imaging of the spine [42] [43]. To overcome this shortcoming of conventional metallic pedicle screws, non-metallic high-strength carbon fiber-reinforced poly(aryl-ether-ether-ketone) (CFR/PEEK) pedicle screws have been developed. CFR/PEEK is radiolucent and non-magnetizable, allowing for the minimization of imaging artifacts in CT and MRI imaging [44][45]. Historically, the availability of polyaromatic polymers came at a time when there was growing interest in the development of "isoelastic" hip stems and fracture fixation plates with stiffness comparable to bone [46]. Although pure (unfilled) polyaromatic polymers can have an elastic modulus in the range of 3 to 4 GPa, the modulus can be tailored to match cortical bone (18 GPa) closely or titanium alloy (110 GPa) by preparing carbon fiber reinforced (CFR) composites with varying fiber length and orientation [46]. It has been shown that orthopedic implants made of CFR-PEEK

composites with carbon fiber content of approximately 60% by volume have mechanical properties (e.g., Young's modulus and fatigue strain) equivalent to those of cortical bone, with promising results in spine surgery [47][48][49][50][51].

1.3 Pull-out Testing

One of the first steps in determining how effective a pedicle screw is at achieving adequate fixation in bone of any density is to perform a pull-out test. The pull-out test for pedicle screws involves applying a constant displacement to the device implanted in either a vertebra or a block of "synthetic bone," creating a gradually increasing axial force. When this force becomes great enough, the screw loses its fixation in the surrounding material. This maximum force achieved is referred to as the pull-out force. Although not commonly seen in a clinical setting, the pull-out test is one of the most efficient methods for testing the fixation of different screw designs in bone, as it is simple to perform and reproducible [52] [53].

While the most observed parameter of the pull-out test is the maximum pull-out force achieved, the test can provide other useful information to describe the interaction between the device and the surrounding bone. For example, stiffness is often measured to determine how quickly axial forces within a system increase when subjected to tension. Looking at the load-displacement curve of a particular pull-out test, stiffness is the slope of the curve before the point of pull-out. The area under the same region of the load-displacement curve can also be used to determine how much mechanical energy must be introduced into the system before the pull-out is reached. This is called energy to failure. In addition, although not commonly used, data can be observed beyond the point of pull-out. For example, the area under the entire load-displacement curve can be used to determine how much mechanical energy is required to completely remove the screw from the bone or block in which it is inserted. This is referred to as toughness [54].

2. Literature Review (Background)

Pedicle screws have revolutionized the surgical treatment of spinal disorders, but their introduction and widespread adoption by spine surgeons has created one of the most challenging regulatory issues ever seen in orthopedics [55].

2.1 History of Spinal Internal Fixation with Pedicle Screws

Hadra [56] first used silver wire internal fixation in 1891 to treat cervical fracture dislocation and tuberculous spondylitis. Later, King [32] introduced facet screws for the treatment of degenerative lumbar conditions. Although Boucher [10] is widely credited with the first use of pedicle screws in North America, his report suggests that his innovation was a longer facet screw that occasionally obtained oblique purchase across the pedicle. His screws were not directed down the long axis of the pedicle. Thus, it appears that Harrington and Tullos [57] deserve credit for the first deliberate attempt to place pedicle screws through the isthmus of the pedicle. Their report, published in 1969, described the attempted reduction of two cases of high-grade spondylolisthesis. The pioneering use of pedicle screw internal fixation continued in the 1970s in France and Switzerland. Clinical success with the screws was reported in the 1980s by investigators such as Cotrel and Dubousset [33], Dick [58], Roy-Camille et al [11] [59], and Louis [60].

A major impetus for the use of the pedicle screw technique in North America was Roy-Camille's presentation at the 1979 meeting of the American Academy of Orthopaedic Surgeons in San Francisco. Subsequently, several American surgeons began using pedicle screws in the United States. Arthur Steffee was the most creative in using them [61]. Steffee et al. [61] developed the Variable Screw Placement (VSP) plate, which allowed pedicle screws to be placed according to the individual patient's anatomy. This device provided much more clinical latitude than the Roy-Camille plate [11] [59], which had fixed screw hole spacing for screw placement (Figure 2.1). Recognizing the clinical utility of pedicle screw fixation, the North American Spine Society and the Scoliosis Research Society collaborated on a series of introductory meetings to educate spine surgeons about this new technique. The first such meeting was held in 1984. These two societies then jointly sponsored the International Meeting on Advanced Spine Techniques, and this annual meeting continues to this day. Since the introduction of pedicle screws, engineers, surgeons, radiologists, neurophysiologists, anatomists, epidemiologists, and statisticians have made fundamental efforts to improve what was universally recognized as a clinical liability in surgical spine care: the lack of truly high-

quality spinal internal fixation as available for long bone internal fixation. The basic and clinical science of pedicle screws evolved from their introduction and infancy in the early 1970s to widespread acceptance, as evidenced by the 1993 and 1996 "State of the Art Treatment" statements of the North American Spine Society, which endorsed the use of pedicle screws by experienced surgeons. Review articles have described the evolution of treatment methods as surgical experience has accumulated [62] [63] [64] [65].

Figure 2.1. The Roy-Camille plate [11][59] (left) and the Steffee variable-screw-placement (VSP) plate [66] (right). The former plate, with its fixed screw-hole distances, was not able to accommodate the individual patient anatomy as well as the latter plate

2.2 Biomechanical Studies of Pedicle-Screw-Based Constructs

In 1986, Gaines et al [67] demonstrated the improved quality of spinal internal fixation provided by a pedicle screw implant with a fixed connection to a plate in the first non-failure stability test for spinal fractures. Gaines et al. also demonstrated the fundamental importance of load transfer through the spine itself along with the implant, a concept known as load sharing [67], which was subsequently widely adopted by the spine surgery community. Biomechanical testing of pedicle screw constructs has demonstrated the fundamental importance of the bone-implant interface, bone density, and screw extraction strength [68][69][70][17]. The essential need for the screw to fit and fill the isthmus of the pedicle has been demonstrated [71] [72] [73]. The direct relationship between pull-out strength and insertion torque has been well demonstrated, and the fundamental improvement in pull-out strength obtained by cross-linking [74][75][76][77] (i.e., the attachment of the two screws in a single vertebra using a metal cross-link) has been documented. The stabilizing influence of using converging screws (high pedicle angle [Figure. 2.2]) when possible has also been emphasized [78] [79] [80]. In addition to in

vitro testing, finite element modeling has been used extensively [81] [82] to analyze stress transfer through implants and implant-based constructs.

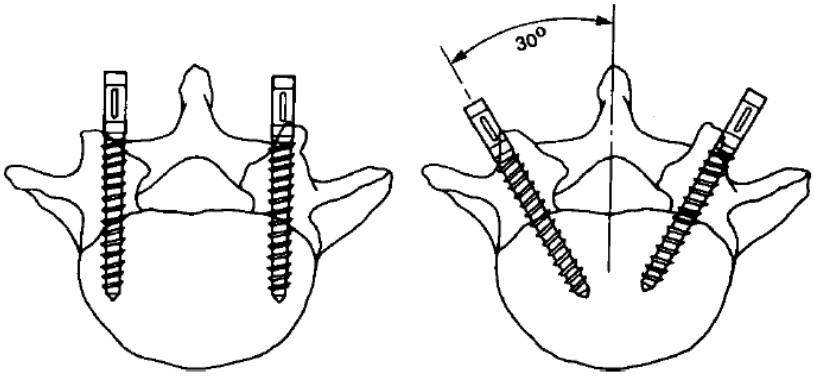

Figure 2.2. Drawings clearly illustrating the benefits of screw triangulation to improve pull-out strength, particularly when the screws are cross-connected to one another [78]

The pull-out test was performed to evaluate the fixation strength and performance of pedicle screws in the trabecular bone. The purpose of the experiment was to measure the maximum force required to remove the screw from the bone and to analyze the factors influencing the pull-out strength. Thread design plays a critical role in the performance of bone screws. It is important to note that other factors, such as screw diameter, length, and material composition, can also affect pull-out strength. These variables were held constant in this study. Further research is needed to evaluate the combined influence of multiple factors on screw fixation strength. Once screw pull-out data has been collected and analyzed, it is of paramount importance to relate and present the primary results understandably and concisely. Pull-out test experimental data (i.e., peak force) in publications vary widely[83][84][85] [86][87][88][89]. This is because in some publications both trabecular and cortical bone was screwed [90]. In this case, the peak force is between 1646 and 3085 N for the human femur, while for the tibia it is between 1100 and 1700 N [91].

2.3 Pedicle screw size

Perhaps the most intuitive technique used to achieve high purchases where little is expected is to increase the diameter of the pedicle screw [36] [92] [17]. This is because it is believed that of all the anatomical considerations in pedicle screw design, the size of the outer diameter best influences the pull-out strength, while the inner diameter determines the fatigue strength. The inner diameter is the most important dimension of the pedicle screw when considering its

fatigue strength [93]. Liu et al [94] showed a 104% increase in fatigue strength following a 27% increase in inner diameter. Hsu et al [36] showed that there was a steady increase in pull-out strength as the diameter increased by approximately 1 mm when testing three different diameters. Zindrick et al [17] observed significantly higher pull-out forces with 6.5 mm cancellous screws than with 4.5 mm cortical screws or 4.5 mm Louis screws. Similarly, Patel et al [92] tested cancellous and cortical screws and found that the 2 mm larger cancellous screws significantly increased fixation strength in a synthetic osteoporotic bone model. Special care must be taken when implanting larger-than-usual pedicle screws in poor-quality bone, as the weakened pedicles are more prone to fracture during screw insertion [95] [96].

In addition to the use of larger diameter screws, adjustments in screw length have been made to increase the depth achieved within the vertebral body in the hope of increasing pull-out strength. It has been suggested that in most cases, advancing the pedicle screw to approximately 80% of the vertebral body will provide adequate fixation [23]; however, Zindrick et al [17] found that in osteoporotic specimens, there did not appear to be much difference between advancing the screw 50% into the vertebral body or fully advancing the screw without penetrating the anterior cortex. In these tests, the differences ranged from a 4% decrease to a 16% increase in pull-out strength with full insertion.

2.4 *Effect of Osteopenic and Osteoporotic on Spinal Fusion*

Osteoporosis and osteopenia are highly prevalent in spine surgery patients, with 34.2% diagnosed with osteoporosis, 43.5% diagnosed with osteopenia, and a combined prevalence of 78.7%. The International Society for Clinical Densitometry (ISCD) recommends bone health assessments for men aged≥70 years and women aged≥65 years undergoing spine surgery, as osteoporosis is more common in women (43.0%) than in men (19.9%) [97]. Fan et al [98] showed an unexpectedly high prevalence of osteoporosis in patients below these cut-off ages. In the age groups 50-59, 60-69, and 70-79 years, the prevalence of osteoporosis is 27.8%, 60.4%, and 75.4% in women and 18.9%, 17.4%, and 26.1% in men. Considering the high rate of osteoporosis and its associated surgical complications, the current screening and treatment of osteoporosis before spinal surgery may not be adequate and needs to raise awareness among orthopedic specialists in the future. Another possible reason is that lumbar degenerative diseases such as scoliosis can lead to significant activity limitation, which is associated with bone loss and osteoporosis [99].

2.5 Pedicle Screw Finite Element Model

The pedicle screw is an important tool used in spinal fusion surgery to attach posterior spinal fixation systems to the vertebrae. Although posterior spinal fixation systems and surgical techniques have been continuously improved over the past two decades, postoperative pedicle screw failures have not been eliminated in postoperative patients [100] [101] [102] [103] [104] [105]. Common complications of pedicle screw-based posterior fixation include screw breakage, screw loosening, and screw extraction [105] [106]. The failure of the pedicle screw can lead to loss of fixation, culminating in pain and ultimately revision surgery [104] [107]. Demir and Camuscu et al [108] reported an average hospitalization cost of over $40,000 and an average hospital stay of over 4 days for spinal fusion surgery. Due to the high cost of revision surgery, there is an increasing clinical need to analyze the interaction between bone and pedicle screw and the effect of the pedicle screw on the biomechanical behavior of the spine [102] [106] [107].

Extensive experimental studies and tests have been carried out to investigate and improve the performance of pedicle screws and posterior spinal fixation systems [108] [109] [110] [111] [112] [113] [114] [115]. Standard test methods have also been developed to measure the performance of pedicle screws inserted into test blocks under static and fatigue loading [109] [111] [112]. Although these tests can quantify the behaviour of pedicle screws by reporting external parameters such as ultimate strength and fatigue life, they cannot reveal information internal to the test configurations, such as the stress at the screw/test block interface, which contributes significantly to screw/bone failure [106] [107]. In addition, test block testing can provide very simplified and limited physiological loading of the spine. Finite Element Analysis (FEA) can provide detailed information at the screw-bone interface and can feasibly test the pedicle screw under physiological spinal loads within the spine FEA model, which has been widely used to study the biomechanics of lumbar spines instrumented with pedicle screws [109] [113].

Varghese et al [116] have developed a 2D axi-symmetric finite element model using ABAQUS to evaluate the pull-out strength of pedicle screws, a critical factor in implant design. The study modeled cancellous bone using homogeneous rigid polyurethane foam. It tested the screw design in extremely osteoporotic and osteoporotic bone, focusing on parameters such as pitch, inner diameter, outer diameter, and thread type. The results showed that an increase in bone density resulted in higher pull-out strength, with the maximum von Mises stress observed at the last thread of the screw.

Biswas et al [117] have modeled L3-L5 spines and used finite element analysis (FEA) to determine optimal pedicle screw and rod configurations. They found that 6 mm diameter pedicle screws, whether stainless steel or Ti6Al4V, were generally optimal in most cases. The study highlighted that applied stress is a critical factor in the long-term success of implants, as excessive stress can lead to bone resorption and eventual loosening of the implant.

Matsukawa et al [118] used 3D finite element analysis (FEA) to investigate the effect of screw size on fixation in osteoporotic vertebrae. They tested pedicle screws of various diameters (4.5, 5.5, 6.5, and 7.5 mm) and lengths (30, 35, 40, 45, 50, and 50 mm), using cobalt chromium for the screw heads and titanium for the shafts. The results showed that larger diameter and longer screws significantly reduced the equivalent stress around the screws while increasing both pull-out strength and overall vertebral fixation strength.

Alisdair et al [119] evaluated three screw-bone interface modeling strategies in mid-shaft tibial fractures stabilized with locking plates: 1) fully bonded interface, 2) screw with a sliding contact, and 3) screw with sliding contact in an undersized pilot hole. While the global load-displacement response showed less than 1% variation between models, the interface significantly affected the local stress-strain environment around the screws. The commonly used tie constraint is suitable for analyzing global load deformation, but different contact interface models affect the mechanical response near screw holes, influencing predictions of screw loosening, bone damage, and stress shielding.

3. Material and Methods

Axial pull-out testing of pedicle screws in bone is a standard technique for evaluating the pull-out strength of orthopedic implants [56]. Such tests include the components shown in Figure 3.1. In recent research, pull-out tests have emerged as a fundamental experimental method for investigating the bond behavior between dissimilar materials. In the pull-out test, a screw is pulled out of the surrounding matrix, simulating the response of the materials under axial loads or shear forces. This method provides valuable insight into the bond strength, anchorage length, and stress distribution at the screw/matrix interface.

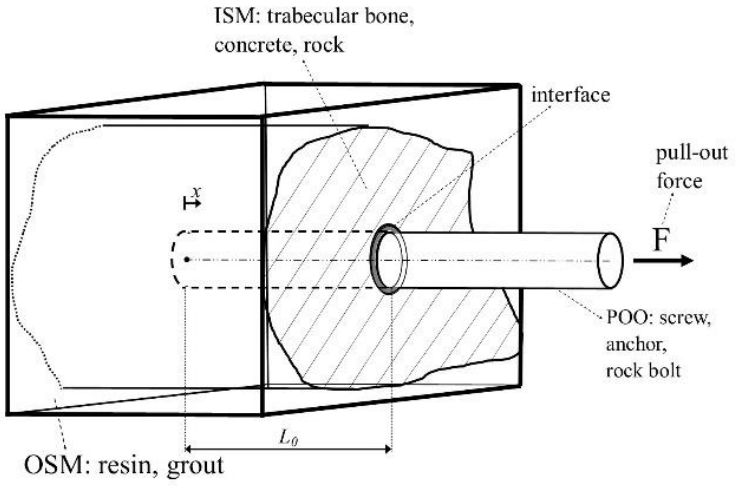

Figure 3.1. Characteristics and components of pull-out tests

3.1 Experimental apparatus and test procedures

3.1.1 Sample preparation and mechanical testing protocol

For the spine, see Figure 3.2, we obtained 13 human lumbar vertebrae (L1-L5) from 5 donors who had written consent for their organs to be used in research and teaching (Table 3.1). The donors were aged between 50 and 67 years. The vertebrae used were free of metastatic or bone disease. According to their BMD measured by qCT scan, 5 were classified as normal, 5 as osteopenic, and 4 as osteoporotic. The soft tissues surrounding the vertebrae were removed and the intervertebral disc was cut to separate the vertebrae of interest from the entire spine. The vertebra was placed in a customised metal mould box (Figure 3.2A) so that the extraction force was perpendicular to the coronal plane; see Figures 3.3 and 3.4. The mould was then filled with low viscosity Araldite epoxy resin (RENCAST, FC53 POLYOL, ISOCYANATE) (Figure 3.2B). This study aims to perform a pull-out test on trabecular bone. Therefore, the specimen

was prepared by cutting the pedicle and lamina from the vertebral body as shown in Figure 3.2C. The embedded specimen was pre-drilled to a depth of 25 mm using a 1.6 mm [120], which is similar to the 20 mm depth recommended by ASTM F543 [121] (Figure 3.2D). We used two specialized pedicle screws (Icotec VADER, BlackArmor, Altstätten, Switzerland). The screws are designed with several features: They are polyaxial, which means that the head of the screw is spherical and enclosed in a casing that allows the screw to move along several different axes relative to the casing. Therefore, there is no torque transmission at the head of the screw. The screws also have a hollow center (cannulated) and contain openings (fenestrated). They are made from a durable material called carbon fiber-reinforced PEEK. Each screw is 45 mm long with an external thread diameter of 6.5 mm and an elastic modulus of E=18 GPa [122]. The inner hollow diameter d^i measures 3.7 mm and the inner thread diameter $d^{thr,i}$ measures 4.8 mm. The average thread diameter is therefore $d^{thr} = \frac{d^{thr,o}+d^{thr,i}}{2} = 5.65$ mm (see Figure 3.5). After placing the K-wire in the bone (Figure 3.2D), we inserted each screw to a depth of 30 mm (Figure 3.2E).

Table 3.1. Donor Demographics

Donor number	*Bone classified*	*Age (y)*	*Sex*	*BMD (mg/ccm)*	*Level*
1	Normal	50	Male	148.59	L4/713
2	Normal	54	Female	144	L1/721
3	Normal	50	Male	154.84	L5/713
4	Normal	67	Male	123.8	L1/302
5	Normal	67	Male	226.1	L2/302
6	Osteopenic	67	Male	84.32	L3/302
7	Osteopenic	67	Male	87.53	L4/302
8	Osteopenic	67	Male	101.37	L5/302
9	Osteopenic	56	Male	105.31	L5/318
10	Osteoporotic	59	Male	32.6	L3/978
11	Osteoporotic	59	Male	23.4	L4/978
12	Osteoporotic	59	Male	43.44	L5/978
13	Osteoporotic	56	Male	78.3	L4/318

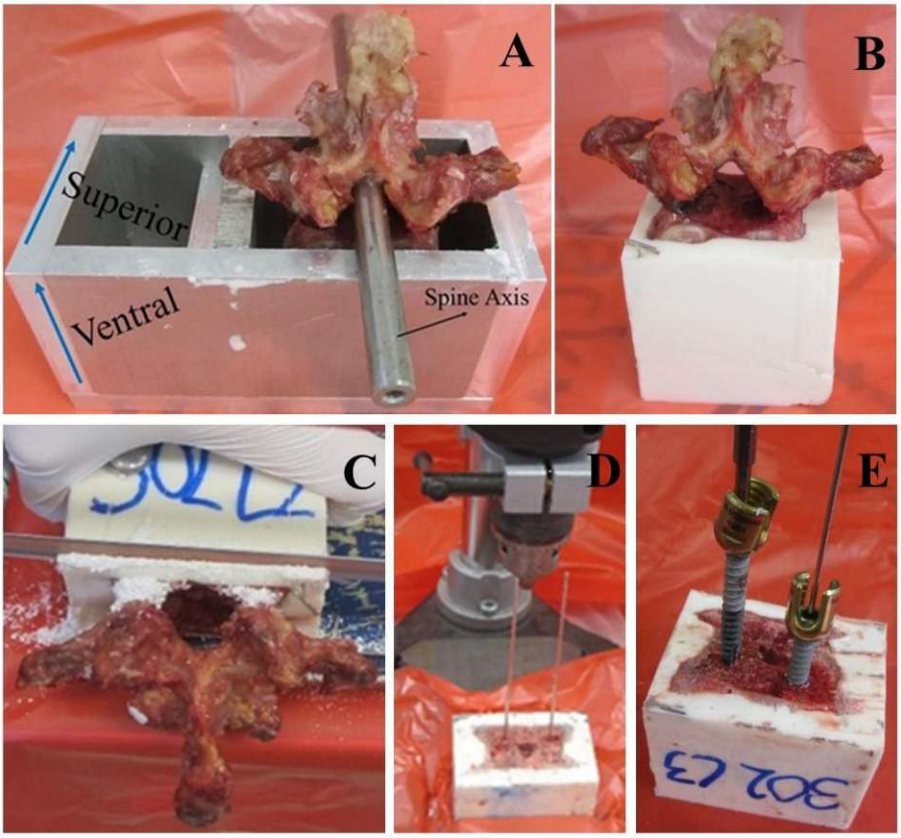

Figure 3.2. Images illustrating the stepwise preparation of a pull-out test sample for biomechanical analysis. (A) Metal embedding model showcasing the simulated anatomical structure. (B) Specimen after embedding. (C) Precision cutting of pedicle and lamina parts to create a defined region for testing. (D) Guide wire insertion to clear the pathway and visualize the intended hole direction. (E) Progressive stages of pedicle screw insertion, a critical step in securing the sample for subsequent biomechanical testing

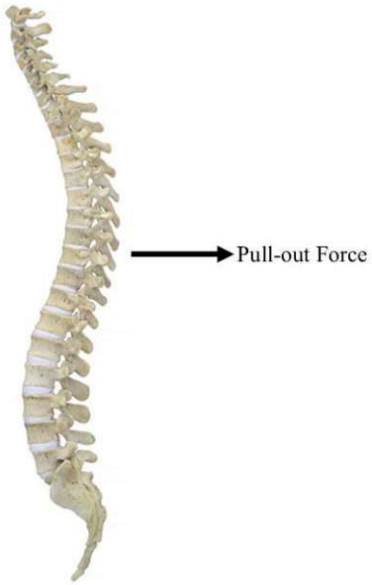

Figure 3.3. Spinal column, with the direction of the pull-out force acting on the lumbar

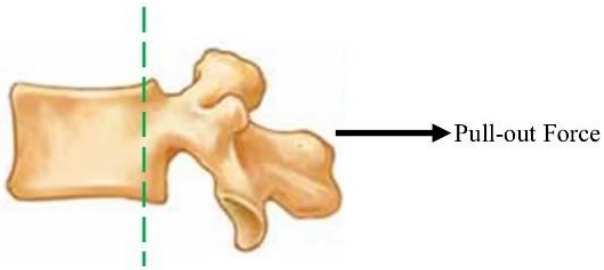

Figure 3.4. Pull-out force direction, orthogonal to coronal plane

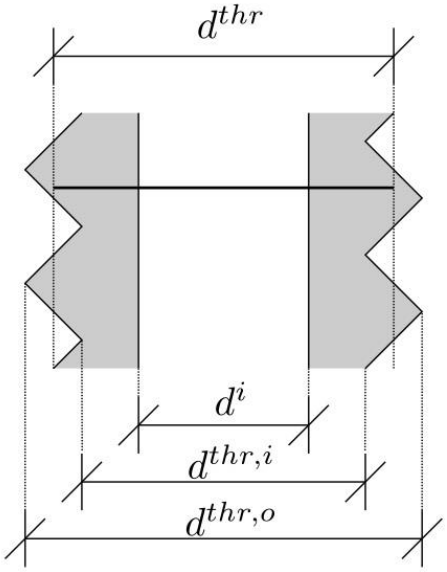

Figure 3.5. Screw diameters: Outer thread diameter $d^{thr,o}$, inner thread diameter $d^{thr,i}$, inner hollow diameter d^{i} and average thread diameter d^{thr}

The pull-out test, based on the ASTM F543 standard [121], was performed using a MTS-858 Mini Bionix ll testing machine, axial torsional, tabletop servo hydraulic system, USA, see Figure 3.6. After placement of the pedicle screw in the vertebrae, the pedicle screw was positioned parallel to the load hook, and the load was set to zero. A displacement control mode was implemented with a 5 mm/min displacement rate. Load-displacement data were recorded at a rate of 50 Hz, starting with a preload of 10 N. The pull-out force versus displacement was recorded for each test case and data acquisition continued until the screw was completely pulled out. We define pull-out stiffness (S_{slope}) as the slope of the linear elastic part of the force-displacement curve. Peak pull-out force (PPF) (F_{peak}) and peak pull-out displacement (PPD) (d_{peak}) were evaluated for all specimens.

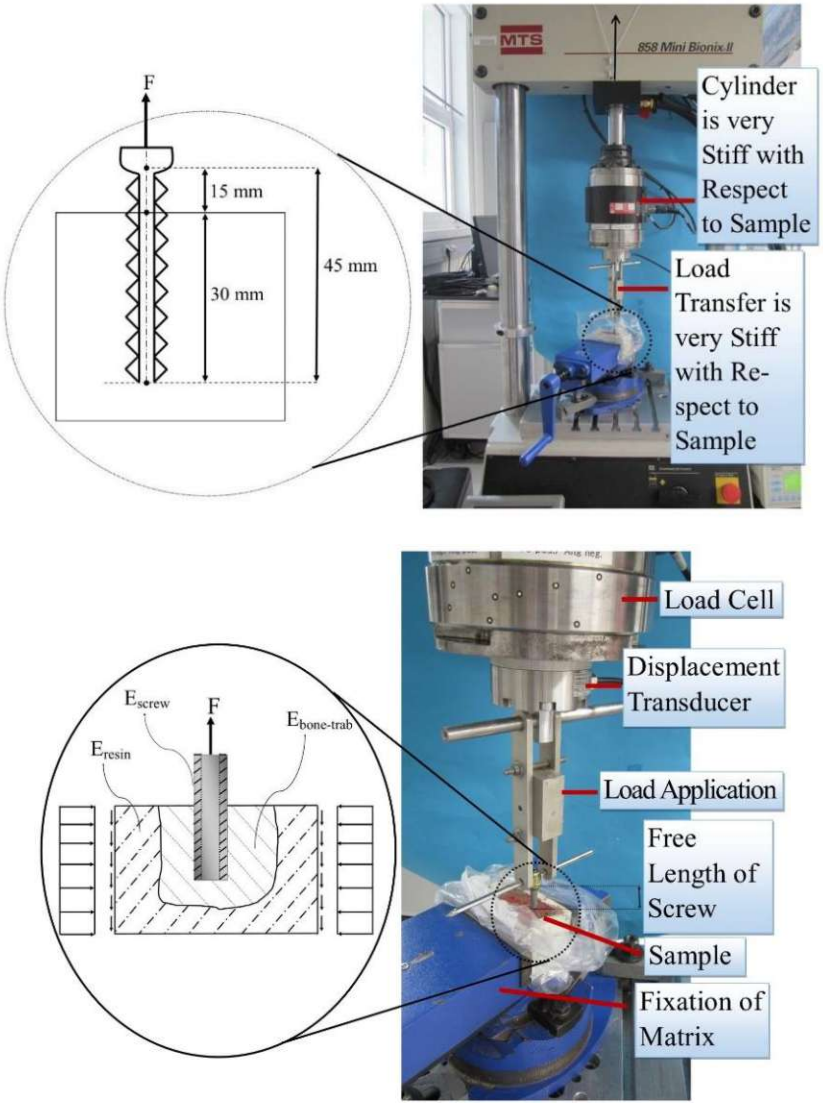

Figure 3.6. photographs of the testing device together with screw dimensions and integrated mechanical system pull-out Performance

3.1.2 Micro-CT imaging and morphometric analysis

The standard method for the quantitative description of bone architecture is the calculation of morphometric indices, also referred to as quantitative morphometry. Historically, the microarchitectural characteristics of trabecular and cortical bone have been studied by examining 2D sections of bone biopsies combined with the calculation of morphometric parameters using stereological methods. While some measurements, such as BV/TV and Bone Surface-to-Volume Ratio (BS/TV), can be obtained directly from 2D images, several key parameters, including trabecular thickness (Tb.Th), trabecular separation (Tb.Sp), and trabecular number (Tb.N), are derived indirectly after assuming a fixed structure model, such as a rod-like or plate-like structure. These highly idealized models can be viewed as two ends of a spectrum in which the real architecture is a mixture of both rods and plates, with the exact composition varying by skeletal location, disease state, treatment, and age. Thus, the

correlations between Tb.Th, Tb.Sp, and Tb.N measurements made using 2D methods that require assumptions about the underlying structure and 3D model-independent measurements of these parameters are modest and vary with skeletal location. Therefore, deviations in the trabecular structure from the assumed plate or rod models will lead to unpredictable errors in the indirectly derived parameters. For this reason, and to take full advantage of volumetric measurements, it is recommended that 3D model-independent algorithms be used to calculate trabecular bone microarchitecture from µCT images [123].

Micro-computed tomography (µCT) has become an essential tool for analysing the three-dimensional structure of bone, particularly the microarchitecture of trabecular bone found in the femur, vertebrae, and calcaneus. This interconnected network of calcified rods and plates plays a crucial role in bone strength, as bone loss often occurs in the trabecular regions, particularly in areas such as the axial spine, forearm, hip, and heel. The reduction in oestrogen associated with menopause is a significant factor in this loss. Researchers have focused on investigating the scale, topological, and geometric properties of trabecular bone, using parameters such as bone volume fraction (BV/TV [%]) is the ratio of the segmented bone volume to the total volume of the region of interest, trabecular thickness (Tb.Th [mm]) is the mean thickness of the trabeculae, trabecular separation (Tb.Sp [mm]) is the trabecular spacing as a parameter of the mean distance between each single trabecula and trabecular number (Tb.N [1/mm]), is the number of trabeculae per volume as a structural parameter. to characterise its microstructure and mechanical properties. Micro-computed tomography (µCT) allows the visualization of three-dimensional (3D) structures and is widely used to evaluate bone quality and morphology in small animals under physiological and pathological conditions. µCT analyses are useful for evaluating the fine structure of bone/cartilage mineral components, particularly in the field of bone and cartilage research [124].

Central dual-energy x-ray absorptiometry (DXA) of the lumbar spine and proximal femur is the preferred method for testing bone mineral density (BMD). Despite the fracture risk statistics, osteoporosis testing with DXA remains underutilized [125] [126]. However, BMD can also be assessed with other radiologic imaging tools, such as quantitative computed tomography (qCT), which may be available when access to DXA is limited [127]. Originally, qCT was developed using thick (approximately 10 mm) CT image slices angled to scan the vertebrae and avoid the cortical endplate. However, this method has been largely superseded using volume images covering regions of interest at the spine or hip. For patients undergoing CT colonography (CTC) screening, there is a potential opportunity for concurrent BMD

screening with qCT without additional imaging, radiation exposure, or patient time [128]. In addition, there are several indications for CT imaging where there is a large overlap between the need for a CT scan and patients with risk factors for osteoporosis. By using the volume-based qCT methodology rather than the older single-slice protocols, these CT images can also be used for BMD measurement by qCT [129] [130]. Such dual use of CT images could increase screening rates or obviate the need for DXA screening in some individuals. Previous studies combining standard CT and qCT have generally focused on BMD measurement at the lumbar spine [131] [132], for which qCT provides a volumetric BMD measure of the trabecular vertebral bone in isolation. This may have the advantage of superior sensitivity due to the higher turnover rate of trabecular bone [133], but qCT T-scores are on average somewhat lower than DXA T-scores for the same age, and the established World Health Organization (WHO) classification of osteoporosis by DXA T-score is not appropriate [134].

Quantitative computed tomography (qCT) and micro-computed tomography (micro-CT) were used at different stages to assess bone quality and structure. Each method serves a different purpose, with qCT used before pedicle screw implantation to classify bone quality and micro-CT used after implantation for detailed analysis of the trabecular bone around the screw.

The main contribution of the current approach is to propose a thresholding technique for image binarisation that exploits the fusion of topological and geometric information. In computed tomography (CT) imaging, different grey levels correspond to specific material densities, so thresholding techniques have been widely used in bone image segmentation [135][136][137][138][139][140]. The key challenge in thresholding is to identify an appropriate threshold to effectively separate bone from other materials. In the present study, after screw insertion, the vertebrae were scanned using a micro-computed tomography (µCT) scanner (Scaco MEDICAL, XtremeCT ll-HR-pQCT, scanco GmbH, Brutisellen, Switzerland). The µCT scan settings were configured as follows: 68 kV, 1460 µA, with a resolution of 61 µm voxel size. Bone morphometric analysis was performed on a specific area around the screw taken from a series of greyscale reconstructed micro-CT images (using µCT Ray version 4.2 software). This area referred to as the volume of interest (VOI) and shown in the image, included both the trabecular bone and the pedicle screw. The images were converted to binary form using a global thresholding technique. The µCT Ray software was then used to calculate various morphometric parameters within the VOI, including bone volume fraction (BV/TV, expressed as a percentage), trabecular thickness (Tb.Th, measured in millimeters), trabecular separation (Tb.Sp, measured in millimeters) and trabecular number (Tb.N, expressed in mm).

3.1.2.1 A Dual-Segmentation Approach for Micro-CT Analysis and Finite Element Simulation of Pedicle Screw Pull-Out in Vertebral Bone

The vertebral body was scanned with a micro-CT (Scaco MEDICAL, XtremeCT ll-HR-pQCT, scanco GmbH, Brutisellen, Switzerland). Materialise Interactive Medical Image Control System (Mimics) is one of the latest image processing software developed by Materialise NV, a Belgian company specialising in additive manufacturing software and technology for the medical, dental and other industries. Mimics is an image processing software for 3D design, 3D surface modelling, 3D measurement and image stack analysis of any 2D image data (e.g., CT, µCT). In this study, two different segmentation approaches were applied to micro-CT scans of vertebral bodies with implanted pedicle screws to support finite element (FE) simulation and volumetric analysis. The first segmentation method included the entire vertebral body to produce accurate 3D models for FE simulation of the pull-out test. This process was completed in Mimics software, where key structures - including the cortical shell, cancellous bone, and screw holes - were isolated. A surface mesh file was then generated from the segmented images and exported as an STL file, which was then imported into CAD software to convert from a surface mesh to a volume mesh, enabling the creation of a 3D volume mesh, which is critical for accurate FE analysis.

In the second segmentation step, a bone subtraction technique was applied within the micro-CT imaging process to isolate the vertebral bone directly contacting the pedicle screw. This involved selective removal of the pedicle screw hole, which allowed the precise calculation of the contact volume between the screw and the surrounding bone. Bone subtraction in micro-CT imaging enhances the clarity of both visual representations and measurements of bone contact features, making it particularly useful for assessing the fine architecture and spatial variations of bone at the screw-bone interface. To define the volume of trabecular bone in contact with the pedicle screw, a 7 mm diameter circle was drawn around the screw, including the 5.5 mm screw diameter plus an additional 1.5 mm surrounding area. This 1.5 mm buffer corresponds to approximately two pixels in the micro-CT scan, where each pixel measures 0.0607 mm. By expanding the region in this way, a cylindrical model representing the trabecular bone surrounding the screw was created, allowing an accurate calculation of the total bone volume around the implant. As part of this step, the bone volume fraction (BV/TV) at the bone-screw interface was also evaluated. This parameter provides an important insight into the local bone density and architecture influencing mechanical fixation. However, it is important to note that micro-CT-derived parameters, including BV/TV, are not representative of the whole trabecular structure of the vertebrae, especially considering the variation in bone mineral

density throughout the vertebral body. Instead, these measurements specifically reflect the localized region of trabecular bone in direct contact with the screw and should be interpreted within this limited context.

BMD was determined from the standard qCT scan using a calibration phantom (EFP) prior to sample selection. Vertebrae with BMD greater than 120 mg/cm^3 were classified as normal, those with BMD between 80-120 mg/cm^3 were classified as osteopenia, and vertebrae with BMD less than 80 mg/cm^3 were classified as osteoporosis (Table 3.2) [141].

Table 3.2. Approximate Spine QCT Diagnostic Categories of WHO DXA Guidelines

QCT Trabecular Spine BMD Range	*Equivalent WHO Diagnostic Category*
BMD$>120\ mg/cm^3$	Normal
$80\ mg/cm^3 \geq BMD \leq 120\ mg/cm^3$	Osteopenia
BMD$< 80\ mg/cm^3$	Osteoporosis

The above categories were derived by selecting thresholds that would result in approximately the same proportion of the population being assigned to a particular category based on QCT spine T-score as would be assigned based on QCT hip T-score. Numbers for the spine would also be similar to DXA spine T-scores. The use of T-scores has been avoided in this categorisation to emphasise the fact that qCT spine T-scores and hip T-scores are often different. Assigning a WHO diagnostic category based on a qCT spine T-score may overestimate a patient's fracture risk [141]. To segment the micro-CT scans, a 7 mm diameter circle was drawn around the screw. This was done to determine the volume of trabecular bone in contact with the pedicle screw. The chosen diameter included 5.5 mm for the screw and the remaining 1.5 mm for the surrounding area of the screw, corresponding to two pixels from the micro-CT scans. (Each pixel is 0.75 mm). To obtain the total bone volume around the screw, the circle was extended to encompass the entire screw, resulting in a cylindrical representation of the trabecular bone in contact with the screw.

3.2 Statistical analysis

The bone mineral density (BMD) of each vertebral body was measured by quantitative computed tomography (qCT). In this study, BMD and bone quality (categorized as normal, osteopenic, and osteoporotic) were considered as independent variables, while peak pull-out force (PPF) was treated as the dependent variable. Linear regression analysis assessed the relationship between BMD, BV/TV, and PPF and PPD. This statistical approach helps to determine how changes in BMD, BV/TV affect PPF and PPD, and whether there is a significant

correlation between these variables. In addition, PPF values were compared between different bone quality groups (normal, osteopenic, and osteoporotic). This test evaluates whether there are statistically significant differences between the PPF values of the three bone quality groups. All statistical analyses were performed using Microsoft Excel 2024 (Microsoft Corp., Redmond, WA, USA). A p-value of less than 0.05 was considered statistically significant, indicating that differences observed between groups were unlikely to be due to random variation alone. Data are presented as means and standard deviations (SDs).

3.3 FE modeling

In this study, we performed micro-CT imaging of vertebral trabecular bone and performed segmentation to analyze its topological and geometric properties, including bone volume fraction (BV/TV), trabecular thickness, and other key parameters. Our approach followed a dual segmentation method aimed at both quantifying trabecular bone properties and creating models for finite element (FE) simulation of pedicle screw extraction. However, due to limitations in scan resolution, we faced challenges in directly using the micro-CT scans for FE analysis. In addition, the available software and hardware were not powerful enough to handle the computational demands of micro-CT-based simulations.

To overcome these challenges, we decided to use alternative CT scans of trabecular vertebral bone. These scans were segmented, and their structural properties were analyzed. We then incorporated key micro-CT-derived parameters, such as BV/TV, into the FE model to ensure that the simulations reflected the microstructural characteristics of trabecular bone. This approach allowed us to proceed with the FE analysis despite limitations in scan resolution and computational resources, ensuring that the study remained methodologically robust while maintaining biomechanical relevance.

Since we prepared the experimental model without the pedicle side, the corresponding FE model was also designed by removing the pedicles, leaving only the vertebral body. This decision was in line with the objective of the study, which focused specifically on the mechanical behavior of trabecular bone. Furthermore, the experimental specimens were prepared without the cortical bone in the posterior wall, and accordingly, the FE model was constructed as a homogenized representation of trabecular bone only. This allowed a consistent comparison between the experimental and numerical results and ensured that the simulation results reflected the mechanical contribution of the trabecular architecture without interference from the surrounding cortical structures.

3.3.1 Geometry and Mesh

Three-dimensional FE models were created from lumbar spine CT images (resolution of $0.8 \times 0.8 \times 1$ mm) of two healthy young individuals aged 21 and 29 years. Although the specific BMD values for these individuals were not available, Ebbesen et al. [142] indicate that the typical BMD for this age group is between 0.8 and 0.9 g/cm^2. These CT datasets have previously been used in several master's theses and research publications by Prof. Navid Arjmand and his biomechanics research group at Sharif University of Technology, Iran, as part of various projects related to spinal biomechanics. The CT scan machine was a Siemens Emotion 16, with a kilovoltage peak (kVp) of 130 kV and a total exposure of ~600 s (Figure 3.9A). Mimics carried out bone segmentation to generate the models (Research 19, Materialise, Leuven, Belgium). Mimics software used a predefined threshold to segment cancellous (predefined threshold range of 148-661 HU). When required, manual segmentation techniques were implemented (Figure 3.9B) [143] [144].

One of the most important steps in the preparation of a finite element (FE) model is the use of computer-aided design (CAD) software to refine the geometry, insert screws, and generate an appropriate mesh. In this project, 3-Matic (Research 11, Materialise, Leuven, Belgium) was used to refine the geometry of the vertebral body (Figure 3.7), implant the pedicle screw, and generate the mesh required for FE simulation.

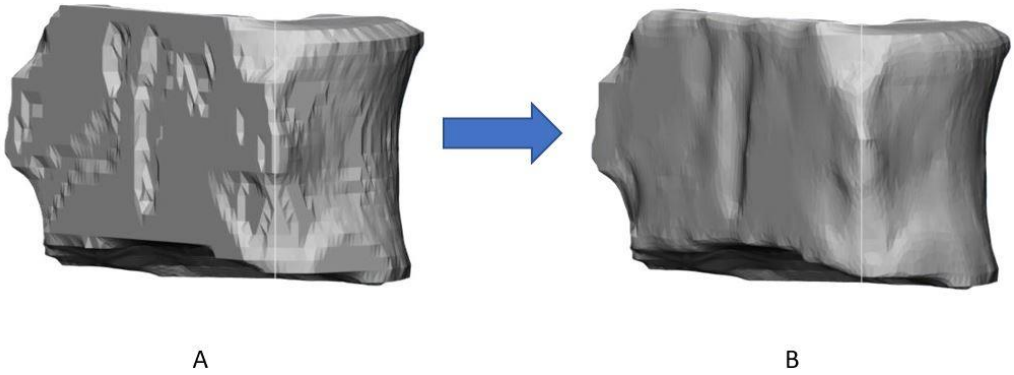

Figure 3.7. Geometry refinement process in 3-Matic: (A) Initial coarse geometry before refinement, (B) smoothed and refined geometry after processing

Posterior elements such as the spinal pedicles and spinous processes were removed using 3-Matic to isolate the vertebral body for analysis. A pedicle screw with a length of 45 mm, diameter of 6.5 mm, pitch of 2.5 mm, helix angle of 23°, and thread angle of 74° was inserted into each vertebra. This was achieved by a Boolean subtraction operation that allowed precise placement of the screw while ensuring a small gap of 0.05 mm between the screw and the surrounding bone (Figure 3.9C). The screw trajectory and placement were modeled to match

the experimental setup and anatomical positioning as closely as possible. After geometric preparation, the vertebral body and screw were meshed. The initial meshing process in 3-Matic produced a surface mesh consisting of triangular elements defining only the outer boundaries of the structures (Figure 3.8A). While suitable for visualization, this surface mesh does not contain any information about the interior of the model and is, therefore, not sufficient for FE simulation. To enable mechanical analysis in ABAQUS, the surface mesh was converted into a volume mesh (Figure 3.8B). This was done using 3-Matic's Volume Meshing tool, which fills the space inside the surface mesh with tetrahedral elements, creating a 3D solid mesh. This volume mesh is essential to accurately calculate the internal stress and strain distributions during the pull-out simulation. It also allows for the correct assignment of material properties, interaction definitions, and boundary conditions throughout the model.

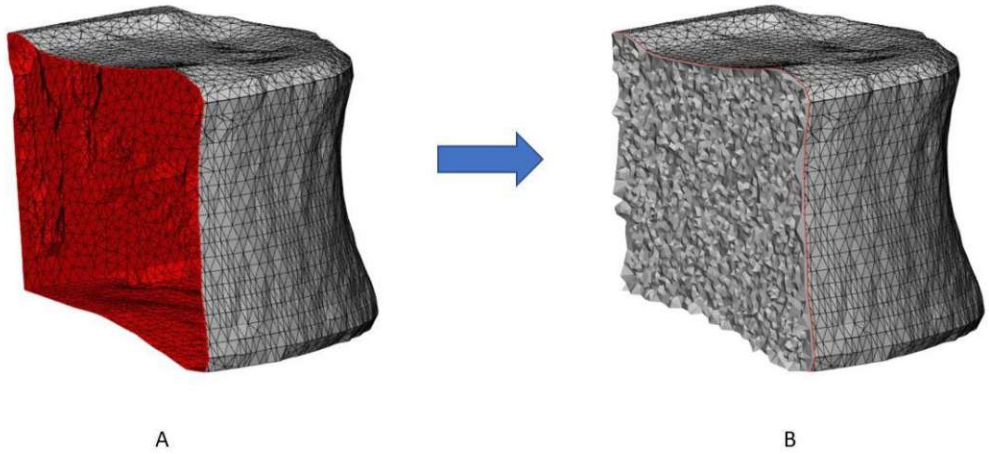

Figure 3.8. Mesh generation process in 3-Matic: (A) surface mesh of the vertebral model, (B) volume mesh created for FE analysis

Each part was meshed and imported into Abaqus (Dassault Systèmes, Vélizy-Villacoublay, France). Tetrahedral elements (specifically C3D4 elements in ABAQUS) were chosen for meshing the vertebrae and screw assembly because of their distinct advantages in modeling complex anatomical geometries. One of the main reasons for using tetrahedral mesh is its ability to conform to irregular and intricate shapes, which is particularly important in biomechanical modeling where anatomical structures, such as vertebrae, have highly detailed and curved surfaces. C3D4 tetrahedral elements were used to mesh the models, with approximately 1,830,000 elements for each vertebra and 168,000 rigid elements for each screw. The average size of each element was 1 mm, and the elements around the screw-bone contact area were further refined to 0.3 mm to improve accuracy in this critical region (Figure 3.9D). Tetrahedral elements also allow for automatic and efficient meshing, making them ideal for geometries reconstructed from medical imaging (e.g., CT or micro-CT) where manual meshing

is impractical. Although linear tetrahedral elements (C3D4) may be less accurate than higher order elements in some scenarios, their lower computational cost, local mesh refinement capability, and ease of generation make them a practical and effective choice for finite element models involving complex biological tissues.. [120] [145] [146] [147] [118] [148].

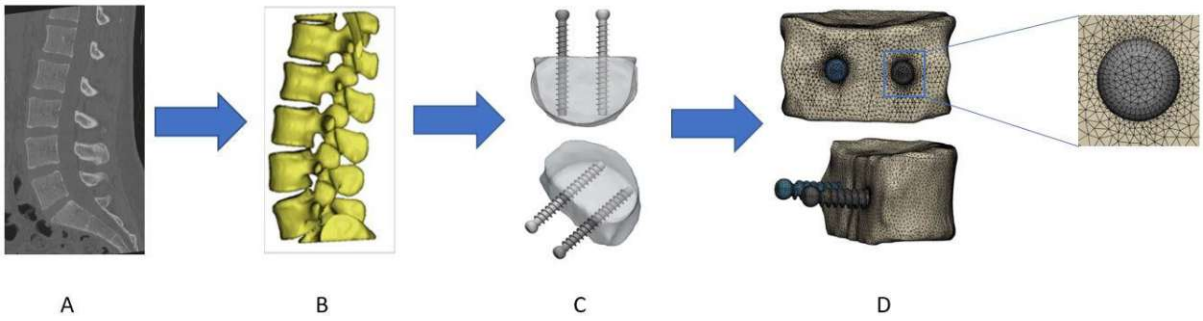

Figure 3.9. A representation of A) raw CT-scan image, B) constructed 3D geometry, segmentation, and smoothing, C) Boolean operation, D) meshing the models

3.3.2 Material Properties

Each vertebra of each subject was modeled using homogeneous elastoplastic materials. The mechanical properties of the cancellous bone tissue were determined from the volume fraction converted to apparent density. This process involved converting BV/TV values to bone apparent density (AD) values, which were then used to derive mechanical properties such as Young's modulus (E) (Table 3.3). The equations for converting apparent densities to mechanical properties (Young's modulus and post-yield behavior) were based on regression equations derived from mechanical tests (compression or tension) performed on different bone specimens with different apparent densities [149] [150] [151] [152]. To account for cortical bone topology, voxels with HU values greater than 500 HU (or a density of 0.6 g/cm^3) were modeled as homogeneous [153].

Table 3.3. Material relationship in the FE simulations

Mechanical Property	*Relations*	*Reference(s)*
Apparent density ($^{g}/_{cm^3}$)	$0.6\frac{BV}{TV}$	[153]
Elastic modulus (MPa)	$E = 4730(Apparent\ density)^{1.56}$	[152] [154]
Yield stress (MPa)	$\sigma_y = 32.6(Apparent\ density)^{1.6}$	[151]
Ultimate stress (MPa)	$\sigma_u = 33.2(Apparent\ density)^{1.53}$	[151]

3.3.3 Interface, boundary conditions, and loading

A general contact model was used for the interface between the screw threads and the threaded hole in the vertebra. The tangential coefficient of friction was set to 0.2 while considering hard contact at the interface [120] [145]. To simulate the pull-out test, an outward axial displacement was applied to the reference point along the longitudinal axis of the screw using a smooth step amplitude (Figure 3.10) [155]. The boundary conditions were in the form of clamps on the superior and inferior shells of the vertebral body (top and bottom of the vertebral body) (Figure 3.10). All nodes on the rigid screw were coupled to a reference point placed on the head of the screw. The loading rate, defined by the ASTM organization [121], has a minimal effect on the predicted pull-out force in low-loading rates [120]. A loading of 0.5 mm/s was considered for simulations. Explicit solver simulations were utilized with a strain-based damage model to accurately simulate bone fractures [151].

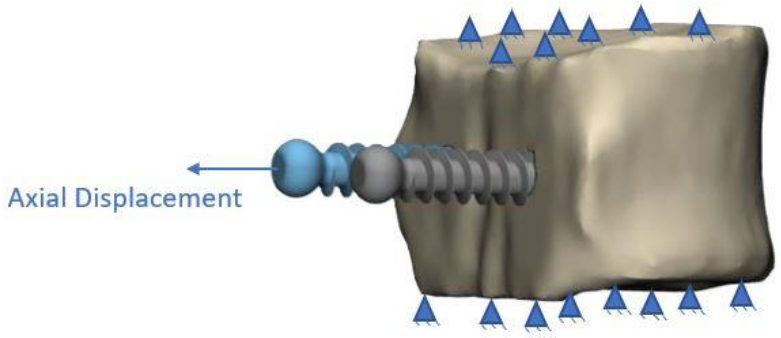

Figure 3.10. Boundary condition and loading

Tables 3.4 and 3.5 show the material properties of bone and pedicle screws used in the study. The bone model was then imported into ABAQUS to calculate the parameters.

Table 3.4. Material properties of the trabecular bone model and pedicle screw (left side) [122] [156]

Property	*713_L4 (Normal)*	*302_L4 (Osteopenic)*	*318_L4 (Osteoporotic)*
Cancellous bone Density (gcm^{-3})	0.17202	0.0777	0.04926
Cancellous bone Young's Modulus (MPa)	303.64	87.88	43.16
Cancellous bone Poisson's ratio	0.25	0.25	0.25
Pedicle screw Density (kg/m^3)	15000	15000	15000
Pedicle screw Young's Modulus (MPa)	18000	18000	18000
Pedicle screw Poisson's ratio	0.4	0.4	0.4
Yield strength (MPa)	1.95	0.54	0.26
Ultimate Strength (MPa)	2.24	0.66	0.33
Ultimate Strain	0.00807	0.00827	0.00839

Table 3.5. Material properties of the trabecular bone model and pedicle screw (right side)

Property	*713_L4 (Normal)*	*302_L4 (Osteopenic)*	*318_L4 (Osteoporotic)*
Cancellous bone Density (gcm^{-3})	0.18132	0.08736	0.06126
Cancellous bone Young's Modulus (MPa)	329.63	105.51	60.65
Cancellous bone Poisson's ratio	0.25	0.25	0.25
Pedicle screw Density (kg/m^3)	15000	15000	15000
Pedicle screw Young's Modulus (MPa)	18000	18000	18000
Pedicle screw Poisson's ratio	0.4	0.4	0.4
*Yield strength (*MPa*)*	2.12	0.65	0.37
*Ultimate Strength (*MPa*)*	2.43	0.79	0.46
Ultimate Strain	0.00806	0.00824	0.00833

4. Results and Discussion

The process of inserting and removing two pedicle screws to evaluate the pedicle screw pull-out test was successfully performed in all 13 vertebrae that were part of this study. The data collected was categorized into three different groups: normal, osteopenic, and osteoporotic. Firstly, one sample was selected from each group and graphs were plotted for the pull-out test. Secondly, the mean pull-out test data were calculated separately for each group. Tables 1, 2, and 3 show the pull-out test results for each group.

4.1 Understanding Pull-Out behavior: Test Findings and Implications

Figures 4.1 to 4.3 illustrate the pull-out test results of the three different groups of left- and right-side screws. These data illustrate a linear elastic behaviour of the specimens up to the peak load for trabecular bone. The value measured by the load cell and linear transducer sensor was plotted on a load-displacement curve. The load-displacement curves were analysed for each screw and this curve was used as the basis for calculating three main parameters: peak pull-out force (PPF), linear domain stiffness (S_{slop}), peak pull-out force-displacement (PPD). PPF (N) was determined as the maximum axial force achieved before disengaging from the bone. Linear stiffness (N/mm) is usually quantified by the slope of the initial linear portion of the force-displacement curve obtained during a pull-out test. The stiffness in the linear domain is calculated from the peak force and peak displacement. Values for bone samples with normal BMD are shown in (Table 4.1). Hereby the first screw pulled out was the left and the second one the right.

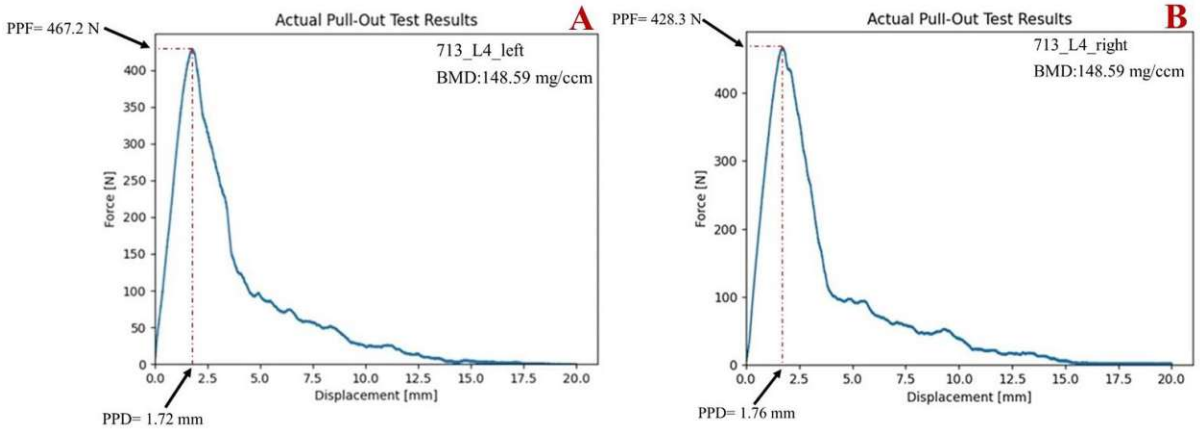

Figure 4.1. Diagram of experimentally measured pull-out force vs. displacement. (A)first screw (left side) for carbon-fiber-reinforced PEEK pedicle screw. (B) second screw (right side) for carbon-fiber-reinforced PEEK pedicle screw, normal bone

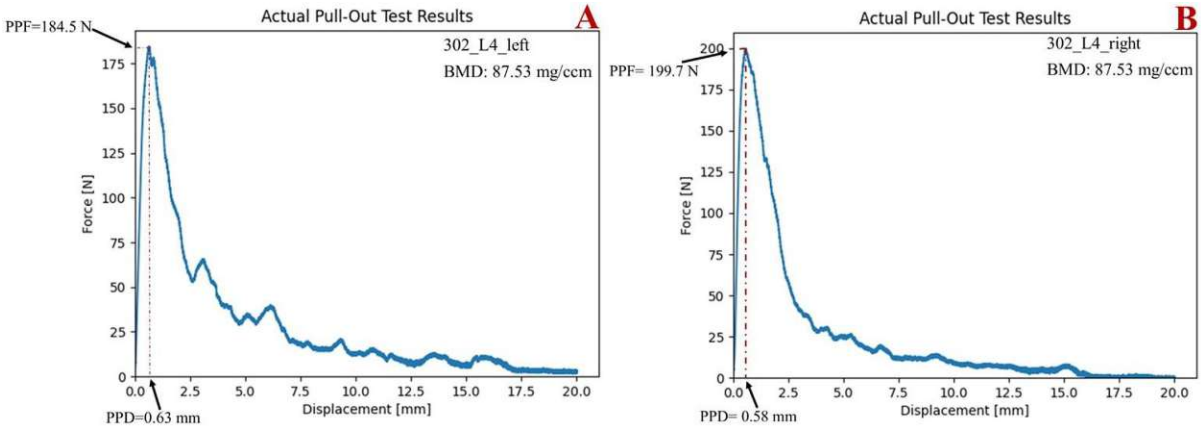

Figure 4.2. Diagram of experimentally measured pull-out force vs. displacement. (A) first screw (left side) for carbon-fiber-reinforced PEEK pedicle screw, Osteopenic Bone (B) second screw (right side) for carbon-fiber-reinforced PEEK pedicle screw, Osteopenic Bone

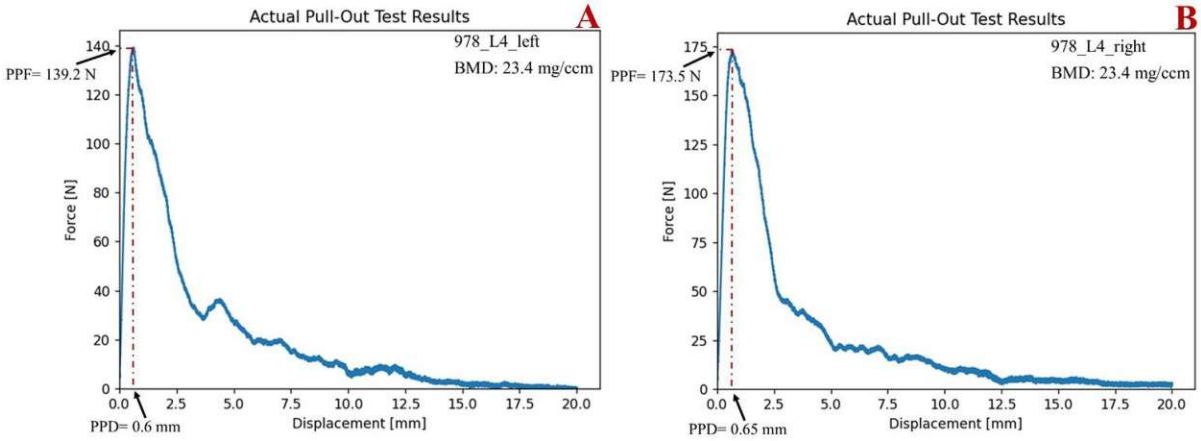

Figure 4.3. Diagram of experimentally measured pull-out force vs. displacement (A) first screw (left side) for carbon-fiber-reinforced PEEK pedicle screw, Osteoporotic Bone (B) second screw (right side) for carbon-fiber-reinforced PEEK pedicle screw, Osteoporotic Bone

Table 4.1. Parameters directly identified from pull-out force vs. displacement plots for the left and right screws in the L4 vertebrae of samples 713, 302, and 978

	Side	*BMD (mg/cm³)*	*S_{slope}(N/mm)*	*PPD (mm)*	*PPF(N)*
713_L4	Right	148.59	181.41	1.72	467.2
713_L4	Left	148.59	196.46	1.76	428.3
302_L4	Right	87.53	43.25	0.58	199.7
302_L4	Left	87.53	38.89	0.63	184.5
978_L4	Right	23.4	43.65	0.65	173.5
978_L4	Left	23.4	36.07	0.6	139.2

Based on the pull-out test, the 13 lumbar vertebrae were stratified into three groups: normal, osteopenic and osteoporotic. The mean PPF values for the subjects were normal left (548.85 N) and right (341.9 N), osteopenic left (187.4 N) and right (200.2 N), osteoporotic left (152.5

N) and right (155.9 N). The other mean values of the pull-out tests are also shown in Tables 4.2-4.4.

Table 4.2. mean Parameters directly identified from pull-out force vs. displacement plots for the left and right screws in the vertebrae of normal samples

	Side	*BMD* (mg/cm^3)	$S_{slope}(N/mm)$	*PPD (mm)*	*PPF (N)*
Normal Group	Left	159.4	196.1	2.8	548.8
Normal Group	Right	159.4	125.1	1.2	341.9
S.D	---	---	50:2	1.13	146.3

Table 4.3. mean Parameters directly identified from pull-out force vs. displacement plots for the left and right screws in the vertebrae of osteopenic samples

	Side	*BMD* (mg/cm^3)	$S_{slope}(N/mm)$	*PPD (mm)*	*PPF (N)*
Osteopenic Group	Left	94.6	46.6	0.8	187.4
Osteopenic Group	Right	94.6	51.9	0.7	200.2
S.D	---	---	3.74	0.07	9.05

Table 4.4. mean Parameters directly identified from pull-out force vs. displacement plots for the left and right screws in the vertebrae of osteoporotic samples

	Side	*BMD* (mg/cm^3)	$S_{slope}(N/mm)$	*PPD (mm)*	*PPF (N)*
Osteoporotic Group	Left	44.4	51.5	1.1	152.5
Osteoporotic Group	Right	44.4	47.4	1.1	155.9
S.D	---	---	2.89	0	2.4

The pull-out test results presented here provide valuable insights into the mechanical behavior of pedicle screws in trabecular bone across different bone quality conditions. By analyzing peak pull-out force (PPF), linear stiffness, peak pull-out displacement (PPD), and bone mineral density (BMD), we can better understand the impact of bone quality on the stability of screw fixation in vertebral bodies.

4.2 Understanding Pull-Out Behavior: Discussion and key Takeaways

4.2.1 Peak Pull-Out Force (PPF)

- The results demonstrate a clear trend in PPF across different bone quality groups, with the normal bone group exhibiting the highest mean PPF values, followed by the osteopenic and osteoporotic groups. For example, the mean PPF in the normal bone group was 548.85 N (left side) and 341.9 N (right side), compared to 187.4 N (left) and 200.2 N (right) in osteopenic bones, and 152.5 N (left) and 155.9 N (right) in osteoporotic bones.

- This trend is consistent with the expected relationship between bone quality and screw fixation strength: bones with higher mineral density (normal group) provide greater resistance to axial loads, leading to higher peak forces before failure. Conversely, lower BMD in osteopenic and osteoporotic bones leads to reduced anchorage, which limits the load the screw can withstand before pulling out.
- The reduction in PPF in the osteopenic and osteoporotic groups suggests that these bone conditions may not provide adequate fixation strength for pedicle screws, raising concerns about stability in clinical applications, especially for osteoporotic patients.

4.2.2 Bone Mineral Density (BMD) and Its Influence

- BMD values align well with the observed PPF results. The normal bone group has the highest BMD (159.4 mg/cm³), while the osteopenic and osteoporotic groups have significantly lower values (94.6 mg/cm³ and 44.4 mg/cm³, respectively).
- The relationship between BMD and PPF suggests that bone mineral density is a key predictor of pull-out strength. This correlation supports the use of BMD as a parameter for preoperative planning and patient selection in orthopedic surgeries, as it directly impacts screw stability.
- Additionally, the symmetrical BMD values between left and right screws within each bone quality group provide consistency and suggest that any differences in PPF between left and right screws are not due to BMD but may be due to anatomical variations or slight differences in screw insertion technique.

4.2.3 Linear Stiffness in the Pull-out Test

- The linear stiffness values further emphasize the impact of bone quality on the mechanical performance of pedicle screw fixation. The mean stiffness in the normal bone group was substantially higher (196.1 N/mm for the left screw and 125.1 N/mm for the right) than in the osteopenic (46.6 N/mm for the left and 51.9 N/mm for the right) and osteoporotic groups (51.5 N/mm for the left and 47.4 N/mm for the right).
- High stiffness in the normal group reflects a strong resistance to initial displacement under load, indicating a more robust interface between the screw and bone. In contrast, the osteopenic and osteoporotic groups exhibit reduced stiffness, suggesting that these bones deform more easily under load, leading to a weaker mechanical anchorage.
- The variability in stiffness values between left and right screws within the same group, particularly in the normal bone, may be due to minor differences in screw positioning

or bone morphology. However, the general trend remains consistent across groups, indicating that bone quality significantly affects stiffness.

4.2.4 Peak Pull-Out Displacement (PPD)

- Peak pull-out displacement values also indicate the bone's mechanical properties. In the normal bone group, the left screw exhibited a higher mean PPD (2.8 mm) compared to the right (1.2 mm), reflecting a larger initial elastic range before peak load. For the osteopenic and osteoporotic groups, PPD values were more similar between the left and right sides, but generally lower than the normal bone group.
- The reduced displacement in osteopenic and osteoporotic bones suggests that these bones reach peak load and failure more quickly, likely due to their reduced structural integrity and weaker bonding with the screw. Lower displacement also indicates a reduced capacity for energy absorption, which may increase the risk of sudden failure under load in clinical settings.
- The observed differences in displacement highlight the importance of considering peak force and displacement when evaluating fixation stability. Higher displacement in normal bones suggests they can sustain deformation over a wider range before failure, potentially offering better shock absorption.

4.3 MicroCT Analysis of Trabecular Bone Microstructure in Normal, Osteopenic, and Osteoporotic Conditions

The micro-CT scans and segmentation of the bone-screw interface showed clear differences in bone structure and density characteristics between the three groups, confirming the initial results of the qCT performed to classify the samples into the three groups. Normal bone had the highest density, osteopenic bone had a moderate reduction, and osteoporotic bone had the lowest bone density. Comparing the bone volume (BV) of the bone-screw interface (Figures 4.4_4.6), we observed that normal bone had the highest BV, followed by osteopenic bone with a moderate reduction. Osteoporotic bone had the lowest BV, indicating a significant loss of bone tissue. Our results show that trabecular thickness (Tb.Th) of bone-screw interface (Figures 4.4_4.6) did not vary significantly between the normal (0.213 mm left screw and 0.211 mm right screw), osteopenic (0.206 mm left and 0.211 mm right) and osteoporotic (0.221 mm left and 0.230 mm on the right side), highlighting a commonality in this specific microarchitectural aspect. The micro-CT scans (Figure 4.6) showed that osteoporotic bone had a greater total volume (TV) (≈123 mm^3) compared to both normal (≈112 mm^3) and osteopenic (≈120 mm^3) bone. However, the ratio of bone volume to total volume (BV/TV) in the bone-

screw interface was still higher in normal bone, suggesting that normal bone had a denser microstructure.

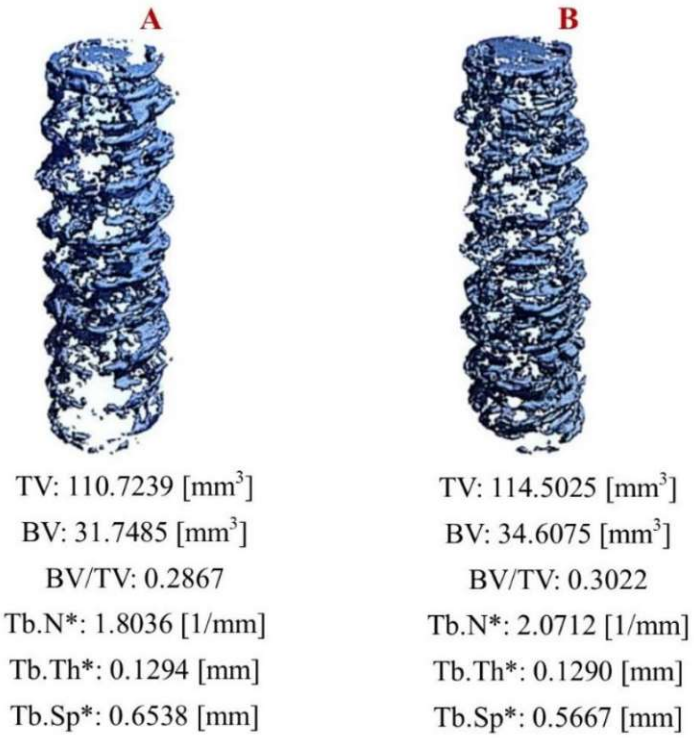

Figure 4.4. Micro CT 3D analyses of vertebrae trabecular bone after insertion of pedicle screw, (A) left screw, (B) right screw, normal bone

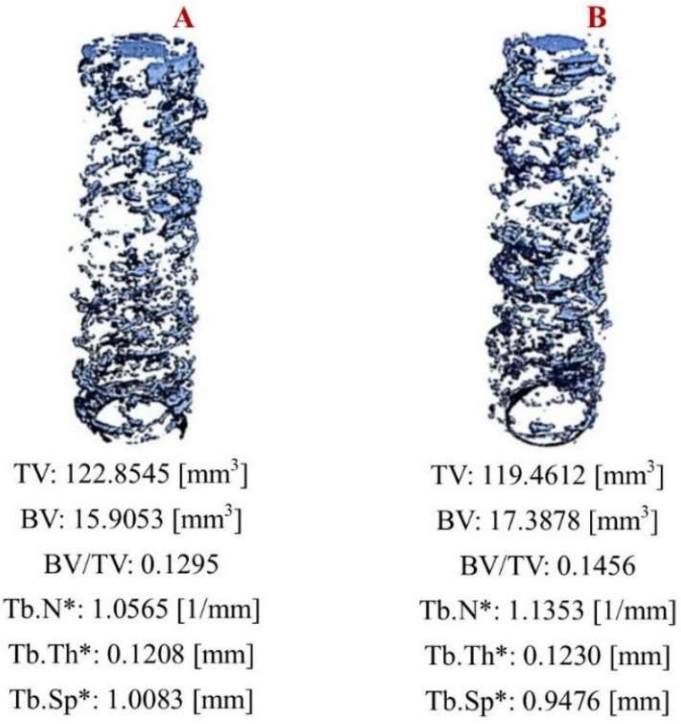

Figure 4.5. Micro CT 3D analyses of vertebrae trabecular bone after insertion of the pedicle screw, (A) left screw, (B) right screw, osteopenic bone

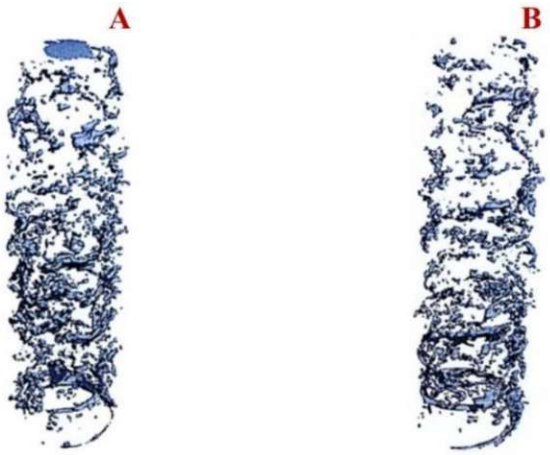

Figure 4.6. Micro CT 3D analyses of vertebrae trabecular bone after insertion of the pedicle screw, (A) left screw, (B) right screw, osteoporotic bone

Micro-CT analysis of the bone-screw interface revealed significant structural differences between normal, osteopenic, and osteoporotic bone, confirming the classifications established by qCT. The normal bone group consistently showed the highest bone density and BV/TV, highlighting its robust microstructural integrity. In comparison, osteopenic bone showed a moderate reduction in density and BV, while osteoporotic bone showed the lowest values in both categories. This pattern is consistent with the expected progression of bone loss in osteoporotic conditions, where reductions in BV are associated with an overall decline in structural integrity.

Interestingly, despite these differences in density and BV, trabecular thickness (Tb.Th) remained relatively consistent across the three groups. This suggests that changes in bone density and volume are not necessarily associated with trabecular thinning but may instead reflect a reduction in the number of trabecular elements or their spacing within the bone matrix. The preserved Tb.Th across groups may indicate that trabecular thickness is a less sensitive indicator of bone quality in early stages of bone loss, when microarchitectural degradation may involve structural separation or trabecular perforation rather than thinning.

In addition, osteoporotic bone was observed to have a greater total volume (TV) than normal bone, which at first seems counterintuitive. This increase in TV can be attributed to the porous nature of osteoporotic bone, where microstructural degradation leads to expanded spaces and reduced density despite a higher apparent volume. The BV/TV ratio further supports this, as normal bone maintained a higher BV/TV despite having a lower total volume compared to osteoporotic bone. This increased BV/TV in normal bone is indicative of a denser and more interconnected trabecular network, which likely contributes to its superior mechanical strength compared to osteopenic and osteoporotic bone.

As mentioned earlier, the number of samples tested in this study were 13, categorized into three groups: normal, osteopenic, and osteoporotic. As observed in Figures 4.17, 4.18, and 4.19, one sample from each group was examined. In Table 4.5, we obtained the mean BV, TV, and BV/TV to facilitate a comparative analysis among all samples in the normal group. The same analysis was performed for the osteopenic group in Table 4.6 and the osteoporotic group in Table 4.7.

Table 4.5. mean Parameters identified from image segmentation of the normal vertebrae group

Bone Classified	*BV [mm³]*	*TV [mm³]*	*BV/TV*
Normal	12.1431	110.652	0.109

Table 4.6. mean Parameters identified from image segmentation of the osteopenic vertebrae group

Bone Classified	*BV [mm³]*	*TV [mm³]*	*BV/TV*
Osteopenic	15.617	111.44	0.14

Table 4.7. mean Parameters identified from image segmentation of the osteoporotic vertebrae group

Bone Classified	*BV [mm³]*	*TV [mm³]*	*BV/TV*
Osteoporotic	10.265	147.685	0.06

Comparative analysis of trabecular bone microstructure in normal, osteopenic, and osteoporotic vertebrae revealed clear differences in bone volume (BV), total volume (TV), and bone volume fraction (BV/TV) between the groups. Normal bone had a BV/TV of 0.109, indicating a relatively dense microstructure, while osteopenic bone had a slightly higher BV/TV of 0.14, despite similar TV values, suggesting some preservation of bone volume. In contrast, osteoporotic bone had the lowest BV/TV ratio of 0.06, confirming a significant loss of bone volume relative to its total volume and reflecting a markedly compromised microstructure.

These results demonstrate that BV/TV is a sensitive indicator of trabecular bone integrity, with significant reductions correlating with osteopenic and osteoporotic conditions. While TV was comparable between groups, the marked decrease in BV/TV in osteoporotic samples highlights a significant microarchitectural deterioration. This finding highlights the role of BV/TV as a key metric for assessing bone quality and suggests that bone volume fraction may be particularly valuable for monitoring changes in bone health in conditions of bone density loss, such as osteoporosis.

4.4 Correlation between parameters of mechanical and radiological measurement

4.4.1 Correlation between BMD and PPF

We employed a pull-out test to investigate how BMD influences the peak pull-out force. Bone mineral density and peak pull-out force are measures related to bone strength and integrity. Test results of BMD, PPF, and PPD are presented in Table 4.8.

Table 4.8. BMD and Pull-out test output for each specimen

Bone Classified	*Age (y)*	*Sex*	*BMD [mg/cm³]*	*Screw Side*	*Level*	*PPF [N]*	*Peak Disp. [mm]*
Normal	54	F	144	L	L1/721	317.4	4.89
Normal	54	F	144	R	L1/721	64.7	0.94
Normal	50	M	148.59	L	L4/713	467.2	1.72
Normal	50	M	148.59	R	L4/713	428.3	1.76
Normal	50	M	154.84	L	L5/713	527.2	1.53
Normal	50	M	154.84	R	L5/713	377.2	1.35
Normal	67	M	123.8	L	L1/302		
Normal	67	M	123.8	R	L1/302	141.8	0.56
Normal	67	M	226.1	L	L2/302	883.6	3.08
Normal	67	M	226.1	R	L2/302	697.5	1.44
Osteopenic	67	M	84.32	L	L3/302	121.9	1.09
Osteopenic	67	M	84.32	R	L3/302	121.9	1.09
Osteopenic	67	M	87.53	L	L4/302	184.5	0.63
Osteopenic	67	M	87.53	R	L4/302	199.7	0.58
Osteopenic	67	M	101.37	L	L5/302	312.4	0.77
Osteopenic	67	M	101.37	R	L5/302	350.9	0.94
Osteopenic	56	M	105.31	L	L5/318	131.1	0.76
Osteopenic	56	M	105.31	R	L5/318	128.4	0.5
Osteoporotic	59	M	32.6	L	L3/978	181.4	1.91
Osteoporotic	59	M	32.6	R	L3/978	129	1.25
Osteoporotic	59	M	23.4	L	L4/978	139.2	0.6
Osteoporotic	59	M	23.4	R	L4/978	173.5	0.65
Osteoporotic	59	M	43.44	L	L5/978	186.1	1.38
Osteoporotic	59	M	43.44	R	L5/978	135.9	1.87
Osteoporotic	56	M	78.3	L	L4/318	103.6	0.6
Osteoporotic	56	M	78.3	R	L4/318	185.3	0.82

As can be seen in Table 4.2, the BMD of normal bones ranged from 144 to 261.1 mg/cm^3, while the PPF ranged from 64.7 to 883.6 N. For the osteopenic samples, the BMD ranged from 84.32 to 105.31 mg/cm^3. The PPF of these later samples ranged between 121.9 N and 350.9 N. The third group was the osteoporotic samples with BMD between 23.4 and 78.3 mg/cm^3 and PPF between 103.6 and 186.1 N. The relationship between BMD and PPF was examined separately for each bone group. This analysis is visualised in Figure 4.10.

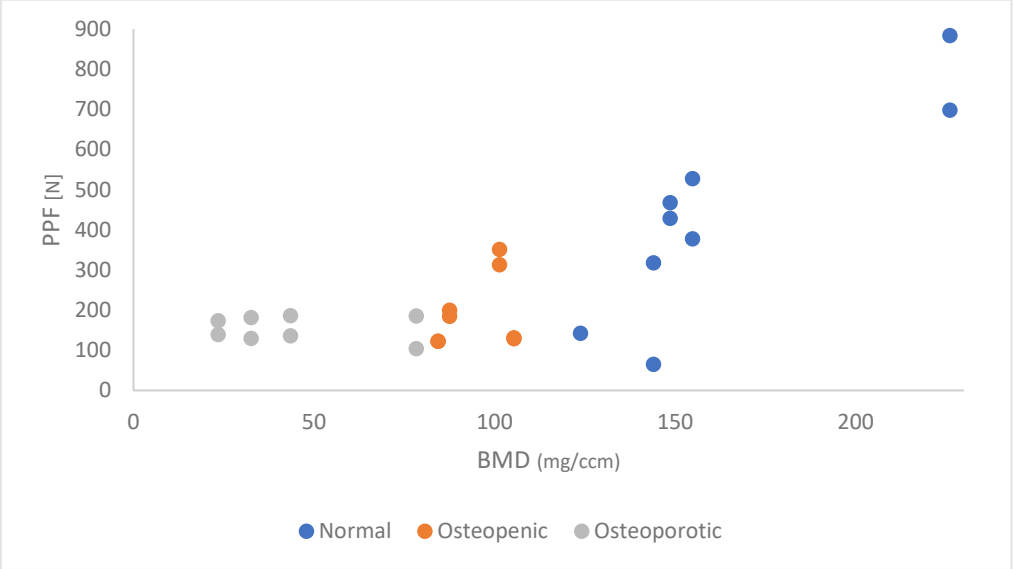

Figure 4.10. The effect of BMD on PPF

Pearson's correlation coefficient (r) is a statistical measure that quantifies the strength and direction of a linear relationship between two continuous variables. It ranges from -1 to 1, where:

- r = 1 indicates a perfect positive linear correlation,
- r = -1 indicates a perfect negative linear correlation, and
- r = 0 indicates no linear correlation between the variables.

In other words, the Pearson correlation coefficient provides information about how closely the data points of two variables lie in a straight line. Positive values indicate that as one variable increases, the other tends to increase as well, while negative values indicate that as one variable increases, the other tends to decrease.

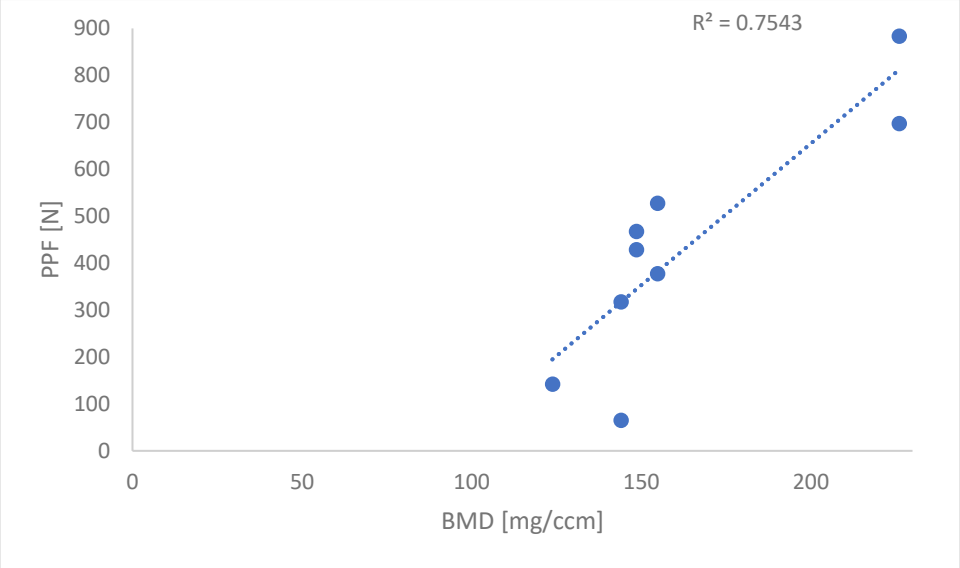

Figure 4.11. Relationship between BMD and PPF. Normal samples

The correlation coefficient (r) for the normal bone group was 0.868 (Figure 4.11). There was a significant positive correlation between BMD and PPF in the normal bone group (R^2=0.75, p<0.002).

In exploring the relationship between PPF and BMD within three different bone groups - normal, osteopenic, and osteoporotic - the initial analysis indicated that a suboptimal linear correlation was considered satisfactory in the normal bone group. However, recognizing the inadequacy of linear correlation in capturing the complex associations within the osteopenic and osteoporotic bone groups, an alternative methodology was implemented. An exponential correlation model (Figure 4.12) was then applied to the data for all three bone groups, resulting in a significantly improved correlation pattern. The application of the exponential model proved more adept at capturing the nuanced relationship between PPF and BMD in conditions associated with osteopenic and osteoporotic bone.

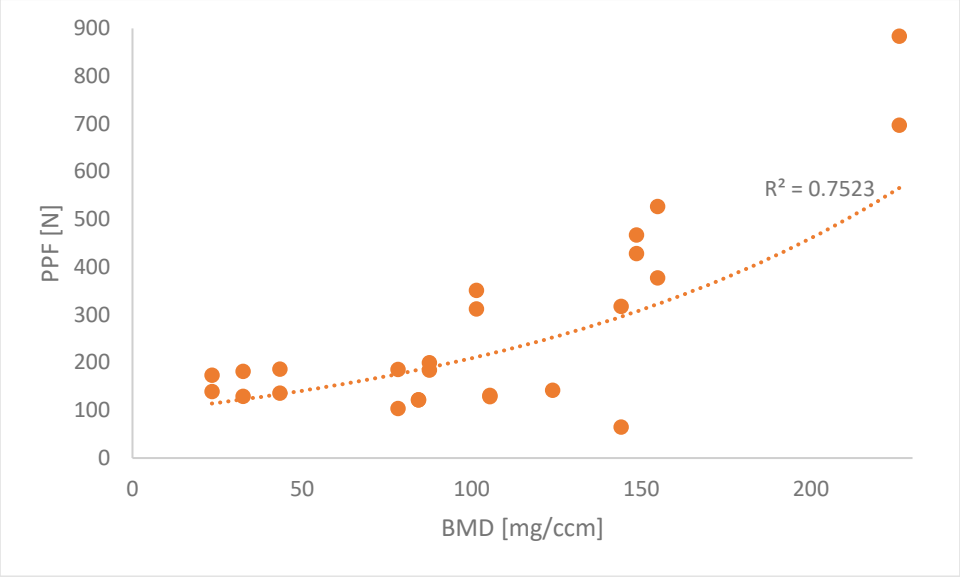

Figure 4.12. Relationship between BMD and PPF. Normal samples, Osteopenic samples, and Osteoporotic samples

4.4.2 Correlation between BMD and PPD

PPD of normal bones was in the range of 0.56 and 4.89 mm (table 4.2). In osteopenic bones PPD encompassed from 0.5 to 1.09 mm, while in osteoporotic ones PPD lied between 0.6 and 1.91 mm. The effect of BMD on PPD for three groups of bones can be seen in Figure 4.13

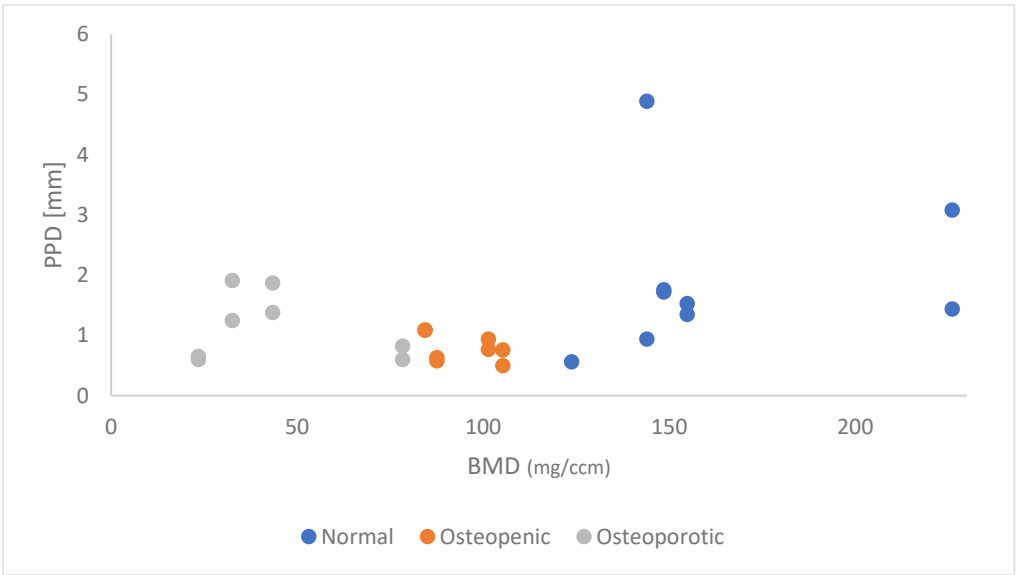

Figure 4.13. The effect of BMD on PPD

The correlation coefficients (r) for the normal bone group were 0.185 as shown in Figure 4.14.

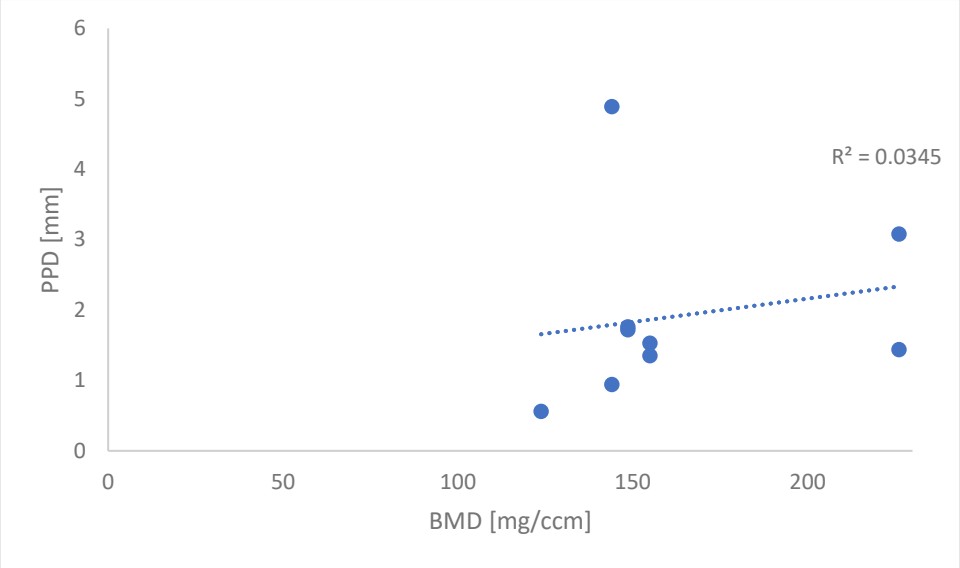

Figure 4.14. Relationship between BMD and PPD: Normal samples

In this case, an R^2 of 0.03 for the normal bone group means that only 3% of the variation in PPD is explained by the independent variable (BMD), suggesting a weak relationship. We know that if the p-value is > 0.05, the result is not statistically significant, meaning that you cannot reject the null hypothesis, and it suggests that there may not be a meaningful relationship. For the normal bone group, a p-value of 0.6 indicates that the relationship between PPD and BMD is not statistically significant. A p-value of 0.6 is much higher than the 0.05 threshold, which means that the observed correlation could be due to chance and is not a reliable indicator of a true relationship. An exponential correlation model ($r=0.38$, $R^2=0.16$, $p<0.05$) (Figure 4.15) was then fitted to the data for all three bone groups, resulting in a significantly improved correlation pattern. The application of the exponential model proved more adept at capturing the nuanced relationship between PPD and BMD in conditions associated with osteopenic and osteoporotic bone. For the normal bone group, this high p-value implies that the observed correlation could be due to chance, and there is no strong evidence to support a meaningful relationship between BMD and PPD in normal bone. These results suggest that, at least in normal bone, BMD alone may not be a sufficient predictor of PPD. It is possible that other factors such as bone microarchitecture, trabecular thickness or overall bone quality may play a more dominant role in influencing PPD. The weak correlation between BMD and PPD in normal bone may also indicate that implant stability and displacement under load may be influenced by factors other than bone mineral density, such as mechanical properties, trabecular connectivity or the presence of cortical bone involvement.

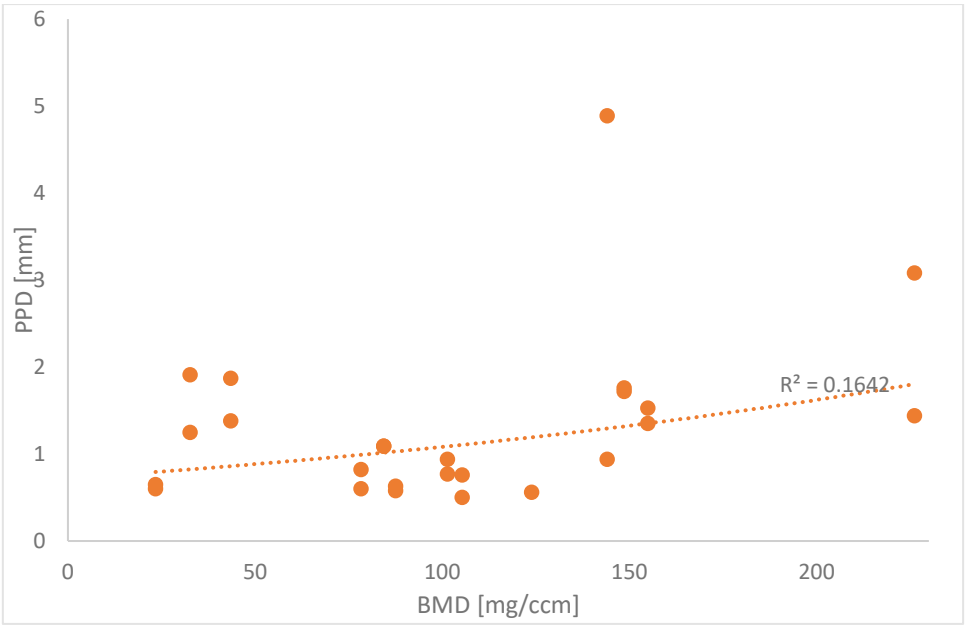

Figure 4.15. Relationship between BMD and PPF. Normal samples, Osteopenic samples, and Osteoporotic samples

4.4.3 Correlation between the BV/TV and PPF

The PPF values recorded in normal bone ranged from 64.7 to 883.6 N, as shown in Table 4.9. In osteopenic bones, the PPF values ranged from 121.9 to 350.9 N, while in osteoporotic bones the PPF values ranged from 129 to 186.1 N. According to the data presented in Table 4.9, the bone volume fraction (BV/TV) for normal bones showed a variability ranging from 0.133 to 0.606. For osteopenic samples, the BV/TV ranged from 0.064 to 0.219. The third group, consisting of osteoporotic bones, showed BV/TV values ranging from 0.012 to 0.128. Figure 4.16 shows the correlation of BV/TV on PPF for three groups of bones.

Table 4.9. Micro-CT values and Pull-out test output for each specimen

Bone Classified	*Age (y)*	*Sex*	*BV/TV*	*Screw Side*	*Level*	*PPF [N]*	*Peak Disp. [mm]*
Normal	54	F	0.1333	L	L1/721	317.4	4.89
Normal	54	F	0.338	R	L1/721	64.7	0.94
Normal	50	M	0.2867	L	L4/713	467.2	1.72
Normal	50	M	0.3022	R	L4/713	428.3	1.76
Normal	50	M	0.3827	L	L5/713	527.2	1.53
Normal	50	M	0.3865	R	L5/713	377.2	1.35
Normal	67	M	0.0834	L	L1/302		
Normal	67	M	0.1004	R	L1/302	141.8	0.56
Normal	67	M	0.4836	L	L2/302	883.6	3.08
Normal	67	M	0.606	R	L2/302	697.5	1.44
Osteopenic	67	M	0.0645	L	L3/302	121.9	1.09
Osteopenic	67	M	0.1746	R	L3/302	121.9	1.09
Osteopenic	67	M	0.1295	L	L4/302	184.5	0.63
Osteopenic	67	M	0.1456	R	L4/302	199.7	0.58
Osteopenic	67	M	0.2192	L	L5/302	312.4	0.77
Osteopenic	67	M	0.1745	R	L5/302	350.9	0.94
Osteopenic	56	M	0.0842	L	L5/318	131.1	0.76
Osteopenic	56	M	0.1149	R	L5/318	128.4	0.5
Osteoporotic	59	M	0.1287	L	L3/978	181.4	1.91
Osteoporotic	59	M	0.1205	R	L3/978	129	1.25
Osteoporotic	59	M	0.1018	L	L4/978	139.2	0.6
Osteoporotic	59	M	0.0839	R	L4/978	173.5	0.65
Osteoporotic	59	M	0.0125	L	L5/978	186.1	1.38
Osteoporotic	59	M	0.0855	R	L5/978	135.9	1.87
Osteoporotic	56	M	0.0821	L	L4/318	103.6	0.6
Osteoporotic	56	M	0.1021	R	L4/318	185.3	0.82

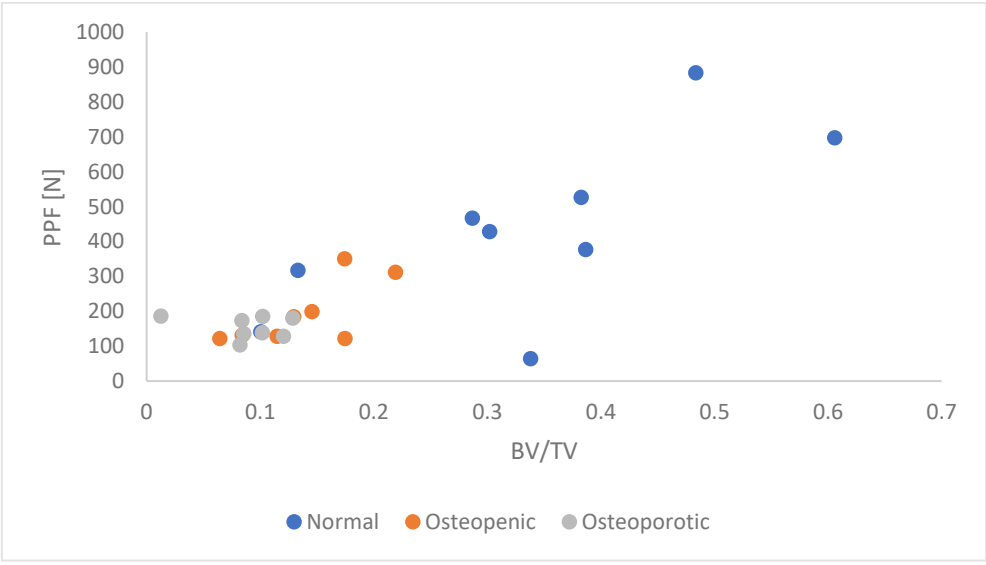

Figure 4.16. The correlation of BV/TV on PPF

The correlation coefficient (r) for the normal bone group was 0.711 (R^2=0.5, p<0.03) as shown in Figure 4.17. A notable observation is the significant positive correlation between BV/TV and PPF in the normal bone group.

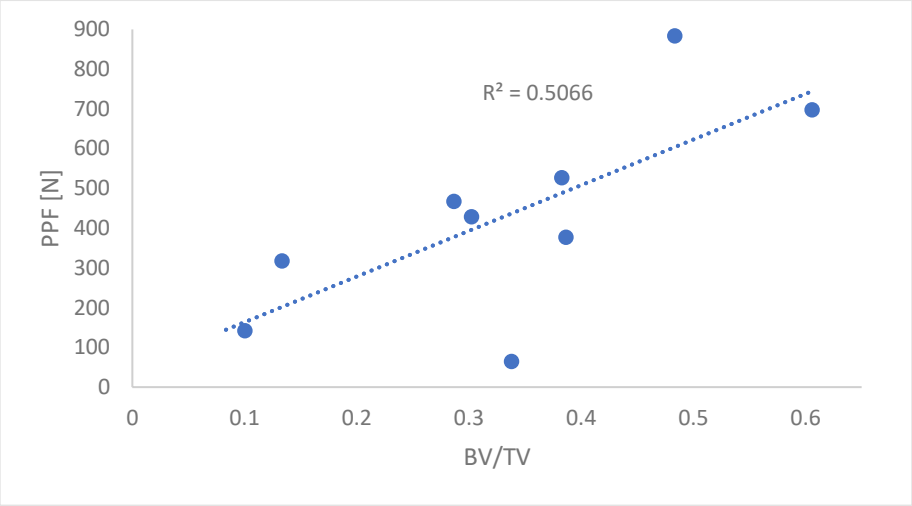

Figure 4.17. Relationship between BV/TV and PPF. Normal samples

In the investigation of the relationship between PPF and BV/TV across three bone groups—normal, osteopenic, and osteoporotic—initial analysis revealed a suboptimal linear correlation in the normal bone group was found to be satisfactory. Recognizing the limitations of linear correlation in capturing the complex associations within the osteopenic and osteoporotic bone groups, an alternative approach was implemented. Subsequently, an exponential correlation (Figure 4.18) (r=0.82, R^2=0.67, p<0.000001) was applied to the data for all three bone groups, resulting in a notably improved correlation pattern. The adoption of the exponential model proved to be more suitable for capturing the nuanced relationship between PPF and BV/TV in osteopenic and osteoporotic bone conditions. This shift in correlation models underscores the importance of considering non-linear relationships in the biomechanical interaction between bone quality and the forces applied, especially in pathological conditions such as osteopenia and osteoporosis.

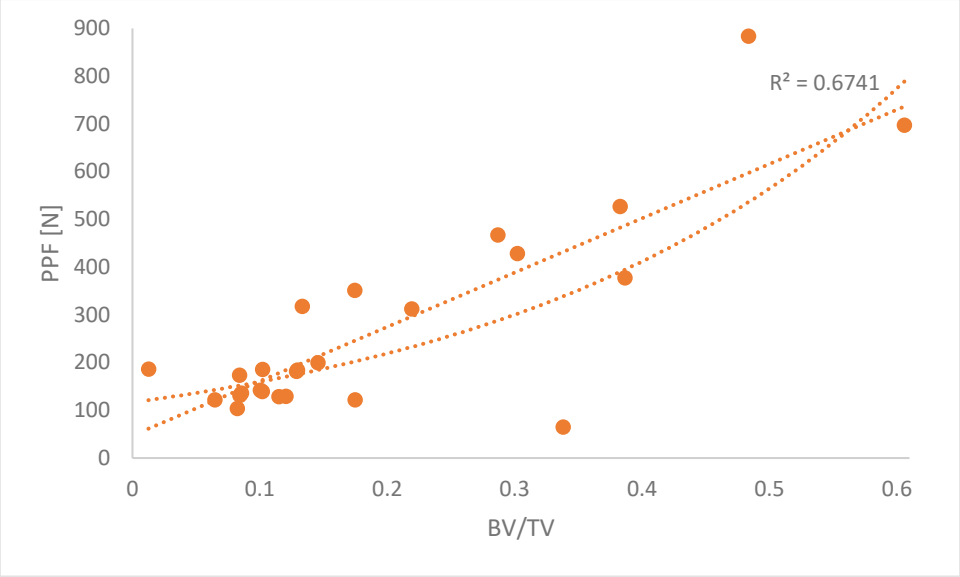

Figure 4.18. Relationship between BV/TV and PPF. Normal samples, Osteopenic samples, and Osteoporotic samples

A high correlation coefficient (r) indicates that there is a strong relationship between the variables, in this case, PPF and BV/TV. This means that when BV/TV increases or decreases, PPF tends to follow a similar pattern. However, the p-value tests whether this observed correlation is likely to have occurred by chance. If the p-value is greater than 0.05, it suggests that the observed correlation may not be statistically significant, meaning that there's a high probability that the relationship occurred by chance. Even if you have a good correlation, the high p-value indicates that there isn't enough evidence to say with confidence that the relationship between PPF and BV/TV is meaningful. This reduces the strength of your finding because it suggests that the correlation may not be reproducible in a larger sample or different population. The correlation between peak pull-out force (PPF) and bone volume fraction (BV/TV) in our study was significantly improved when an exponential model was applied to the data in all three bone groups - normal, osteopenic and osteoporotic. With a correlation coefficient (r) of 0.82, this suggests a strong positive relationship between BV/TV and PPF, indicating that as bone volume fraction increases, the pull-out force also increases significantly. In addition, the R^2 value of 0.67 indicates that 67% of the variance in PPF can be explained by BV/TV. The p-value < 0.000001 confirms the statistical significance of this relationship, leaving very little chance that this correlation occurred by chance.

4.4.4 Correlation between the BV/TV and PPD

The relationship between BV/TV and PPD was investigated in this study (Figure 4.19). The correlation analysis aimed to uncover any possible relationship between bone microstructure and the amount of displacement during the pull-out test. Investigating this correlation provided insight into how bone density and architecture influence the mechanical behaviour of the bone-implant interface.

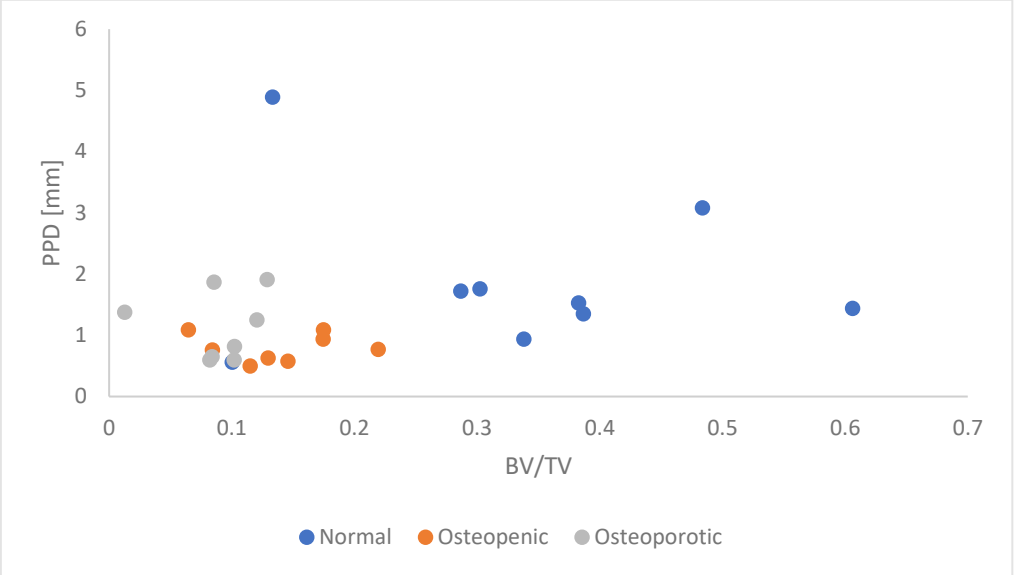

Figure 4.19. The effect of BV/TV on PPD

For the normal bone group, we observed a linear correlation between PPD and BV/TV in Figure 4.20 with a correlation coefficient ($r=-0.165$), R^2 value of 0.02, and very low p-value ($p<0.000001$), indicating statistical significance.

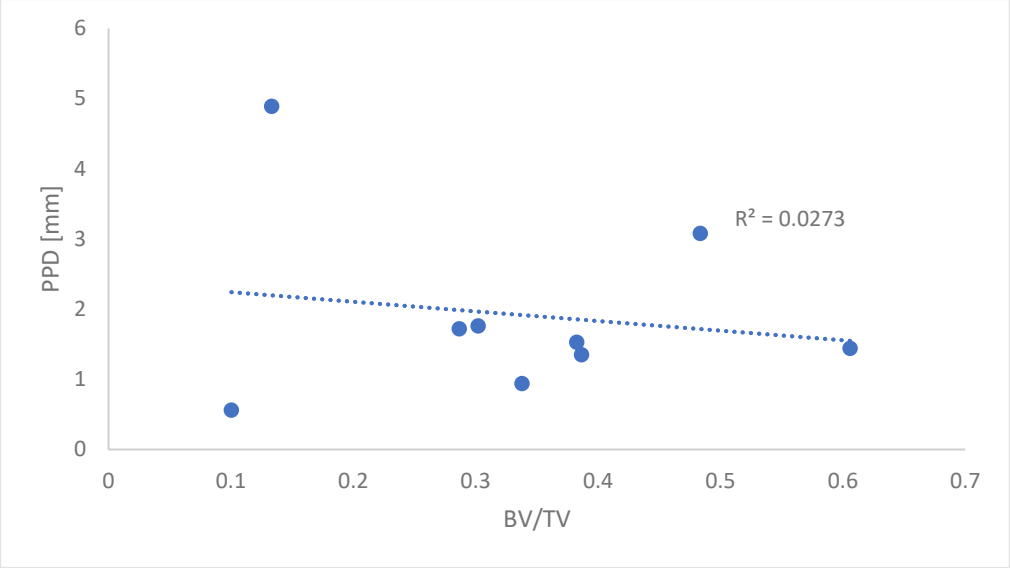

Figure 4.20. Relationship between BV/TV and PPD. Normal samples

For the normal bone group, a linear correlation was observed between PPD and BV/TV, yielding a correlation coefficient of r=-0.165, R^2 value of 0.02, and a highly significant p-value ($p<0.00001$). these results suggest a very weak negative linear relationship between BV/TV and PPD in normal bone, with a significant p-value but limited predictive power, as BV/TV accounts for only 2% of the variability in PPD. the correlation coefficient ($r=-0.165$) indicates a weak negative relationship between BV/TV and PPD. This implies that in normal bones, an increase in bone volume fraction is associated with a slight reduction in peak pull-out displacement. However, given the small magnitude of this relationship, this effect is minimal. The low R^2 of 0.02 further confirms that BV/TV alone does not significantly predict PPD, as only 2% of the variation in PPD is explained by changes in BV/TV. The statistically significant p-value ($p<0.00001$) shows that the observed correlation is unlikely to be due to random chance, but the practical significance remains low due to the weak correlation strength. In the context of bone biomechanics, a statistically significant but weak correlation indicates that while BV/TV may have some influence, it is not a primary driver of PPD in normal bones. This suggests that other microstructural characteristics of bone, beyond BV/TV, may play more influential roles in determining pull-out displacement behavior.

The linear correlation between PPD and BV/TV in normal bone is statistically significant but weak, suggesting that BV/TV has a limited role in predicting pull-out displacement. This points to the need for a multifactorial approach in analyzing pull-out behavior, integrating BV/TV with other bone quality metrics for a more accurate assessment of implant stability and bone-implant interactions in normal bone.

The analysis of PPD and BV/TV across all three groups (normal, osteopenic, and osteoporotic) revealed a weak exponential correlation with a correlation coefficient (r=0.26) R^2 value of 0.069 (Figure 4.21), and a high p-value (p=0.2).

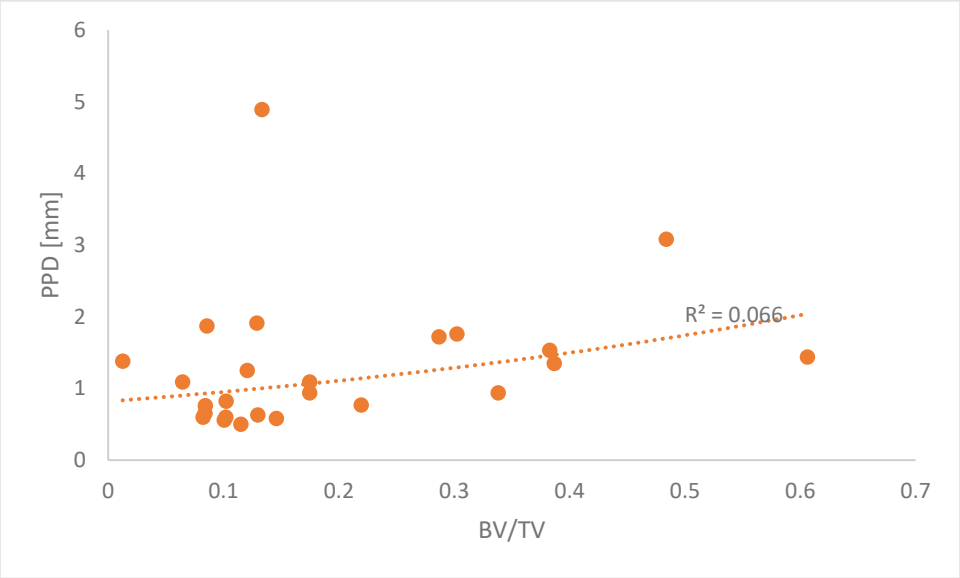

Figure 4.21. Relationship between BV/TV and PPD. Normal samples, Osteopenic samples, and Osteoporotic samples

For the combined analysis of PPD and BV/TV across the three bone groups (normal, osteopenic, and osteoporotic), an exponential correlation was applied, resulting in a correlation coefficient of r=0.26, R^2 value of 0.066, and a p-value of 0.2. These findings indicate a low correlation strength between PPD and BV/TV in the combined dataset, with limited predictive capability. The correlation coefficient (r=0.26) indicates a weak positive relationship between PPD and BV/TV when considering all three bone groups together. This implies a slight tendency for PPD to increase as BV/TV increases; however, given the low magnitude of this relationship, the effect is minimal. The R^2 value of 0.066 suggests that only 6.6% of the variability in PPD is explained by BV/TV across these bone types, indicating that BV/TV alone is not a strong predictor of PPD in a mixed-quality bone sample. The p-value of 0.2 is above the conventional threshold for statistical significance (0.05), suggesting that the observed relationship between PPD and BV/TV in this analysis could be due to chance. Thus, the correlation observed is not statistically reliable, meaning it does not provide strong evidence of a meaningful relationship between BV/TV and PPD across the combined bone types. The weak correlation might be attributable to differences in how BV/TV impacts PPD in each bone group. Normal, osteopenic, and osteoporotic bones have distinct microstructural properties and

mechanical responses to pull-out loads, potentially diluting meaningful patterns that may exist within each individual group. This mixed analysis might obscure group-specific effects, as BV/TV's influence on PPD can vary depending on the bone's density and microarchitecture.

The weak, non-significant exponential correlation between PPD and BV/TV across normal, osteopenic, and osteoporotic bones suggests that BV/TV alone does not meaningfully predict PPD in this mixed sample. These results emphasize the need for group-specific analysis or more comprehensive models incorporating additional bone quality metrics to better understand the relationship between BV/TV and PPD in diverse bone conditions.

4.4.5 Correlation between the BV/TV and BMD

Our study investigated the relationship between BMD and Bone Volume Fraction (BV/TV) in three different bone groups: normal, osteopenic, and osteoporotic (Figure 4.22). Notably, we observed a robust and positive correlation between BMD and BV/TV in the normal bone group ($r=0.872$, $R^2=0.76$, $p=0.0009$) (Figure 4.23), indicating a strong relationship between bone mineral density and bone microstructure.

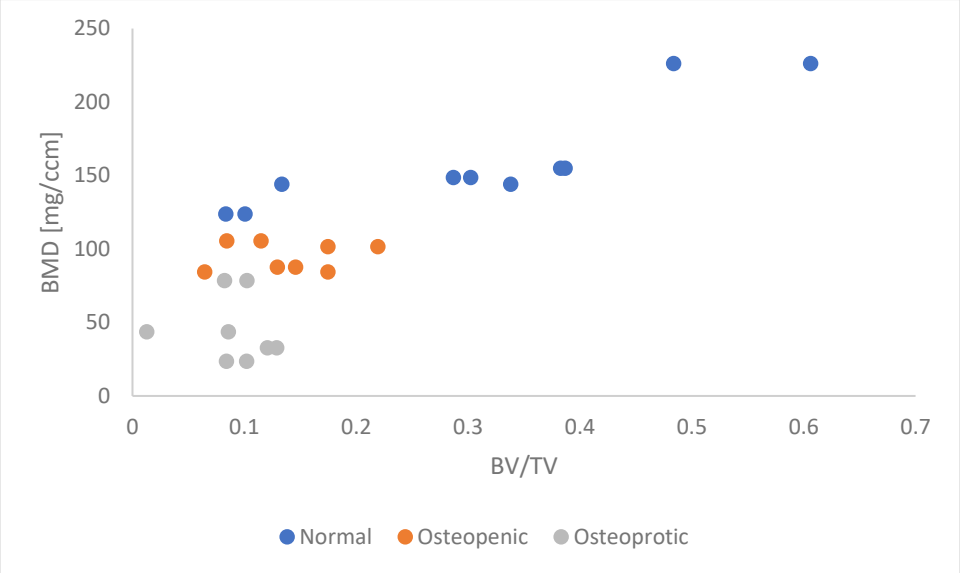

Figure 4.22. The effect of BV/TV on BMD

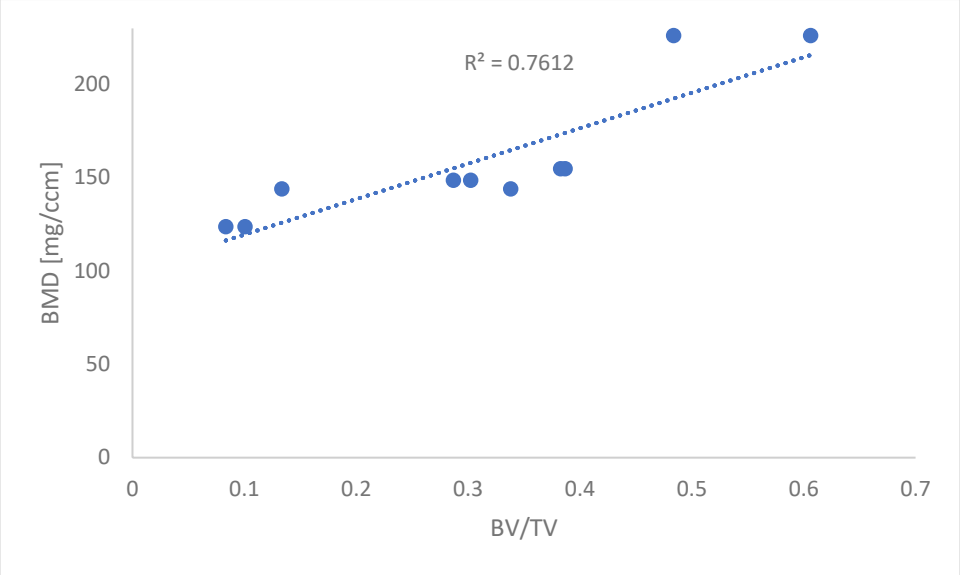

Figure 4.23. Relationship between BV/TV and BMD: Normal samples

For the normal bone group, a strong linear correlation was observed between BMD and BV/TV, with a correlation coefficient of r=0.872, an R^2 value of 0.76, and a statistically significant p-value of 0.0009. These results indicate a robust and significant relationship, suggesting that BMD is strongly associated with BV/TV in normal bone. The high correlation coefficient (r=0.872) indicates a strong positive relationship between BMD and BV/TV in normal bone, meaning that as bone volume fraction increases, BMD tends to increase proportionally. The high R^2 value of 0.76 further supports this finding, showing that 76% of the variability in BMD can be explained by BV/TV in normal bone. This suggests that BV/TV is a reliable predictor of BMD in normal bone quality, reflecting a well-defined relationship between these two parameters in healthy bone tissue. The p-value of 0.0009, which is well below the conventional threshold of 0.05, indicates that this observed relationship is statistically significant, providing strong evidence that the correlation between BMD and BV/TV in normal bone is not due to random chance. This significant result confirms that BV/TV provides meaningful insights into the bone density of normal bone. The strong correlation between BMD and BV/TV in normal bone suggests that BV/TV could be used as a surrogate marker to assess bone density in cases where direct measurement of BMD is not possible or is limited. As BV/TV is a measure of the structural composition of bone, its strong association with BMD underline the close relationship between bone structure and density in healthy bone tissue, where higher bone volume fraction is well correlated with higher mineral density. The strong and statistically significant linear correlation between BMD and BV/TV in normal bone demonstrates that BV/TV is a reliable predictor of bone mineral density in healthy

bone tissue. This correlation has important applications in clinical and modelling contexts, where BV/TV can serve as an effective proxy for BMD in normal bone, facilitating assessments and simulations that require accurate representations of bone density.

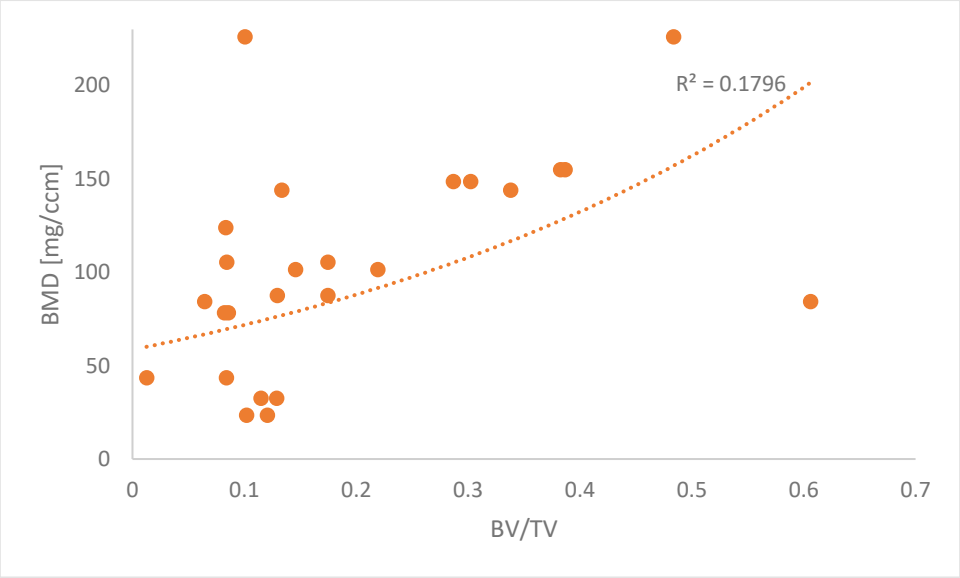

Figure 4.24. Relationship between BV/TV and BMD. Normal samples, Osteopenic samples, and Osteoporotic samples

For the combined data analysis of BMD and BV/TV across all three bone groups, an exponential correlation was applied. The analysis resulted in a moderate correlation coefficient (r=0.48), an R^2 value of 0.233, and p-value of 0.014. These findings suggest a modest but statistically significant relationship between BMD and BV/TV across different bone types, though with a relatively low explanatory power. The correlation coefficient (r=0.48) indicates a moderate positive relationship between BMD and BV/TV across the pooled dataset of normal, osteopenic, and osteoporotic bones. This suggests a tendency for BMD to increase as BV/TV increases across bone types, though the effect is not particularly strong. The moderate nature of this correlation reflects the diversity in bone quality and structural characteristics inherent in the different bone groups. The R^2 value of 0.233 suggests that BV/TV accounts for approximately 23.3% of the variability in BMD across these bone types, leaving a large portion of the variance unexplained by BV/TV alone. This indicates that while BV/TV is relevant to predicting BMD, other factors not captured in this analysis likely play a substantial role in determining BMD, particularly when considering different bone quality groups together. The p-value of 0.014, which is below the conventional significance threshold of 0.05, indicates that the observed correlation is statistically significant. This suggests that the relationship between BMD and BV/TV across all three bone types is unlikely to be due to chance, providing

evidence for a real association between these variables despite the moderate strength of the correlation.

4.5 Discussion of Correlation between Test Parameters and MicroCT Scans

The modest correlation strength could be influenced by the heterogeneity in bone quality among the normal, osteopenic, and osteoporotic groups. Each group exhibits unique structural and compositional characteristics that may alter the relationship between BMD and BV/TV. In normal bone, for example, a strong linear relationship may exist, while osteopenic and osteoporotic bones, with their structural degradation, may exhibit a weaker or more variable relationship. This mix likely reduces the overall correlation strength when all groups are analyzed together, as BV/TV may not have a consistent impact on BMD across varying bone conditions. The exponential correlation between BMD and BV/TV across normal, osteopenic, and osteoporotic bone groups shows a moderate but statistically significant association. This finding suggests BV/TV is somewhat predictive of BMD across diverse bone qualities, though other factors likely impact BMD in varying bone conditions. For both clinical and modelling purposes, additional bone quality parameters should be considered alongside BV/TV to improve predictions of BMD, especially in heterogeneous bone samples.

4.6 Results of Finite Element Analysis of Pull-Out Test

In the osteoporotic group, a different specimen was selected for the finite element analysis (FEA) compared to the experimental test. This decision was made due to the discrepancy in peak pull-out force (PPF) between the experimental and FEA results for the originally selected specimen. Several factors could explain this discrepancy, with the most likely reason being the segmentation accuracy of BV/TV for this particular specimen. In this work, we segmented the bone-screw interface and achieved the BV/TV of this region. As we know, BV/TV varies in different regions of the vertebral body, and it appears that an inaccurate BV/TV value was assigned during the segmentation of specimen 978_L5. Unfortunately, resegmentation was not possible for all specimens, making it difficult to correct the problem. To ensure a more reliable comparison between FEA and experimental results, another osteoporotic specimen was selected for FEA simulation.

4.6.1 Mesh Sensitivity

A mesh sensitivity analysis was performed to determine the optimal mesh size for accurate simulation results of pull-out behavoir of a pedicle screw in trabecular vertebral bone. The normal bone 713_L4_L was chosen for mesh sensitivity (Table 4.10). A mesh size of 1 mm was used for the vertebral body, while a mesh size of 0.5 mm was used for the screw in all simulations. The interface between the bone and the screw was tested with different mesh sizes, including 0.3 mm, 0.25 mm, 0.4 mm, and 0.5 mm. The analysis showed (Figure 4.25) that a 0.3 mm mesh size for the interface provided the closest match to the experimental PPF values, making it the optimal choice for capturing the mechanical response at the bone-screw interface.

Table 4.10. Mesh sensitivity done on bone-screw interface

Level	*Seed Size (mm)*	*No. of elements*	*No. of nodes*	*PPF (N)*	*Region of interest*
713_L4_left	0.25	2242000	367000	522.8	Bone-screw interface
713_L4_L	0.3	1830000	298000	516.8	Bone-screw interface
713_L4_L	0.4	1468000	237000	559.7	Bone-screw interface
713_L4_L	0.6	1250000	201000	614.5	Bone-screw interface

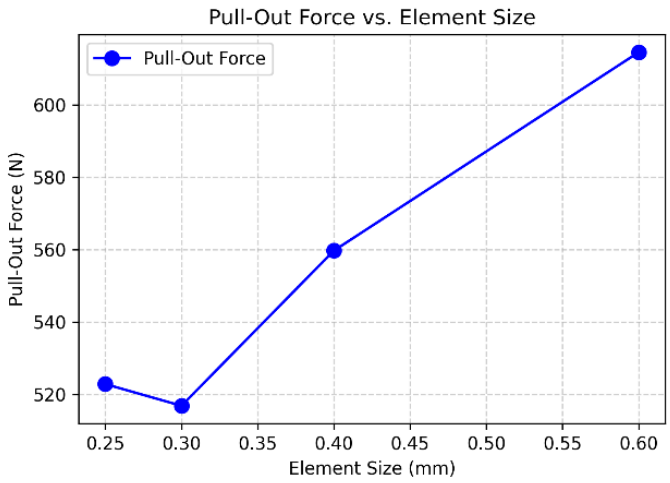

Figure 4.25. Mesh sensitivity study

4.6.2 Understanding Pull-out Behavior: Numerical Findings

Figures 4.26 through 4.28 illustrate the Finite Element (FE) pullout test results for the three different bone quality groups, showing the left and right screw simulations. The Peak Pullout Force (PPF) values obtained from the simulations are summarized as follows:

In the normal bone group, the PPF for the left-side screw was 516.8 N, while the right-side screw had a slightly higher PPF of 559.3 N. In the osteopenic bone group, the PPF was significantly lower, with values of 150.2 N for the left-side screw and 180.7 N for the right-side screw. Similarly, the lowest extraction forces were observed in the osteoporotic bone group, with a PPF of 74.3 N for the left screw and 104.3 N for the right screw.

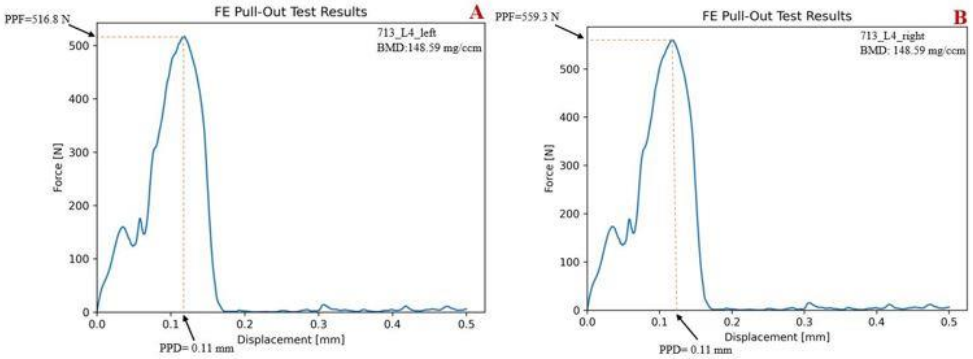

4.26. Diagram of numerically measured pull-out force vs. displacement. (A) first screw (left side) for carbon-fiber reinforced PEEK pedicle screw, Normal Bone (B) second screw (right side) for carbon-fiber reinforced PEEK pedicle screw, Normal Bone

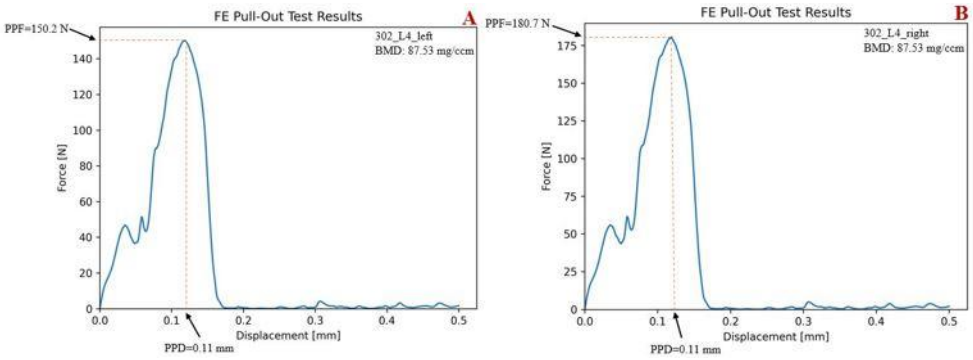

4.27. Diagram of numerically measured pull-out force vs. displacement. (A) first screw (left side) for carbon-fiber reinforced PEEK pedicle screw, Osteopenic Bone (B) second screw (right side) for carbon-fiber reinforced PEEK pedicle screw, Osteopenic Bone

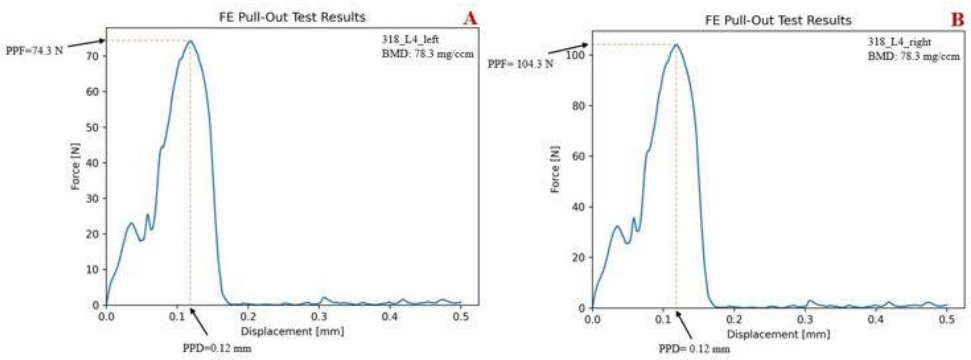

4.28. Diagram of numerically measured pull-out force vs. displacement. (A) first screw (left side) for carbon-fiber reinforced PEEK pedicle screw, Osteoporotic Bone (B) second screw (right side) for carbon-fiber reinforced PEEK pedicle screw, Osteoporotic Bone

These results indicate a clear trend of decreasing PPF with decreasing bone quality, which will be further analyzed in the following discussion in comparison to experimental results.

4.7 FE Analysis: Discussion

This study investigated the pull-out behavior of pedicle screws in vertebral trabecular bone by comparing Finite Element (FE) simulations with experimental pull-out tests. The FE models were constructed from CT images of normal, osteopenic, and osteoporotic vertebrae, with screws ideally placed on the left and right sides. After meshing, elastoplastic mechanical properties were assigned to the material, and a 0.5 mm/s axial displacement was applied to the top of each screw. The pull-out tests were then simulated for each pedicle screw using the developed FE models. The FE PPF for all three bone groups fell within the range of experimental data (Figure 4.29), with an observed difference of approximately 9-43% between experiment and FE for three groups of bones.

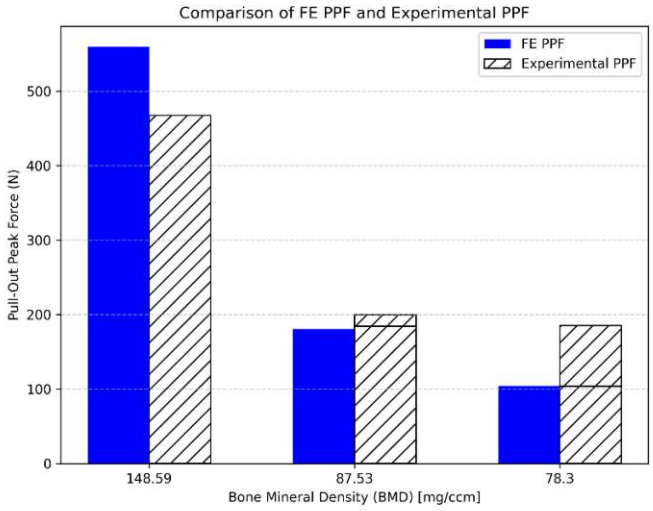

Figure 4.29. Experimental vs Finite Element studies

The results of the experimental studies were compared with those of the finite element (FE) analysis. As shown in Figure 4.29 and Figures 4.30 through 4.32, both methods indicate that pedicle pull-out force (PPF) increases with bone density. Experimentally, the highest PPF was observed in normal bone (148.59 mg/ccm), reaching 467.2 N for the left screw and 428.3 N for the right screw (Figures 4.29 and 4.30). In comparison, the lowest values were recorded in osteoporotic bone (78.3 mg/ccm) with 185.3 N and 103.6 N for the right and left screws, respectively (Figures 4.29 and 4.32). In osteopenic bone (87.53 mg/ccm), the PPF was 199.7 N for the right screw and 184.5 N for the left screw (Figures 4.29 and 4.32). In the case of finite element studies, PPF was highest in bone density at 148.59 mg/ccm representing normal bone at 559.3 N and 516.8 N for the right and left screws, respectively. These values were 30% higher for the right screw and 10% higher for the left screw than the experimental PPF values (Figures 4.29 and 4.30). In the case of osteopenic bone, represented by the bone with a density of 87.53 mg/ccm, the FE model predicted a PPF of 180.7 N and 150.2 N for the right and left screws, respectively, which were 9% for the right screw and 18% for the left screw lower than the values obtained in the experimental study (Figures 4.29 and 4.31). In the case of the osteoporotic bone model with a density of 78.3 mg/ccm, the PPF values were 104.3 N and 74.3 N for the right and left screws, respectively. The values obtained are 43% lower for the right screw and 28% lower for the left screw than those obtained in the experimental study (Figures 4.29 and 4.32).

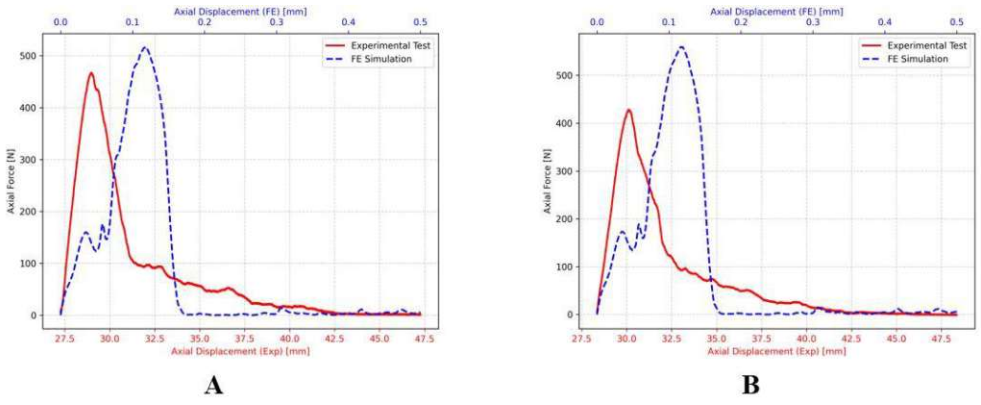

Figure 4.30. Comparison between the experimental and numerical force-displacement curves obtained for the tested cadaveric vertebrae, (A) first screw (left side) for carbon-fiber reinforced PEEK pedicle screw, Normal Bone (B) second screw (right side) for carbon-fiber reinforced PEEK pedicle screw, Normal Bone

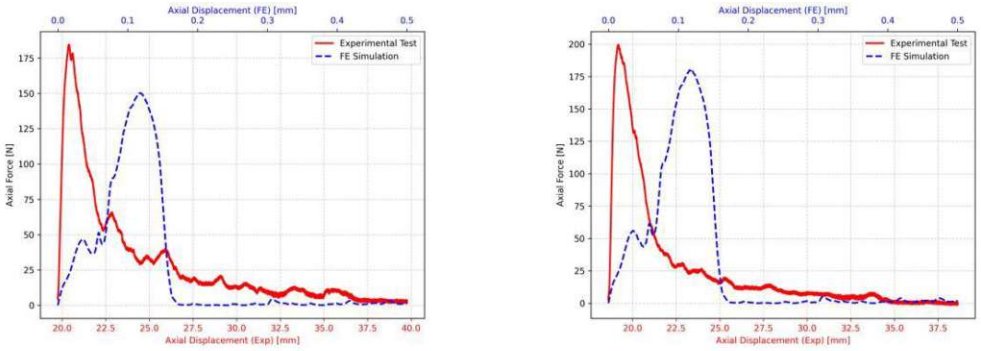

Figure 4.31. Comparison between the experimental and numerical force-displacement curves obtained for the tested cadaveric vertebrae, (A) first screw (left side) for carbon-fiber reinforced PEEK pedicle screw, Osteopenic Bone (B) second screw (right side) for carbon-fiber reinforced PEEK pedicle screw, Osteopenic Bone

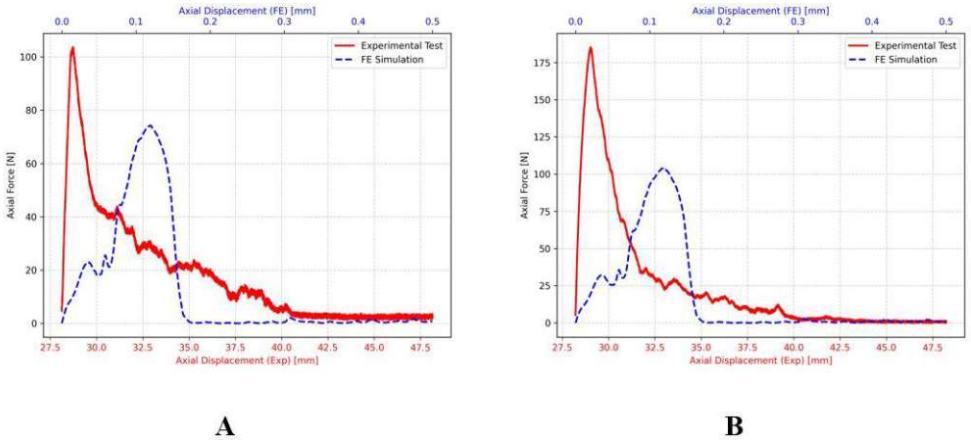

Figure 4.32. Comparison between the experimental and numerical force-displacement curves obtained for the tested cadaveric vertebrae, (A) first screw (left side) for carbon-fiber reinforced PEEK pedicle screw, Osteoporotic Bone (B) second screw (right side) for carbon-fiber reinforced PEEK pedicle screw, Osteoporotic Bone

4.7.1 Model validation

To validate the Finite Element (FE) model, the simulated Peak Pull-Out Force (PPF) values were compared with experimental results for all three bone groups. The comparison showed a reasonable agreement, confirming the accuracy of the material properties, boundary conditions, and loading conditions applied in the simulations.

However, some discrepancies were observed between the FE model and the experimental results for different bone groups:

- Normal Bone:
    - The FE PPF in the right screw was 30% higher than the experimental result.

    - The FE PPF in the left screw was 10% higher than the experimental result.
- Osteopenic Bone:
    - The FE PPF in the right screw was 9% lower than the experimental result.
    - The FE PPF in the left screw was 18% lower than the experimental result.
- Osteoporotic Bone:
    - The FE PPF in the right screw was 43% lower than the experimental result.
    - The FE PPF in the left screw was 28% lower than the experimental result.

The discrepancies between the FE model and experimental results can be attributed to several factors, including simplifications in the FE model, assumptions regarding material homogeneity, and the limitations in modeling the bone-screw interaction. The variability in trabecular bone microstructure, differences in boundary constraints, and potential inconsistencies in experimental conditions could also contribute to these variations.

Despite these differences, the FE simulations effectively captured the overall trends observed in the experimental data (Figure 4.29). The relatively small deviation in most cases suggests that the FE model provides a reasonable representation of the mechanical behavior of the bone-screw interface.

Overall, the FE model remains a valuable tool for predicting screw fixation strength and can be further refined by incorporating more detailed material properties, improved boundary conditions, and better representation of bone anisotropy to enhance its predictive capability.

4.7.2 Limitations

This study used micro-CT imaging of vertebral trabecular bone to segment and analyze topological and geometric properties, including bone volume fraction (BV/TV) and trabecular thickness. A dual segmentation approach was used to both quantify bone properties and generate FE models to simulate pedicle screw extraction. However, certain limitations must be acknowledged:

- Scan Resolution Limitations - The resolution of the micro-CT scans posed a challenge in directly incorporating them into FE models, resulting in necessary simplifications in the representation of the bone structure.

- Computational Limitations - Available software and hardware lacked the computational power required for highly detailed micro-CT-based FE simulations, limiting the degree of mesh refinement and model complexity.
- Segmentation Challenges - One of the key challenges was segmenting the bone-screw interface region to calculate BV/TV and other morphometric parameters. Due to the heterogeneous nature of trabecular bone and regional variations in BV/TV across the vertebral body, it was not possible to resegment the entire vertebra. As a result, the quantitative parameters obtained from the segmented region reflect only the local microarchitecture surrounding the screw and do not represent the overall bone quality of the vertebral body. This is a limitation in generalizing the findings to the entire structure.

Despite these limitations, the study provides valuable insights into the mechanical behavior of pedicle screws in different bone quality conditions and establishes a strong foundation for future improvements in FE modeling and simulation accuracy.

5. Conclusions

This study investigated the pull-out behavior of pedicle screws in vertebral trabecular bone using both experimental testing and finite element (FE) simulation. The objective of the research was to evaluate the mechanical performance of screws in normal, osteopenic, and osteoporotic bone and to gain insight into how bone quality affects screw fixation strength. In the experimental phase, vertebral trabecular bone specimens were prepared and subjected to pull-out tests to measure peak pull-out force (PPF). After testing, the specimens were scanned using micro-CT and key trabecular parameters, including bone volume fraction (BV/TV) and trabecular thickness, were calculated to characterize bone quality. For the numerical phase, FE models of the specimens were developed for comparison with the experimental results. Due to computational and resolution constraints, direct micro-CT scans could not be used for FE modeling. Instead, BV/TV values were used to estimate the mechanical properties of the bone based on established relationships between BV/TV and apparent density. Simulations were performed on homogeneous FE models with mechanical properties assigned according to the density and elasticity relationships derived from BV/TV. Comparison between the FE and experimental results showed reasonable agreement, confirming the effectiveness of the FE approach in capturing the general trends in screw pull-out behavior. However, some discrepancies were observed, particularly in osteoporotic bone, which may be attributed to simplifications in the FE model, material property estimates, and assumptions regarding bone homogeneity.

Despite these limitations, this study provides valuable insight into the mechanical behavior of pedicle screws in different bone conditions. The results highlight the importance of bone quality on screw fixation strength and provide a strong foundation for future refinements in FE modeling. Future work should aim to improve simulation accuracy by incorporating more detailed bone microarchitecture, anisotropic material properties, and improved bone-screw interaction models.

6. Bibliography

[1] T. Cheng, R.-G. Xia, S.-K. Dong, X.-Y. Yan, and C.-F. Luo, "Interlocking Intramedullary Nailing Versus Locked Dual-Plating Fixation for Femoral Shaft Fractures in Patients with Multiple Injuries: A Retrospective Comparative Study," *J. Invest. Surg.*, vol. 32, no. 3, pp. 245–254, Apr. 2019, doi: 10.1080/08941939.2017.1400131.

[2] N. Enninghorst, D. McDougall, J. A. Evans, K. Sisak, and Z. J. Balogh, "Population-based epidemiology of femur shaft fractures," *J. Trauma Acute Care Surg.*, vol. 74, no. 6, pp. 1516–1520, Jun. 2013, doi: 10.1097/TA.0b013e31828c3dc9.

[3] S. T. Salminen, H. K. Pihlajam??ki, V. J. Avikainen, and O. M. B??stman, "Population Based Epidemiologic and Morphologic Study of Femoral Shaft Fractures:," *Clin. Orthop.*, vol. 372, pp. 241–249, Mar. 2000, doi: 10.1097/00003086-200003000-00026.

[4] T. W. O'Neill *et al.*, "The prevalence of vertebral deformity in European men and women: The european vertebral osteoporosis study," *J. Bone Miner. Res.*, vol. 11, no. 7, pp. 1010–1018, Jul. 1996, doi: 10.1002/jbmr.5650110719.

[5] L. J. Melton, A. W. Lane, C. Cooper, R. Eastell, W. M. O'Fallon, and B. L. Riggs, "Prevalence and incidence of vertebral deformities," *Osteoporos. Int.*, vol. 3, no. 3, pp. 113–119, May 1993, doi: 10.1007/BF01623271.

[6] D. J. Burval, R. F. McLain, R. Milks, and S. Inceoglu, "Primary Pedicle Screw Augmentation in Osteoporotic Lumbar Vertebrae: Biomechanical Analysis of Pedicle Fixation Strength," *Spine*, vol. 32, no. 10, pp. 1077–1083, May 2007, doi: 10.1097/01.brs.0000261566.38422.40.

[7] Cooper, C., & Melton, L. J. (1992). How large is the silent epidemic. *Br Med J*, *304*, 793-794.

[8] B. Ettinger *et al.*, "Contribution of vertebral deformities to chronic back pain and disability," *J. Bone Miner. Res.*, vol. 7, no. 4, pp. 449–456, Apr. 1992, doi: 10.1002/jbmr.5650070413.

[9] V. Gupta, P. M. Pandey, and V. V. Silberschmidt, "Rotary ultrasonic bone drilling: Improved pullout strength and reduced damage," *Med. Eng. Phys.*, vol. 41, pp. 1–8, Mar. 2017, doi: 10.1016/j.medengphy.2016.11.004.

[10] Boucher, H. H. (1959). A method of spinal fusion. *The Journal of Bone & Joint Surgery British Volume*, *41*(2), 248-259.

[11] R. Roy-Camille, G. Saillant, and C. Mazel, "Internal Fixation of the Lumbar Spine with Pedicle Screw Plating:," *Clin. Orthop.*, vol. 203, no. NA;, p. 7???17, Feb. 1986, doi: 10.1097/00003086-198602000-00003.

[12] M. Einafshar, A. Hashemi, and G. H. Van Lenthe, "Homogenized finite element models can accurately predict screw pull-out in continuum materials, but not in porous materials," *Comput. Methods Programs Biomed.*, vol. 202, p. 105966, Apr. 2021, doi: 10.1016/j.cmpb.2021.105966.

[13] Hirano, T., Hasegawa, K., Takahashi, H. E., Uchiyama, S., Hara, T., Washio, T., ... & Ikeda, M. (1997). Structural characteristics of the pedicle and its role in screw stability. *Spine*, *22*(21), 2504-2510.

[14] Lim, T. H., An, H. S., Evanich, C., Hasanoglu, K. Y., McGrady, L., & Wilson, C. R. (1995). Strength of anterior vertebral screw fixation in relationship to bone mineral density. *Clinical Spine Surgery*, *8*(2), 121-125.

[15] Myers, B. S., Belmont Jr, P. J., Richardson, W. J., Yu, J. R., Harper, K. D., & Nightingale, R. W. (1996). The role of imaging and in situ biomechanical testing in assessing pedicle screw pull-out strength. *Spine*, *21*(17), 1962-1968.

[16] Zink, P. M. (1996). Performance of ventral spondylodesis screws in cervical vertebrae of varying bone mineral density. *Spine*, *21*(1), 45-52.

[17] Zindrick, M. R., Wiltse, L. L., Widell, E. H., THOMAS, J. C., Holland, W. R., FIELD, B. T., & SPENCER, C. W. (1986). A biomechanical study of intrapeduncular screw fixation in the lumbosacral spine. *Clinical Orthopaedics and Related Research (1976-2007)*, *203*, 99-112.

[18] Q. H. Zhang, S. H. Tan, and S. M. Chou, "Investigation of fixation screw pull-out strength on human spine," *J. Biomech.*, vol. 37, no. 4, pp. 479–485, 2004, doi: 10.1016/j.jbiomech.2003.09.005.

[19] P. Chaynes, J.-C. Sol, Ph. Vaysse, J. Bécue, and J. Lagarrigue, "Vertebral pedicle anatomy in relation to pedicle screw fixation: a cadaver study," *Surg. Radiol. Anat.*, vol. 23, no. 2, pp. 85–90, Jun. 2001, doi: 10.1007/s00276-001-0085-z.

[20] A. Hashemi, D. Bednar, and S. Ziada, "Pullout strength of pedicle screws augmented with particulate calcium phosphate: An experimental study," *Spine J.*, vol. 9, no. 5, pp. 404–410, May 2009, doi: 10.1016/j.spinee.2008.07.001.

[21] Hounsfield, G. N. (1973). Computerized transverse axial scanning (tomography): Part 1. Description of system. *The British journal of radiology*, *46*(552), 1016-1022.

[22] J. D. Silva, "Automation of pedicle screw placement by coupling distal bone bio-impedance measurements and robotics".

[23] J. N. Weinstein, B. L. Rydevik, and W. Rauschning, "Anatomic and Technical Considerations of Pedicle Screw Fixation:," *Clin. Orthop.*, vol. 284, p. 34???46, Nov. 1992, doi: 10.1097/00003086-199211000-00006.

[24] C. M. Bono and T. A. Einhorn, "Overview of osteoporosis: pathophysiology and determinants of bone strength," *Eur. Spine J.*, vol. 12, no. 0, pp. S90–S96, Oct. 2003, doi: 10.1007/s00586-003-0603-2.

[25] Varacallo, M., Seaman, T. J., Jandu, J. S., & Pizzutillo, P. (2018). Osteopenia.

[26] R. Bartl and B. Frisch, *Osteoporosis: Diagnosis, Prevention, Therapy*, 2. 2nd ed. 2009. Berlin, Heidelberg: Springer Berlin Heidelberg, 2009. doi: 10.1007/978-3-540-79527-8.

[27] Kanis, J. A. (2007). Assessment of osteoporosis at the primary health-care level. *WHO Collaborating Centre for Metabolic Bone Diseases, University of Sheffield*.

[28] V. K. Goel, K. Sairyo, S. L. Vishnubhotla, A. Biyani, and N. Ebroheim, "Spine Disorders: Implications for Bioengineers," *Spine Technol. Handb.*.

[29] "Spinal Disorders: Fundamentals of Diagnosis and Treatment," *Am. J. Neuroradiol.*, vol. 30, no. 3, pp. e44–e44, Mar. 2009, doi: 10.3174/ajnr.A1299.

[30] Deyo, R. A., Nachemson, A., & Mirza, S. K. (2004). Spinal-fusion surgery—the case for restraint. *The Spine Journal*, *4*(5), S138-S142.

[31] K.-U. Lewandrowski, D. L. Wise, and D. J. Trantolo, *Advances in Spinal Fusion: Molecular Science, Biomechanics and Clinical Management*. Hoboken: Marcel Dekker Inc, 2003.

[32] D. King, "INTERNAL FIXATION FOR LUMBOSACRAL FUSION," *Am. J. Surg.*, 1944.

[33] King, H. A. (1988). Selection of fusion levels for posterior instrumentation and fusion in idiopathic scoliosis. *The Orthopedic clinics of North America*, *19*(2), 247-255.

[34] S. Becker *et al.*, "Assessment of different screw augmentation techniques and screw designs in osteoporotic spines," *Eur. Spine J.*, vol. 17, no. 11, pp. 1462–1469, Nov. 2008, doi: 10.1007/s00586-008-0769-8.

[35] L.-H. Chen *et al.*, "Pullout strength for cannulated pedicle screws with bone cement augmentation in severely osteoporotic bone: Influences of radial hole and pilot hole tapping," *Clin. Biomech.*, vol. 24, no. 8, pp. 613–618, Oct. 2009, doi: 10.1016/j.clinbiomech.2009.05.002.

[36] C. Hsu, C. Chao, J. Wang, S. Hou, Y. Tsai, and J. Lin, "Resea r c h Increase of pullout strength of spinal pedicle screws with conical core : biomechanical tests and finite element analyses," vol. 23, pp. 788–794, 2005.
[37] S. Inceoglu, L. Ferrara, and R. F. McLain, "Pedicle screw fixation strength: pullout versus insertional torque," *Spine J.*, vol. 4, no. 5, pp. 513–518, Sep. 2004, doi: 10.1016/j.spinee.2004.02.006.
[38] S. M. Renner, T.-H. Lim, W.-J. Kim, L. Katolik, H. S. An, and G. B. J. Andersson, "Augmentation of Pedicle Screw Fixation Strength Using an Injectable Calcium Phosphate Cement as a Function of Injection Timing and Method:," *Spine*, vol. 29, no. 11, pp. E212–E216, Jun. 2004, doi: 10.1097/00007632-200406010-00020.
[39] S.-B. Lien, N.-H. Liou, and S.-S. Wu, "Analysis of anatomic morphometry of the pedicles and the safe zone for through-pedicle procedures in the thoracic and lumbar spine," *Eur. Spine J.*, vol. 16, no. 8, pp. 1215–1222, Aug. 2007, doi: 10.1007/s00586-006-0245-2.
[40] G. F. Solitro, K. Whitlock, F. Amirouche, A. I. Mehta, and A. Mcdonnell, "Currently Adopted Criteria for Pedicle Screw Diameter Selection," *Int. J. Spine Surg.*, vol. 13, no. 2, pp. 132–145, Apr. 2019, doi: 10.14444/6018.
[41] K. J. Karami *et al.*, "Biomechanical Evaluation of the Pedicle Screw Insertion Depth Effect on Screw Stability Under Cyclic Loading and Subsequent Pullout," *J. Spinal Disord. Tech.*, vol. 28, no. 3, pp. E133–E139, Apr. 2015, doi: 10.1097/BSD.0000000000000178.
[42] P. Stradiotti, A. Curti, G. Castellazzi, and A. Zerbi, "Metal-related artifacts in instrumented spine. Techniques for reducing artifacts in CT and MRI: state of the art," *Eur. Spine J.*, vol. 18, no. S1, pp. 102–108, Jun. 2009, doi: 10.1007/s00586-009-0998-5.
[43] Rudisch, A., Kremser, C., Peer, S., Kathrein, A., Judmaier, W., & Daniaux, H. (1998). Metallic artifacts in magnetic resonance imaging of patients with spinal fusion: a comparison of implant materials and imaging sequences. *Spine*, *23*(6), 692-699.
[44] S. M. Kurtz and J. N. Devine, "PEEK biomaterials in trauma, orthopedic, and spinal implants," *Biomaterials*, vol. 28, no. 32, pp. 4845–4869, Nov. 2007, doi: 10.1016/j.biomaterials.2007.07.013.
[45] F. Ringel *et al.*, "Radiolucent Carbon Fiber–Reinforced Pedicle Screws for Treatment of Spinal Tumors: Advantages for Radiation Planning and Follow-Up Imaging," *World Neurosurg.*, vol. 105, pp. 294–301, Sep. 2017, doi: 10.1016/j.wneu.2017.04.091.
[46] H. B. Skinner, "Composite Technology for Total Hip Arthroplasty:," *Clin. Orthop.*, vol. 235, no. NA;, p. 224???236, Oct. 1988, doi: 10.1097/00003086-198810000-00022.
[47] C. S. Li, C. Vannabouathong, S. Sprague, and M. Bhandari, "The Use of Carbon-Fiber-Reinforced (CFR) PEEK Material in Orthopedic Implants: A Systematic Review," *Clin. Med. Insights Arthritis Musculoskelet. Disord.*, vol. 8, p. CMAMD.S20354, Jan. 2015, doi: 10.4137/CMAMD.S20354.
[48] D. J. Hak, C. Mauffrey, D. Seligson, and B. Lindeque, "Use of Carbon-Fiber-Reinforced Composite Implants in Orthopedic Surgery," *Orthopedics*, vol. 37, no. 12, pp. 825–830, Dec. 2014, doi: 10.3928/01477447-20141124-05.
[49] G. Tedesco, A. Gasbarrini, S. Bandiera, R. Ghermandi, and S. Boriani, "Composite PEEK/Carbon fiber implants can increase the effectiveness of radiotherapy in the management of spine tumors," *J. Spine Surg.*, vol. 3, no. 3, pp. 323–329, Sep. 2017, doi: 10.21037/jss.2017.06.20.
[50] S. Boriani *et al.*, "Carbon-fiber-reinforced PEEK fixation system in the treatment of spine tumors: a preliminary report," *Eur. Spine J.*, vol. 27, no. 4, pp. 874–881, Apr. 2018, doi: 10.1007/s00586-017-5258-5.

[51] O. Uri, Y. Folman, G. Laufer, and E. Behrbalk, “A Novel Spine Fixation System Made Entirely of Carbon-Fiber-Reinforced PEEK Composite: An In Vitro Mechanical Evaluation,” *Adv. Orthop.*, vol. 2020, pp. 1–7, Jun. 2020, doi: 10.1155/2020/4796136.
[52] Breeze, S. W., Doherty, B. J., Noble, P. S., LeBlanc, A., & Heggeness, M. H. (1998). A biomechanical study of anterior thoracolumbar screw fixation. *Spine*, *23*(17), 1829-1831.
[53] J. Seebeck, J. Goldhahn, H. Städele, P. Messmer, M. M. Morlock, and E. Schneider, “Effect of cortical thickness and cancellous bone density on the holding strength of internal fixator screws,” *J. Orthop. Res.*, vol. 22, no. 6, pp. 1237–1242, Nov. 2004, doi: 10.1016/j.orthres.2004.04.001.
[54] T. M. Shea, “Localized Expansion of Pedicle Screws for Increased Stability and Safety in the Osteoporotic Spine”.
[55] R. W. Gaines, “The Use of Pedicle-Screw Internal Fixation for the Operative Treatment of Spinal Disorders*:,” *J. Bone Jt. Surg.-Am. Vol.*, vol. 82, no. 10, pp. 1458–1476, Oct. 2000, doi: 10.2106/00004623-200010000-00013.
[56] Hadra, B. E. (1891). Wiring the spinous processes in Pott's disease. *JBJS*, *1*(1), 206-210.
[57] PR, H. (1969). Reduction of severe spondylolisthesis in children. *South Med J*, *62*, 1-7.
[58] Dick, W. (1987). The “fixatuer interne” as a versatile implant for spine surgery. *Spine*, *12*(9), 882-900.
[59] R. Roy-Camille, G. Saillant, and Ch. Mazel, “Plating of Thoracic, Thoracolumbar, and Lumbar Injuries with Pedicle Screw Plates,” *Orthop. Clin. North Am.*, vol. 17, no. 1, pp. 147–159, Jan. 1986, doi: 10.1016/S0030-5898(20)30425-9.
[60] R. Louis, “Fusion of the Lumbar and Sacral Spine by Internal Fixation with Screw Plates:,” *Clin. Orthop.*, vol. 203, no. NA;, p. 18???33, Feb. 1986, doi: 10.1097/00003086-198602000-00004.
[61] A. D. Steffee, R. S. Biscup, and D. J. Sitkowskj, “Segmental Spine Plates with Pedicle Screw Fixation A New Internal Fixation Device for Disorders of the Lumbar and Thoracolumbar Spine:,” *Clin. Orthop.*, vol. 203, no. NA;, p. 45???53, Feb. 1986, doi: 10.1097/00003086-198602000-00006.
[62] Crawford, M. J., & Esses, S. I. (1994). Indications for pedicle fixation: Results of NASS/SRS faculty questionnaire. *Spine*, *19*(22), 2584-2589.
[63] GURR, K. R., & McAFEE, P. C. (1988). Cotrel-Dubousset instrumentation in adults: a preliminary report. *Spine*, *13*(5), 510-520.
[64] Matsuzaki, H., Tokuhashi, Y., MATSUMOTO, F., HOSHINO, M., KIUCHI, T., & TORIYAMA, S. (1990). Problems and solutions of pedicle screw plate fixation of lumbar spine. *Spine*, *15*(11), 1159-1165.
[65] Vaccaro, A. R., & Garfin, S. R. (1995). Internal fixation (pedicle screw fixation) for fusions of the lumbar spine. *Spine*, *20*, 166S.
[66] Steffee, A. D., Biscup, R. S., & SITKOWSKJ, D. J. (1986). Segmental Spine Plates with Pedicle Screw Fixation A New Internal Fixation Device for Disorders of the Lumbar and Thoracolumbar Spine. *Clinical Orthopaedics and Related Research (1976-2007)*, *203*, 45-53.
[67] GAINES, R. W., SATTERLEE, C. C., & GROH, G. I. (1991). Experimental evaluation of seven different spinal fracture internal fixation devices using nonfailure stability testing: The load-sharing and unstable-mechanism concepts. *Spine*, *16*(8), 902-909.
[68] Bennett, G. J., Serhan, H. A., Sorini, P. M., & Willis, B. H. (1997). An experimental study of lumbar destabilization: restabilization and bone density. *Spine*, *22*(13), 1448-1453.

[69] Coe, J. D., Warden, K. E., ENGR, M., HERZIG, M. A., & McAFEE, P. C. (1990). Influence of bone mineral density on the fixation of thoracolumbar implants a comparative study of transpedicular screws, laminar hooks, and spinous process wires. *Spine*, *15*(9), 902-907.

[70] Kumano, K., Hirabayashi, S., Ogawa, Y., & Aota, Y. (1994). Pedicle screws and bone mineral density. *Spine*, *19*(10), 1157-1161.

[71] Law, M., Tencer, A. F., & Anderson, P. A. (1993). Caudo-cephalad loading of pedicle screws: mechanisms of loosening and methods of augmentation. *Spine*, *18*(16), 2438-2443.

[72] Mc Lain Robert, F., Moseley, T. A., & Sharkey, N. A. (1995). Lumbar pedicle screw salvage: pullout testing of three different pedicle screw designs. *Clinical Spine Surgery*, *8*(1), 62-68.

[73] Anna, G. U., & Jack, K. M. (1994). The Effect of Pedicle Screw Fit An in Vitro Study. *Spine*, *19*(15), 1752.

[74] Dick, J. C., Zdeblick, T. A., Bartel, B. D., & Kunz, D. N. (2000). Mechanical evaluation of cross-link designs in rigid pedicle screw systems. *Spine*, *25*(6S), 13S-18S.

[75] Hadjipavlou, A. G., Nicodemus, C. L., Al-Hamdan, F. A., Simmons, J. W., & Pope, M. H. (1997). Correlation of bone equivalent mineral density to pull-out resistance of triangulated pedicle screw construct. *Clinical Spine Surgery*, *10*(1), 12-19.

[76] Lynn, G., Mukherjee, D. P., Kruse, R. N., Sadasivan, K. K., & Albright, J. A. (2000). Mechanical stability of thoracolumbar pedicle screw fixation: the effect of crosslinks. *Spine*, *25*(6S), 31S-35S.

[77] Pintar, F. A., Maiman, D. J., Yoganandan, N., Droese, K. W., Hollowell, J. P., & Woodard, E. (1995). Rotational stability of a spinal pedicle screw/rod system. *Clinical Spine Surgery*, *8*(1), 49-55.

[78] Barber, J. W., Boden, S. D., Ganey, T., & Hutton, W. C. (1998). Biomechanical study of lumbar pedicle screws: does convergence affect axial pullout strength?. *Clinical Spine Surgery*, *11*(3), 215-220.

[79] Carson, W. L., Duffield, R. C., Arendt, M., Ridgely, B. J., & Gaines Jr, R. W. (1990). Internal forces and moments in transpedicular spine instrumentation the effect of pedicle screw angle and transfixation—the 4R-4Bar linkage concept. *Spine*, *15*(9), 893-901.

[80] Ruland, C. M., McAfee, P. C., Warden, K. E., & Cunningham, B. W. (1991). Triangulation of pedicular instrumentation: a biomechanical analysis. *Spine*, *16*(6S), S270-S276.

[81] Goel, V. K., Kim, Y. E., Lim, T. H., & WEINSTEIN, J. N. (1988). An analytical investigation of the mechanics of spinal instrumentation. *Spine*, *13*(9), 1003-1011.

[82] T.-H. Lim, V. K. Goel, J. N. Weinstein, and W. Kong, “Stress analysis of a canine spinal motion segment using the finite element technique,” *J. Biomech.*, vol. 27, no. 10, pp. 1259–1269, Oct. 1994, doi: 10.1016/0021-9290(94)90279-8.

[83] M. S. R. Aziz, B. Nicayenzi, M. C. Crookshank, H. Bougherara, E. H. Schemitsch, and R. Zdero, “Biomechanical measurements of cortical screw purchase in five types of human and artificial humeri,” *J. Mech. Behav. Biomed. Mater.*, vol. 30, pp. 159–167, Feb. 2014, doi: 10.1016/j.jmbbm.2013.11.007.

[84] R. Zdero, K. Elfallah, M. Olsen, and E. H. Schemitsch, “Cortical Screw Purchase in Synthetic and Human Femurs,” *J. Biomech. Eng.*, vol. 131, no. 9, p. 094503, Sep. 2009, doi: 10.1115/1.3194755.

[85] R. Zdero, M. Olsen, H. Bougherara, and E. H. Schemitsch, “Cancellous bone screw purchase: A comparison of synthetic femurs, human femurs, and finite element analysis,” *Proc. Inst. Mech. Eng. [H]*, vol. 222, no. 8, pp. 1175–1183, Nov. 2008, doi: 10.1243/09544119JEIM409.

[86] R. Zdero and E. H. Schemitsch, “The Effect of Screw Pullout Rate on Screw Purchase in Synthetic Cancellous Bone,” *J. Biomech. Eng.*, vol. 131, no. 2, p. 024501, Feb. 2009, doi: 10.1115/1.3005344.
[87] S. E. Tankard, S. C. Mears, D. Marsland, E. R. Langdale, and S. M. Belkoff, “Does Maximum Torque Mean Optimal Pullout Strength of Screws?,” *J. Orthop. Trauma*, vol. 27, no. 4, pp. 232–235, Apr. 2013, doi: 10.1097/BOT.0b013e318279791f.
[88] Lyon, W. F., Cochran, J. R., & Smith, L. (1941). Actual holding power of various screws in bone. *Annals of surgery*, *114*(3), 376.
[89] G. L. Westmoreland, T. M. McLaurin, and W. C. Hutton, “Screw Pullout Strength: A Biomechanical Comparison of Large-fragment and Small-fragment Fixation in the Tibial Plateau:,” *J. Orthop. Trauma*, vol. 16, no. 3, pp. 178–181, Mar. 2002, doi: 10.1097/00005131-200203000-00007.
[90] S. Nagaraja and V. Palepu, “Comparisons of Anterior Plate Screw Pullout Strength Between Polyurethane Foams and Thoracolumbar Cadaveric Vertebrae,” *J. Biomech. Eng.*, vol. 138, no. 10, p. 104505, Oct. 2016, doi: 10.1115/1.4034427.
[91] R. Zdero, M. S. R. Aziz, and B. Nicayenzi, “Pullout Force Testing of Cortical and Cancellous Screws in Whole Bone,” in *Experimental Methods in Orthopaedic Biomechanics*, Elsevier, 2017, pp. 117–132. doi: 10.1016/B978-0-12-803802-4.00008-1.
[92] P. S. D. Patel, D. E. T. Shepherd, and D. W. L. Hukins, “The effect of screw insertion angle and thread type on the pullout strength of bone screws in normal and osteoporotic cancellous bone models,” *Med. Eng. Phys.*, vol. 32, no. 8, pp. 822–828, Oct. 2010, doi: 10.1016/j.medengphy.2010.05.005.
[93] W. Cho, S. K. Cho, and C. Wu, “The biomechanics of pedicle screw-based instrumentation,” *J. BONE Jt. Surg.*, vol. 92, no. 8, 2010.
[94] LIU, Y. K., NJUS, G. O., Bahr, P. A., & Geng, P. O. (1990). Fatigue Life Improvement of Nitrogen-Ion–Implanted Pedicle Screws. *Spine*, *15*(4), 311-317.
[95] S. D. Cook, J. Barbera, M. Rubi, S. L. Salkeld, and T. S. Whitecloud, “Lumbosacral fixation using expandable pedicle screws: an alternative in reoperation and osteoporosis,” *Spine J.*, 2001.
[96] W. Lei and Z. Wu, “Biomechanical evaluation of an expansive pedicle screw in calf vertebrae,” *Eur. Spine J.*, vol. 15, no. 3, pp. 321–326, Mar. 2006, doi: 10.1007/s00586-004-0867-1.
[97] P. A. Anderson *et al.*, “Use of Bone Health Evaluation in Orthopedic Surgery: 2019 ISCD Official Position,” *J. Clin. Densitom.*, vol. 22, no. 4, pp. 517–543, Oct. 2019, doi: 10.1016/j.jocd.2019.07.013.
[98] Z. Fan *et al.*, “Prevalence of osteoporosis in spinal surgery patients older than 50 years: A systematic review and meta-analysis,” *PLOS ONE*, vol. 18, no. 5, p. e0286110, May 2023, doi: 10.1371/journal.pone.0286110.
[99] Y.-J. Tang, W. H.-H. Sheu, P.-H. Liu, W.-J. Lee, and Y.-T. Chen, “Positive associations of bone mineral density with body mass index, physical activity, and blood triglyceride level in men over 70 years old: a TCVGHAGE study,” *J. Bone Miner. Metab.*, vol. 25, no. 1, pp. 54–59, Dec. 2006, doi: 10.1007/s00774-006-0727-7.
[100] M. Xu, J. Yang, I. H. Lieberman, and R. Haddas, “Finite element method-based study of pedicle screw–bone connection in pullout test and physiological spinal loads,” *Med. Eng. Phys.*, vol. 67, pp. 11–21, May 2019, doi: 10.1016/j.medengphy.2019.03.004.
[101] Y. Amaritsakul, C.-K. Chao, and J. Lin, “Biomechanical evaluation of bending strength of spinal pedicle screws, including cylindrical, conical, dual core and double dual core designs using numerical simulations and mechanical tests,” *Med. Eng. Phys.*, vol. 36, no. 9, pp. 1218–1223, Sep. 2014, doi: 10.1016/j.medengphy.2014.06.014.

[102] P. Chazistergos, G. Ferentinos, E. A. Magnissalis, and S. K. Kourkoulis, “The Pull-Out Strength of Transpedicular Screws in Posterior Spinal Fusion,” in *Fracture of Nano and Engineering Materials and Structures*, E. E. Gdoutos, Ed., Dordrecht: Springer Netherlands, 2006, pp. 417–418. doi: 10.1007/1-4020-4972-2_206.
[103] K.-H. Chao *et al.*, “Biomechanical analysis of different types of pedicle screw augmentation: A cadaveric and synthetic bone sample study of instrumented vertebral specimens,” *Med. Eng. Phys.*, vol. 35, no. 10, pp. 1506–1512, Oct. 2013, doi: 10.1016/j.medengphy.2013.04.007.
[104] B. D. Elder *et al.*, “The biomechanics of pedicle screw augmentation with cement,” *Spine J.*, vol. 15, no. 6, pp. 1432–1445, Jun. 2015, doi: 10.1016/j.spinee.2015.03.016.
[105] C.-S. Chen, W.-J. Chen, C.-K. Cheng, S.-H. E. Jao, S.-C. Chueh, and C.-C. Wang, “Failure analysis of broken pedicle screws on spinal instrumentation,” *Med. Eng. Phys.*, vol. 27, no. 6, pp. 487–496, Jul. 2005, doi: 10.1016/j.medengphy.2004.12.007.
[106] S. Liu, W. Qi, Y. Zhang, Z.-X. Wu, Y.-B. Yan, and W. Lei, “Effect of bone material properties on effective region in screw-bone model: an experimental and finite element study,” *Biomed. Eng. OnLine*, vol. 13, no. 1, p. 83, Dec. 2014, doi: 10.1186/1475-925X-13-83.
[107] C.-K. Chao, C.-C. Hsu, J.-L. Wang, and J. Lin, “Increasing Bending Strength and Pullout Strength in Conical Pedicle Screws: Biomechanical Tests and Finite Element Analyses,” *J. Spinal Disord. Tech.*, vol. 21, no. 2, pp. 130–138, Apr. 2008, doi: 10.1097/BSD.0b013e318073cc4b.
[108] T. Demir and N. Camuşcu, “Design and performance of spinal fixation pedicle screw system,” *Proc. Inst. Mech. Eng. [H]*, vol. 226, no. 1, pp. 33–40, Jan. 2012, doi: 10.1177/0954411911427351.
[109] L. La Barbera, C. Ottardi, and T. Villa, “Comparative analysis of international standards for the fatigue testing of posterior spinal fixation systems: the importance of preload in ISO 12189,” *Spine J.*, vol. 15, no. 10, pp. 2290–2296, Oct. 2015, doi: 10.1016/j.spinee.2015.07.461.
[110] H. Kovacı, A. F. Yetim, and A. Çelik, “Biomechanical analysis of spinal implants with different rod diameters under static and fatigue loads: an experimental study,” *Biomed. Eng. Biomed. Tech.*, vol. 64, no. 3, pp. 339–346, May 2019, doi: 10.1515/bmt-2017-0236.
[111] T. Villa, L. La Barbera, and F. Galbusera, “Comparative analysis of international standards for the fatigue testing of posterior spinal fixation systems,” *Spine J.*, vol. 14, no. 4, pp. 695–704, Apr. 2014, doi: 10.1016/j.spinee.2013.08.032.
[112] L. La Barbera, F. Galbusera, T. Villa, F. Costa, and H.-J. Wilke, “ASTM F1717 standard for the preclinical evaluation of posterior spinal fixators: Can we improve it?,” *Proc. Inst. Mech. Eng. [H]*, vol. 228, no. 10, pp. 1014–1026, Oct. 2014, doi: 10.1177/0954411914554244.
[113] L. La Barbera, F. Galbusera, H.-J. Wilke, and T. Villa, “Preclinical evaluation of posterior spine stabilization devices: can the current standards represent basic everyday life activities?,” *Eur. Spine J.*, vol. 25, no. 9, pp. 2909–2918, Sep. 2016, doi: 10.1007/s00586-016-4622-1.
[114] L. La Barbera and T. Villa, “Toward the definition of a new *worst-case* paradigm for the preclinical evaluation of posterior spine stabilization devices,” *Proc. Inst. Mech. Eng. [H]*, vol. 231, no. 2, pp. 176–185, Feb. 2017, doi: 10.1177/0954411916684365.
[115] “Veterinary Surgery - 2015 - Boero Baroncelli - Effect of Screw Insertion Torque on Push-Out and Cantilever Bending.pdf.”
[116] V. Varghese, “A Finite Element Analysis Based Sensitivity Studies on Pull Out Strength of Pedicle Screw in Synthetic Osteoporotic Bone Models,” pp. 382–387, 2016, doi: 10.1109/IECBES.2016.7843478.

[117] J. Biswas, S. Karmakar, S. Majumder, P. S. Banerjee, S. Saha, and A. Roychowdhury, "Optimization of spinal implant screw for lower vertebra through finite element studies," *J. Long. Term Eff. Med. Implants*, vol. 24, no. 2–3, pp. 99–108, 2014, doi: 10.1615/JLongTermEffMedImplants.2014006264.
[118] K. Matsukawa, Y. Yato, and H. Imabayashi, "Impact of Screw Diameter and Length on Pedicle Screw Fixation Strength in Osteoporotic Vertebrae: A Finite Element Analysis," *Asian Spine J.*, vol. 15, no. 5, pp. 566–574, Oct. 2021, doi: 10.31616/asj.2020.0353.
[119] A. R. MacLeod, P. Pankaj, and A. H. R. W. Simpson, "Does screw-bone interface modelling matter in finite element analyses?," *J. Biomech.*, vol. 45, no. 9, pp. 1712–1716, 2012, doi: 10.1016/j.jbiomech.2012.04.008.
[120] J. Widmer, M.-R. Fasser, E. Croci, J. Spirig, J. G. Snedeker, and M. Farshad, "Individualized prediction of pedicle screw fixation strength with a finite element model," *Comput. Methods Biomech. Biomed. Engin.*, vol. 23, no. 4, pp. 155–167, Mar. 2020, doi: 10.1080/10255842.2019.1709173.
[121] F04 Committee, *Specification and Test Methods for Metallic Medical Bone Screws*. doi: 10.1520/F0543-13E01.
[122] K.-T. Kang, Y.-G. Koh, J. Son, J. S. Yeom, J.-H. Park, and H.-J. Kim, "Biomechanical evaluation of pedicle screw fixation system in spinal adjacent levels using polyetheretherketone, carbon-fiber-reinforced polyetheretherketone, and traditional titanium as rod materials," *Compos. Part B Eng.*, vol. 130, pp. 248–256, Dec. 2017, doi: 10.1016/j.compositesb.2017.07.052.
[123] M. L. Bouxsein, S. K. Boyd, B. A. Christiansen, R. E. Guldberg, K. J. Jepsen, and R. Müller, "Guidelines for assessment of bone microstructure in rodents using micro–computed tomography," *J. Bone Miner. Res.*, vol. 25, no. 7, pp. 1468–1486, Jul. 2010, doi: 10.1002/jbmr.141.
[124] Y. Zhang, Z. He, S. Fan, K. He, and C. Li, "Automatic Thresholding of Micro-CT Trabecular Bone Images," in *2008 International Conference on BioMedical Engineering and Informatics*, Sanya, China: IEEE, May 2008, pp. 23–27. doi: 10.1109/BMEI.2008.13.
[125] J. R. Curtis *et al.*, "Longitudinal Trends in Use of Bone Mass Measurement Among Older Americans, 1999–2005," *J. Bone Miner. Res.*, vol. 23, no. 7, pp. 1061–1067, Jul. 2008, doi: 10.1359/jbmr.080232.
[126] A. H. Warriner *et al.*, "Effect of Self-referral on Bone Mineral Density Testing and Osteoporosis Treatment," *Med. Care*, vol. 52, no. 8, pp. 743–750, Aug. 2014, doi: 10.1097/MLR.0000000000000170.
[127] A. D. Brett and J. K. Brown, "Quantitative computed tomography and opportunistic bone density screening by dual use of computed tomography scans," *J. Orthop. Transl.*, vol. 3, no. 4, pp. 178–184, Oct. 2015, doi: 10.1016/j.jot.2015.08.006.
[128] P. J. Pickhardt, B. D. Pooler, T. Lauder, A. M. Del Rio, R. J. Bruce, and N. Binkley, "Opportunistic Screening for Osteoporosis Using Abdominal Computed Tomography Scans Obtained for Other Indications," *Ann. Intern. Med.*, vol. 158, no. 8, pp. 588–595, Apr. 2013, doi: 10.7326/0003-4819-158-8-201304160-00003.
[129] H. K. Genant, "Quantitative Computed Tomograplhy of Vertebral Spongiosa: A Sensitive Method for Detecting Early Bone Loss After Oophorectomy," *Ann. Intern. Med.*, vol. 97, no. 5, 1982.
[130] D. L. Kopperdahl *et al.*, "Assessment of incident spine and hip fractures in women and men using finite element analysis of CT scans," *J. Bone Miner. Res.*, vol. 29, no. 3, pp. 570–580, Mar. 2014, doi: 10.1002/jbmr.2069.
[131] R. M. Summers *et al.*, "Feasibility of Simultaneous Computed Tomographic Colonography and Fully Automated Bone Mineral Densitometry in a Single

Examination:," *J. Comput. Assist. Tomogr.*, vol. 35, no. 2, pp. 212–216, Mar. 2011, doi: 10.1097/RCT.0b013e3182032537.
[132] P. J. Pickhardt *et al.*, "Simultaneous screening for osteoporosis at CT colonography: Bone mineral density assessment using MDCT attenuation techniques compared with the DXA reference standard," *J. Bone Miner. Res.*, vol. 26, no. 9, pp. 2194–2203, Sep. 2011, doi: 10.1002/jbmr.428.
[133] J. E. Adams, "Quantitative computed tomography," *Eur. J. Radiol.*, vol. 71, no. 3, pp. 415–424, Sep. 2009, doi: 10.1016/j.ejrad.2009.04.074.
[134] K. G. Faulkner, E. Von Stetten, and P. Miller, "Discordance in Patient Classification Using T-Scores," *J. Clin. Densitom.*, vol. 2, no. 3, pp. 343–350, Sep. 1999, doi: 10.1385/JCD:2:3:343.
[135] C. M. Langton, T. J. Haire, P. S. Ganney, C. A. Dobson, and M. J. Fagan, "Dynamic Stochastic Simulation of Cancellous Bone Resorption," vol. 22, no. 4.
[136] O. B. Olurin, M. Arnold, C. Körner, and R. F. Singer, "The investigation of morphometric parameters of aluminium foams using micro-computed tomography," *Mater. Sci. Eng. A*, vol. 328, no. 1–2, pp. 334–343, May 2002, doi: 10.1016/S0921-5093(01)01809-3.
[137] A. S. Issever *et al.*, "A micro-computed tomography study of the trabecular bone structure in the femoral head".
[138] M. Rossi, F. Casali, D. Romani, and M. L. Carabini, "3D micro-CT analysis of cancellous bone architecture," presented at the International Symposium on Optical Science and Technology, U. Bonse, Ed., San Diego, CA, USA, Jan. 2002, p. 349. doi: 10.1117/12.452863.
[139] B. R. Gomberg, P. K. Saha, Hee Kwon Song, S. N. Hwang, and F. W. Wehrli, "Topological analysis of trabecular bone MR images," *IEEE Trans. Med. Imaging*, vol. 19, no. 3, pp. 166–174, Mar. 2000, doi: 10.1109/42.845175.
[140] M. Ding, A. Odgaard, and I. Hvid, "Accuracy of cancellous bone volume fraction measured by micro-CT scanning," *J. Biomech.*, vol. 32, no. 3, pp. 323–326, Mar. 1999, doi: 10.1016/S0021-9290(98)00176-6.
[141] American College of Radiology. (2023). *ACR–SPR–SSR practice parameter for the performance of quantitative computed tomography (QCT) bone mineral density*.
[142] E. N. Ebbesen, J. S. Thomsen, H. Beck-Nielsen, H. J. Nepper-Rasmussen, and L. Mosekilde, "Age- and Gender-Related Differences in Vertebral Bone Mass, Density, and Strength," *J. Bone Miner. Res.*, vol. 14, no. 8, pp. 1394–1403, Aug. 1999, doi: 10.1359/jbmr.1999.14.8.1394.
[143] A. Rouyin, M. Einafshar, and N. Arjmand, "A novel personalized homogenous finite element model to predict the pull-out strength of cancellous bone screws," *J. Orthop. Surg.*, vol. 19, no. 1, p. 732, Nov. 2024, doi: 10.1186/s13018-024-05169-x.
[144] H. Huang, C. Xiang, C. Zeng, H. Ouyang, K. K. L. Wong, and W. Huang, "Patient-specific geometrical modeling of orthopedic structures with high efficiency and accuracy for finite element modeling and 3D printing," *Australas. Phys. Eng. Sci. Med.*, vol. 38, no. 4, pp. 743–753, Dec. 2015, doi: 10.1007/s13246-015-0402-1.
[145] R. J. Bianco, P. J. Arnoux, E. Wagnac, J. M. Mac-Thiong, and C. É. Aubin, "Minimizing Pedicle Screw Pullout Risks: A Detailed Biomechanical Analysis of Screw Design and Placement," *Clin. Spine Surg.*, vol. 30, no. 3, pp. E226–E232, 2017, doi: 10.1097/BSD.0000000000000151.
[146] Y. X. Ye, D. G. Huang, D. J. Hao, J. Y. Liu, J. J. Ji, and J. N. Guo, "Screw Pullout Strength After Pedicle Screw Reposition: A Finite Element Analysis," *Spine*, vol. 48, no. 22, pp. E382–E388, 2023, doi: 10.1097/BRS.0000000000004553.

[147] S. Takenaka *et al.*, "Influence of novel design alteration of pedicle screw on pull-out strength: A finite element study," *J. Orthop. Sci.*, vol. 25, no. 1, pp. 66–72, Jan. 2020, doi: 10.1016/j.jos.2019.03.002.
[148] K. Matsukawa, Y. Yato, H. Imabayashi, and N. Hosogane, "Biomechanical evaluation of fixation strength among different sizes of pedicle screws using the cortical bone trajectory : what is the ideal screw size for optimal fixation ?," pp. 465–471, 2016, doi: 10.1007/s00701-016-2705-8.
[149] Li. Mosekilde, Le. Mosekilde, and C. C. Danielsen, "Biomechanical competence of vertebral trabecular bone in relation to ash density and age in normal individuals," *Bone*, vol. 8, no. 2, pp. 79–85, Jan. 1987, doi: 10.1016/8756-3282(87)90074-3.
[150] T. S. Keller, "Predicting the compressive mechanical behavior of bone," *J. Biomech.*, vol. 27, no. 9, pp. 1159–1168, Sep. 1994, doi: 10.1016/0021-9290(94)90056-6.
[151] D. L. Kopperdahl and T. M. Keaveny, "Yield strain behavior of trabecular bone," *J. Biomech.*, vol. 31, no. 7, pp. 601–608, Jul. 1998, doi: 10.1016/S0021-9290(98)00057-8.
[152] E. F. Morgan, H. H. Bayraktar, and T. M. Keaveny, "Trabecular bone modulus–density relationships depend on anatomic site," *J. Biomech.*, vol. 36, no. 7, pp. 897–904, Jul. 2003, doi: 10.1016/S0021-9290(03)00071-X.
[153] L. Molinari, C. Falcinelli, A. Gizzi, and A. Di, "Journal of the Mechanical Behavior of Biomedical Materials Effect of pedicle screw angles on the fracture risk of the human vertebra : A patient-specific computational model," *J. Mech. Behav. Biomed. Mater.*, vol. 116, no. December 2020, p. 104359, 2021, doi: 10.1016/j.jmbbm.2021.104359.
[154] J. Y. Rho, M. C. Hobatho, and R. B. Ashman, "Relations of mechanical properties to density and CT numbers in human bone," *Med. Eng. Phys.*, vol. 17, no. 5, pp. 347–355, Jul. 1995, doi: 10.1016/1350-4533(95)97314-F.
[155] A. Rouyin, H. Nazemi, N. Arjmand, and M. J. Einafshar, "Effect of pedicle screw misplacement on the pull-out strength using personalized finite element modeling," *Comput. Biol. Med.*, vol. 183, pp. 109290–109290, Dec. 2024, doi: 10.1016/j.compbiomed.2024.109290.
[156] A. Garo, P. J. Arnoux, E. Wagnac, and C. E. Aubin, "Calibration of the mechanical properties in a finite element model of a lumbar vertebra under dynamic compression up to failure," *Med. Biol. Eng. Comput.*, vol. 49, no. 12, pp. 1371–1379, Dec. 2011, doi: 10.1007/s11517-011-0826-z.